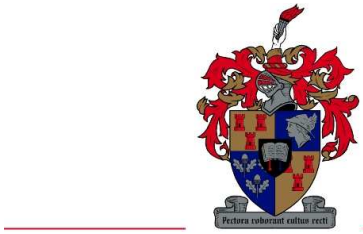

UNIVERSITEIT • STELLENBOSCH • UNIVERSITY

Mathematical modelling on interaction between malaria parasites and the host immune system

by

Theresia Marijani

Dissertation presented in full fulfilment of the
academic requirements for the degree of
Doctor of Philosophy in Mathematics
at the Stellenbosch University

Promoter: Prof. Edward M. Lungu (University of Botswana)
Co-Promoter: Prof. John Hargrove (University of Stellenbosch)

March 2012

Declaration

I, the undersigned, hereby declare that the work contained in this dissertation is my own original work and has not previously, in its entirety or in part, been submitted at any university for a degree.

---------- ----------

Theresia Marijani Date

Abstract

Malaria is a deadly tropical disease caused by protozoa of the genus plasmodium. The malaria parasite life cycle involves three cycles namely the sporogony (mosquito stages), exo-erythrocytic schizogony (human liver stages), and the erythrocytic schizogony (human blood stage). We consider a mathematical model for malaria involving, susceptible red blood cells, latent infected red blood cells, active infected red blood cells, intracellular parasites, extracellular parasites and effector cells. We extend the model to include all the three stages of the malaria life cycle. The effect of treatment on the prognosis of malaria is also introduced in these models. The models are analysed mathematically and numerically. One of the question addressed in our study is: what replicative characteristics offer the parasite opportunities to evade the host immune system? The results showed that the longer it takes to produce the parasites, the higher the chance that an infected red blood cell will be identified and apoptosised by the effector cells. Our sensitivity analysis results show that poor parametric estimation has serious implications on the prognosis of the disease. Treatment results suggest that a high drug efficacy can stop the development of the disease. The study has revealed that the parasite replicative characteristics enable the parasite to evade the immune response during the red blood stage malaria. Firstly, we have found that the parasite has a strategy of infecting older red blood cells as a strategy to evade immune surveillance. Secondly, we discovered that the administration of an effective drug can prevent malaria in all stages despite the current belief that only a malaria vaccine can reliably protect against all stages malaria infection. We recommend treatment to be used in areas where anti-malarial drugs do not show resistance to the parasites. We also recommend that individuals with malaria or showing some symptoms should be treated for both malaria and chronic infections.

Opsomming

Malaria is 'n dodelike tropiese siekte wat veroorsaak word deur die protoso ë van die genus Plasmodium. Die malariaparasiet lewensiklus bestaan uit drie siklusse naamlik die sporogony (muskiet stadiums), exo-erythrocytic schizogony (menslike lewer stadiums), en die erythrocytic schizogony (menslike bloed stadium). Ons kyk na 'n wiskundige model vir malaria, vatbaar rooibloedselle, latente besmet rooi bloedselle, aktief besmette rooibloedselle, intrasellul êre parasiete, ekstrasellulêre parasiete en effektor selle. Ons brei die model om al die drie fases van die lewensiklus malaria te sluit. Die effek van behandeling op die voorspelling van malaria is ook in hierdie modelle ingevoer. Die modelle is wiskundig en numeries ontleed. Een van die vraag in ons studie is: watter replicative eienskappe bied die parasiet geleenthede om die gasheer se immuunrespons te ontduik? Die resultate het getoon dat hoe langer dit neem om die parasiete te produseer, hoe groter die kans dat besmette rooibloedselle sal geïdentifiseer word en deur die effektor selle apoptosised. Ons sensitiwiteitsanalise resultate toon dat die arme parametriese beraming het ernstige implikasies vir die voorspelling van die siekte. Behandeling resultate dui daarop dat 'n hoë dwelm doeltreffendheid kan die ontwikkeling van die siekte stop. Die studie het getoon dat die parasiet replicative eienskappe die parasiet in staat stel om die immuunreaksie tydens die rooi bloed stadium malaria te ontduik. Eerstens, het ons gevind dat die parasiet het 'n strategie van besmet om ouer rooi bloed selle as' n strategie om immuun toesig te ontduik. Tweedens, het ons ontdek dat die administrasie van 'n doeltreffende middel kan malaria in alle stadiums voorkom ten spyte van die huidige oortuiging dat slegs' n malaria-entstof betroubaar kan beskerm teen alle stadia malaria infeksie. Ons raai dat behandeling gebruik word in gebiede waar die anti-malaria medisyne nie weerstand toon aan die parasiete. Ons beveel ook aan dat individue met malaria of wat sekere simptome het, behandel moet word vir beide malaria en chroniese malaria infeksies.

Dedication

I dedicate this dissertation to the greater glory of God, to his grace and power, to the people who suffers with malaria, to my beloved parents Mr. and Mrs. Marijani.

Acknowledgments

I would like thank almighty God for his grace, inspiration, strength and guidance, to God be the glory!

I would like to thank my beloved parents for their encouragement and prayer through all the time.

I would like give thank my promoter Prof. Edward Lungu, for his valuable guidance and supervision. He has been an excellent supervisor, a wise mentor, an inspiring and motivational teacher available in moments of need. His help during the time in need is real appreciated. My sincere thanks go to Mrs. Elizabeth Lungu.

I deeply appreciate my co-promoter Prof. John Hargrove for his valuable suggestions and insightful comments on this dissertation.

I real appreciate the direction and help by the Director of South African Centre of Epidemiological Modelling and Analysis (SACEMA) Dr. Alex Welte, research manager Lynnemore Scheepers, assistant director training Dr. Gavin Hitchcock, administrator Natalie Roman, Dr. Rashid Ouifki, all the staff at SACEMA, University of Stellenbosch, International office at Stellenbosch University. University of Botswana, mathematics department at University of Botswana, Office of International Education and Partnerships at University of Botswana during these years of my study. My special thanks to them for all official assistance they gave me and the personal concern they showed me.

I would like to thank all my fellow students at SACEMA and at University of Botswana for their help and support in personally and academically.

My special thanks go to Huba Boshoff and Tebogo Magetse for their help and support

during the time of exchanging my studies from Stellenbosch University to Botswana University.

This thesis is supported by SACEMA and OWSD (Organization for Women in Science for the Developing World). International office at Stellenbosch University, Office of International Education and Partnerships at University of Botswana. I would like to thank all these sponsors.

To my family members, my sisters, my brothers' in-law, my brother, sister's in-law, thank you for being patient with me during this time of my study, especially for my nephews (Godwin and Crispin) and my nieces (Winlove, Immaculata and Agnes). Thank you so much my family for your support, encouragement and prayers I real appreciate.

Last, but not least, my deepest acknowledgement to all my friends, Angelina Lutambi, Asha Kalula, Sara Mkango, Rose Kibechu, Doreen Mbabazi, Joseph Ssebuliba, Amani Lusekelo, Maggie Goosen, Boitumelo Mogaleemang, Malebogo, Christina Meela and Fazia Du Plessis thanks for their help on reading and comments.

Glossary

Abbreviation	Meaning
RBCs	Red Blood Cells
LVCs	Liver Cells
MGCs	Midgut Cells
CD in CD4	Cluster of Differentiation 4
CD in CD8	Cluster of Differentiation 8
HIV	Human immunodeficiency virus
AIDS	Acquired Immunodeficiency Syndrome
ODE	Ordinary Differential Equation
T in T-cell	Thymus
ACT	Artemisin-based Combination Therapy
WHO	World Health Organization
DDT	Dichloro-Diphenyl-Trichloroethane
UNICEF	United Nations Children's Fund
SIV	Simian Immunodeficiency Virus
CDC	Centers for Disease Control & Prevention

Contents

List of Figures

List of Tables

Chapter 1

Introduction

1.1 Background

Malaria is a mosquito borne infectious disease caused by protozoan of genus plasmodium [73]. The four species that can infect humans are; Plasmodium falciparum, which causes severe disease and possibly death [41, 92] if not diagnosed and treated promptly, the other three plasmodium vivax, plasmodium ovale and plasmodium malariae generally cause milder disease that is rarely fatal. [50]. The parasite was discovered in 1880 by Charles Laveran [45], who was working in the military hospital in Constantine, Algeria. He observed the parasites in a blood smear taken from a patient who had just died of malaria. But Laveran linked the cause of malaria with the monkeys [8]. In 1902 Sir Ronald Ross discovered the malaria parasite in the gastrointestinal tract of the anopheles mosquito. This led to the realization that malaria was transmitted by the Anopheles mosquito [98]. This study [98] laid the foundation for combating the disease such as the use of the pesticide Dichloro-Diphenyl -Trichloroethane (DDT) for the control of mosquitoes during world war II [63] and the treatment drug chloroquine in 1950.

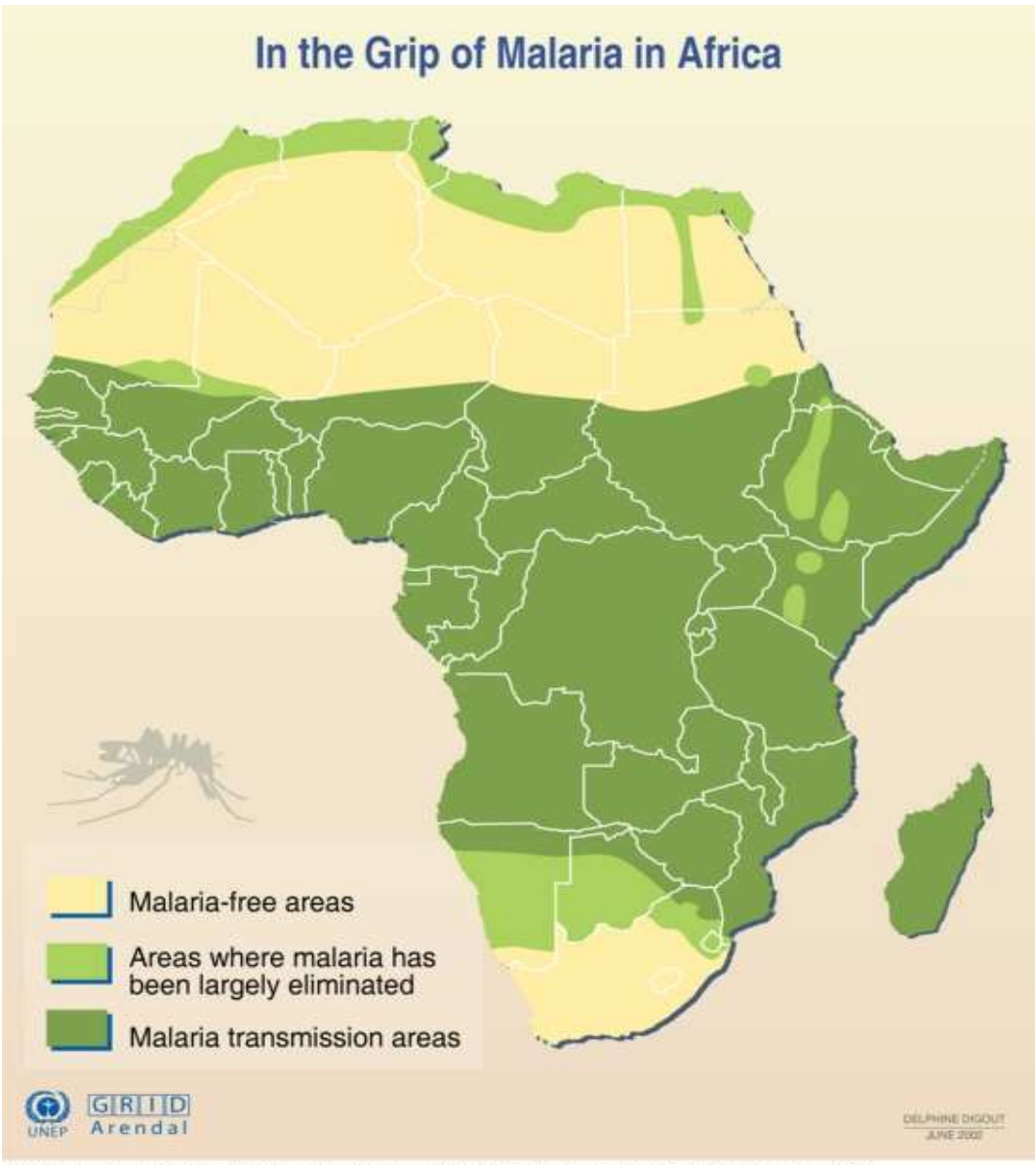

FIG. 1.1. A diagram showing malaria endemic area in Africa.

Malaria remains a burden in terms of morbidity and mortality for developing countries (FIG. 1.1) with tropical and subtropical climates. Malaria is prevalent in these regions because of heavy rainfall, warm consistent temperatures and high humidity conditions that are conducive to the development of the larvae. Temperature determines vector survival, incubation period and transmission while heavy rainfall causes the stagnant waters in which their larvae mature and provide mosquito with the environment needed for continuous

breeding [23, 77].

It is estimated that half of the world's population, over 3.3 billion lives in malaria endemic areas. There are about 300 to 500 million cases of clinical malaria reported [24, 67, 80, 96], resulting in 1.5 to 2.7 million deaths annually. sub-Sahara Africa is the region with the highest infection rate [96]. In this region alone, the disease kills at least one million people each year and is responsible for as many as half of the deaths in African children under the age of 5 [96], and accounts for 20% of all childhood deaths globally. Malaria decreases the gross domestic product by as much as 1.3% in countries with high disease rate [70, 96]. This contributes to poverty and underdevelopment in most sub-Sahara countries.

The Malaria parasites are introduced into the human blood stream after a bite by a female anopheles mosquito. Parasites in the form of sporozoites, enter the liver where they divide several times before maturing into schizonts which rupture and release merozoites which completing the initial parasite replication in the liver (exo-erythrocytic schizogony). During this initial stage, two species, namely, plasmodium vivax and plasmodium ovale can remain dormant (hypnozoites) in the liver and cause replace by invading the blood stream weeks, or even years later. After this initial replication in the liver, the merozoites enter the blood stage where they undergo asexual multiplication in the erythrocytes (erythrocytic schizogony). Mature merozoites in the blood stream are capable of invading the red blood cell. At this point the symptoms of disease will start to manifest, in the form of fever, headache, vomiting, chills, weakness and sweating. These symptoms are intermittent depending on the immunity of the host. Some merozoites differentiate and develop into sexual forms of the parasite, called male and female gametocytes, that circulate in the bloodstream [2, 11, 41, 45, 101].

When a mosquito bites an infected human, it ingests the gametocytes which initiate parasite multiplication replication in the mosquito known as the sporogonic cycle. In the mosquito's stomach, male and female gametes fuse to form diploid zygotes which develop into ookinetes that invade the mosquito midgut wall and form oocysts. The oocysts grow, rupture, and release thousands of sporozoites. Sporozoites invade the mosquito salivary glands from where they can be injected into human hosts to continue the infection process when the mosquito takes a blood meal [45, 50]. Malaria can be prevented [41, 46, 92] mainly through awareness of risk; People at risk include those who have no or those with

low immunity to malaria like young children, pregnant woman and visitors that travel to tropical areas from malaria free areas. Malaria can be prevented by preventing bites from infected mosquitoes. This can be achieved by wearing long clothes that cover as much of the skin as possible, treating exposed parts of the body with insect repellent, using insecticide-impregnated bed nets while sleeping and spraying indoors with insecticide around sleeping areas. People visiting malaria endemic areas are advised to take anti-malarial drugs before entering these area. It is advisable for all residents of malaria endemic areas to be diagnosed for malaria routinely and be treated if they test positive.

Despite the intense research and number of clinical trial, currently there is no effective vaccine [23, 64] and there has been very little success in producing such vaccines [64].

Accurate diagnosis of malaria is an integral part of treatment of malaria patients and prevention of further spread of malaria in the community. Treating malaria depends on many factors including disease severity, the species of malaria parasite causing the infection and the part of the world in which the infection was acquired. The use of a simple, inexpensive and rapid diagnosis tests for malaria may be of increasing importance as countries in Africa shift from low-cost anti-malarial to more expensive drugs Artemisin-based Combination Therapy (ACT). ACT is the most effective strategy for plasmodium falciparum infection recommended by WHO in the face of wide spread drug resistance [63, 96].

Parasites have become resistance due to usual anti-malarial drug like chloroquine which was the drug of choice to treat malaria for decades following World War II; it was stopped after parasites became resistant to it. Also the mosquito has became resistant to most insecticide [6, 54], DDT which was a very effective vector control pesticide was stopped because the mosquito became resistant to it [63]. Malaria can be managed with proper diagnosis and prompt treatment. Early diagnosis and prompt treatment are the principle technical components of the global strategy to control malaria and is highly dependent on the efficacy, safety, availability, affordability and acceptability of anti-malarial drugs [91]. An effective anti-malarial drug not only reduces mortality and morbidity of malaria but also reduces the risk of drug resistance. Due to drug resistance of parasites towards, available anti-malarial drugs for various regions are given below;

TABLE. 1.1. The table that shows the drug resistance for anti-malarial drug

Anti-malarial drug	Places that shows drug resistance
Chloroquine	Plasmodium falciparum species all areas of the world except the following: North Africa; the Middle East (though cases have been reported in Oman, Yemenand Iran);Haiti; Dominican Republic; rural areas of Mexico; and Central America,north and west of the Panama canal [86].
Fansidar	South East Asia;the Indian sub-continent; the Amazon basin; many countries in Africa south of the Sahara; and Oceania [90].
Mefloquine	South East Asia especially in Thailand; parts of Africa and South America; the Middle East; and Oceania [90].
Quinine	South East Asia;parts of Africa; Brazil; and Oceania [90].
Halofantrine	Thailand and shows cross resistance with mefloquine, fansidar and sulfadoxine-pyrimethamine [90].

1.2 Statement of the problem

In-host mathematical models are important and necessary to enhance our understanding of the dynamics of the Malaria parasites [58]. Such models can also be used to give an insight into the effectiveness of treatment drug and other intervention strategies. In this study, we investigate the dynamics of the malaria parasite during the red blood cycle, then extend the model to look at all the stages of the malaria life cycle, namely; liver stage, red blood cell stage and mosquito stage. These models, which also include the effector cells will be used to address the following questions:

(i) What replicative characteristics offer the parasite opportunities to evade the host immune system?

(ii) Can we find the critical effector cell killing rates which must be maintained (or exceeded) to ensure that the parasite does not establish itself within the host?

(iii) What are the effect of therapy on the prognosis of the malaria disease?

(iv) What are these models' contribution to the public health?

1.3 Objectives of the study

Malaria remains one of the world's worst problem. It is shown that more people are clinically ill with malaria than any other disease [96]. According to WHO estimates, in 2008 alone, there occurred $190 - 311$ million clinical cases of malaria [11, 96]. Hopes that malaria might be eradicated have proved impossible to realize. In many tropical areas, the threat of epidemic malaria is increasing and the control measures are becoming less effective. For this malaria associated burden to be reduced, we conduct a study whose objectives are summarized as follows;

- To understand biological processes that enable the parasites to evade the immune response.
- To gaining insights into the dynamics between the malaria parasites and the immune system
- To investigate the effect of anti-malarial therapy on the prognosis of the disease.
- To contribution policy recommendations on management of malaria.

1.4 Organization of the work

This work is organized as follows: Chapter 2 reviews various studies about malaria. Chapter 3 provides mathematical and numerical tools necessary for this study. Chapter 4 presents the model with the following classes; susceptible RBCs, latent RBCs, active infected RBCs, intracellular parasites, extracellular parasites and effector cells. Also presents the effects of treatment. The model is analysed mathematically and numerically, and the results are discussed. Chapter 5 presents the treatment model with three stages of the malaria life cycle, namely; (i) the liver stage which comprises of; susceptible liver cells

(LVCs), infected liver cells (LVCs), sporozoites and schizonts inside the liver cells (LVCs), (ii) the blood stage which consist of; susceptible red blood cells (RBCs), infected RBCs, merozoites, trophozoites, and schizonts inside the red blood cells (RBCs), (iii) the mosquito stage which has; susceptible midgut cells (MGCs), infected midgut cells (MGCs), gametocytes. The model also has an effector cell class. The mathematical and numerical simulations are done, the results are also discussed. Chapter 6 concludes what has been discussed in the results and suggests limitations, recommendations, and possibilities of future work. This is followed by the appendix.

Chapter 2

Literature review

It is over one hundred years since malaria was recognized as a disease in humans. Initially, malaria was known as mal′aria implying that the disease was caused by bad or spoiled air. The fever clinical symptoms were related to swaps and low lying water. In 1880, Laveran discovered parasites inside red blood cells of a sick person and mistakenly related the disease to monkeys following his earlier study which identified the same parasites inside a monkey's red blood cells [8].

The study by Ross (see [8] and the references therein) on malaria has become the basis of epidemiological studies of malaria including vector spread, treatment etc. and these have led to immunological studies of the disease [8, 41]. To demonstrate the seriousness of the malaria epidermic, we have analysed available records for the trend. Records regarding malaria clinical cases and mortality before the year 1950 are not available. The treatment drug chloroquine was discovered in 1950 and at almost the same time the pesticide DDT was discovered. From available records depicted by FIG. 2.1, it is evident that malaria clinical cases were in decline between 1950 and 1975 due to effective vector control programs and the effectiveness of the treatment drug chloroquine [66, 76]. Over a long period of administration of chloroquine, the parasites developed resistance to the drug [6, 54] and currently, chloroquine is not recommended for treatment of malaria in sub-Sahara Africa [66]. The trend for malaria clinical cases has been on the increase since 1975 (FIG. 2.1).

There appears to be a link between malaria and HIV/AIDS (FIG. 2.1). During the late 1980's, HIV/AIDS became an epidemic in most sub-Sahara Africa. Coincidentally, when

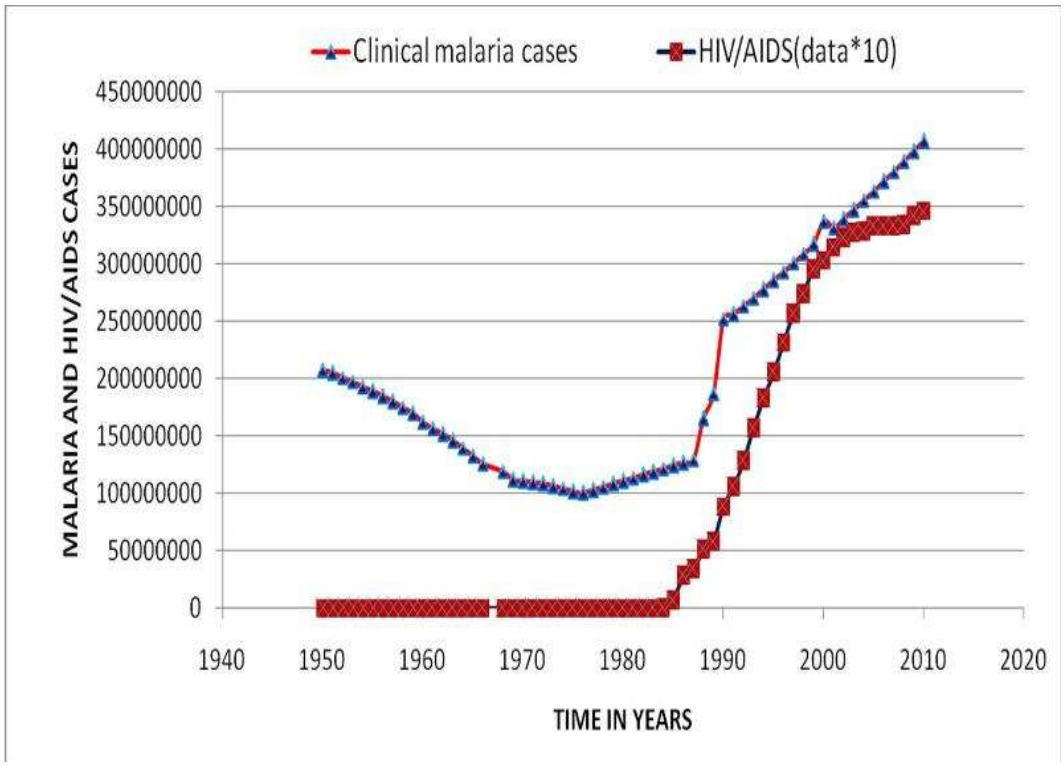

FIG. 2.1. A diagram showing amplified relationship between HIV and malaria

HIV/AIDS exploded malaria clinical cases also started to increase rapidly.

We want to exercise caution about the link mentioned above and to note that the rapid increase in malaria clinical cases during the late 1980's could also be related to other factors such as the collapse of the vector control programs following the deterioration in most economies in sub-Sahara Africa, but it may also be due to weakened immune responses in patients co-infected with HIV and malaria.

There are four species of plasmodium that are known to infect humans namely, Plasmodium falciparum, Plasmodium malariae, Plasmodium vivax, and Plasmodium ovale. The distribution of the various malaria parasites are indicated in the [TABLE 2.1]. Plasmodium falciparum, which causes more deaths in humans, is found mainly in tropical and subtropical areas of the world which include sub-Sahara Africa and most of the poor regions of Asia. These parasites develop through a cycle depicted in (FIG.2.2) and discussed in detail in [26, 50]. Clearly from this figure, the malaria life cycle is very complex and involves stages within the mosquito and the human host. If malaria is to be controlled and/or

TABLE. 2.1. The table shows plasmodium species and characteristics.

Species	Global distribution	Recur	Type of RBCs	Infection
P. falciparum	Tropical and sub-tropical worldwide	Recrudescence	All	Severe anaemia
P. malariae	Worldwide	Recrudescence	Older RBCs	Milder disease
P. ovale	Africa	Relapse	Young RBCs	Normal infection
P. vivax	Asia, Latin America some part of Africa	Relapse	Young RBCs	Normal infection

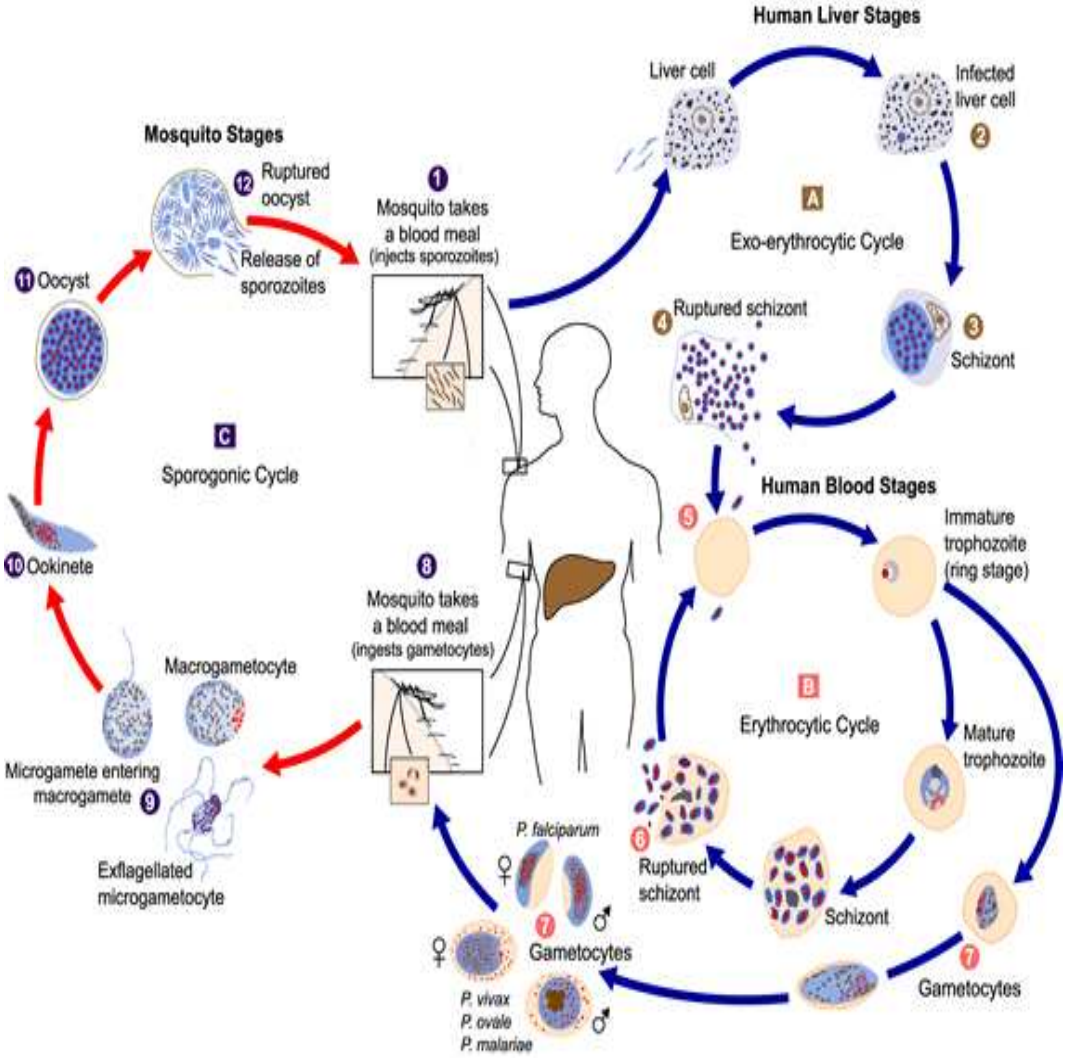

FIG. 2.2. Malaria life cycles, copied from *Parasite image library* [10]

.

eradicated, it is important to understand the factors that influence malaria pathogenesis [1, 31]. It is evident from (FIG.2.2) that the important questions for the mathematical study of malaria are both epidemiological and immunological and span several levels of biological organization.

Knowing the factors involved in pathogenesis, however, is only the first step towards quantifying how each factor influences the result [51]. As a sequel to the study by Anderson *et al.* [1], several studies Hetzel and Anderson [31], Antia *et al.* [2], etc., have studied the within-host cellular dynamics of blood stage malaria. Hetzel and Anderson [31] investigated the properties of a mathematical model of blood stage infection of malaria. The analysis [31], done in the absence of the host immune response to demonstrate the relationship between host and parasites parameters, led to the determination of parameters necessary for the successful invasion and persistence of the parasites. The parameters in Hetzel and Anderson [31] are used in this study as a first approximation in our model to understand the role of treatment and innate immune response to malaria pathogenesis.

A more recent study by Antia *et al.* [2] has considered acute malaria infections with a view to determine the dynamics of parasite and anaemia during acute primary malaria infections and why some strains of malaria reach higher densities and cause greater anaemia than others. While most studies agree that specific immunity does not play a major role in the initial dynamics of pathogenesis, there is considerable controversy over which factors drive the dynamics shortly after infection [1, 30, 31, 55].

Despite these numerous studies on malaria pathogenesis, the relative significance of different factors influencing malaria pathogenesis cited in [1, 2, 31], the development of the disease is far from clear [60]. So far, many studies focus on the innate immune response [31, 34] to understand the RBC-parasites interaction and a few on adaptive immune response. However the fact that researchers have successfully categorized the immune responses does not imply understanding of these processes. For example, Stevenson and Riley [82] have discussed how several adaptive immune response components like macrophages and natural killer cells are involved in the innate immune response and concluded that the interaction of those cells remains speculative and conflicting experimental data has opened a way for mathematical models of pathogenesis to be used as tools to achieve deeper understanding of this process [31].

Several studies on the innate immune response to malaria infection have been formulated [13, 65, 84, 89]. A study by Su *et. al* [84] on the synchronization of parasite replication in different red blood cells, considers an age-structural human malaria infection of red blood cells. The numerical simulation results in this study show that synchronization with regular periodic oscillation occurs when the replication rates increase. A more recent study by Niger and Gumel [65] has investigated the innate immune response to malaria infection and the effect of imperfect vaccines. The simulation results [65] show that a vaccine efficacy of at least 87% is necessary to eliminate Infected Red Blood Cells (IRBCs)in vivo.

The study by McQueen and McKenzie [55] considers the susceptibility of red blood cells and the dynamics of malaria infection. The authors [55] assume a predator-prey type relationship between a population of replicating parasites and a replenishing population of red blood cells. The study explores the hypothesis that some malaria-parasite species that infect humans such as Plasmodium malariae and Plasmodium vivax have preference for particular age classes of red blood cells. Our study considers the infection of red blood cells by Plasmodium falciparum which has different infection characteristics [34, 55]. We want to investigate whether Plasmodium falciparum too has a tendency for age selection like the other malaria species, noting that the difference in infection characteristics between Plasmodium falciparum and the species considered by McQueen and McKenzie [55] occurs primarily in the range of parameters used [34].

A review by Engwerda and Good [23] considered the interaction between malaria parasites and the host immune system and revealed the potential for designing and implementing new vaccine and drug programs through understanding of cell-immune, cell-parasite interaction. This study [23] included the adaptive response which is not part of this study but provides insight into the cell-parasite dynamics which has guided our study.

A review by Mideo *et al.* [58] recommended the use of mathematical models as a tool for refining knowledge of within-host processes and has suggested why under certain circumstances mathematical models may be better than experimentation. Generally, however, Mideo *et al.* [58] recommends the use of both approaches since together these approaches possess the potential for informing the design of intervention and health policy for addressing lingering questions about the basic biology of malaria which should guide the model formulation. The malaria parasite replication is a very complex process and involves three

stages as shown in (FIG. 2.2). This complicated replication cycle has implications regarding eradication of malaria which is too expensive and probably unrealistic for poor resource sub-Sahara African countries. A treatment or vaccination strategy suggested by mathematical models may contribute to cutting cost of intervention programs.

This study will attempt to quantitatively predict the pattern of pathogenesis as a function some underlying within-host regulatory facts. However, as the biology of malaria pathogenesis is very complex and involves many factors, this study will include only those biological process that we believe can plausibly explain the dynamic of malaria pathogenesis.

McKenzie and Bossert [34, 53, 55] modelled malaria pathogenesis using a system of coupled differential equations involving only uninfected RBCs, infected RBCs and merozoites. These studies omitted the detailed biology such as how the merozoites are replicated asexually and concentrated on the basic infection dynamics that lead to clinical malaria. The aim in those studies was to understand pathogenesis and not how the immune system responds to infection. However, the study by Hoshen *et al.* [34] gives useful insights and conclusions that have guided our study. The question one ask is whether a simplified model such as Hoshen *et al.* [34] can yield reliable information to guide planning and policy. Furthermore, one wonders whether these simple models can reliably estimate the severity of the disease?

Some larger models [61] have included more biological process such as innate and adaptive immune responses. However, such studies have lacked clinically determined parameter values to calibrate and validate their models. The objective behind such large models is to determine parasite replication mechanisms but in the absence of biologically determined laws it has proved difficult to justify results from such models. It is known that when merozoites infect red blood cells, to initiate the asexual replication of the merozoite population [55, 61], not all infected red blood cells contribute to the population of merozoites since some of them are apoptosed by the natural killer cells. Adjustment to reflect this fact has been done in an ad hoc manner [40]. The differences in accounting for the replication laws for malaria, TB and HIV [25, 55] are indicative of the absence of clear biological understanding of the processes. Some authors have assumed very simple laws [34, 55] to keep the models parsimonious. The lack of biological facts on this subject has affected our

definition of the parasite replication law which we admit has no biological basis.

These complex mathematical models on malaria pathogenesis have considered the development of cerebral malaria in children and adult travelers living in non endemic malaria areas and have concluded that severe malaria is an immune-mediated disease [4]. This study [4] considered the role of innate and adaptive immune responses in terms of (i) protection from clinical malaria and (ii) their potential role in immunopathology and the subsequence development of clinical immunity. Another study [3] has determined the potential contribution of innate immune responses to the early pro-inflammatory cytokine response to Plasmodium falciparum malaria. The study examined the kinetics and cellular sources of interferon-gamma production in response to infection of red blood cells. The study concludes that early interferon-gamma response could reduce red blood cells infection.

There is considerable controversy over which factors drive the malaria pathogenesis shortly after infection [1, 30, 31, 55]. Some of the assumptions made to explain the differences in the initial dynamics of malaria strains include virulence evolution [2, 14, 27, 49], (ii) red blood cell age specific infection strategy [55] and (iii) innate or early specific immune responses to regulate the initial dynamics of infection and anaemia [21, 29]. Antia *et al.* [2], however, have given two reasons why it is difficult to ascertain the contribution of these factors to the dynamics of acute infection namely (i) limited data on the dynamics of the parasite and loss of RBCs following infection of humans with human malaria parasites and (ii) the dynamics of the infection could involve many interacting populations.

Several studies have investigated the potential for a vaccine as the best strategy to combat malaria targeting the liver stage for a vaccine [23, 33, 59]. According to [23], this stage poses many obstacles to anti-infection vaccines and drugs. These include: (i) the liver stage malaria parasites have distinct metabolism which helps them to evade anti-malarial drugs (ii) Plasmodium malaria parasites can lie dormant in the liver and relapse to blood infection after months or even years. According to Morrow and Moss [63], liver stage parasites cannot be targeted by any licensed drug except primaquine which is fatal to pregnant women and diabetic individuals.

Our hypothesis in this study follows from the observation made by McQueen and McKenzie [55]. We ask the question whether Plasmodium falciparum targets older red blood cells as a strategy for accelerating parasite replication. Although we have not developed an age-

structured model, we have manipulated the natural death term in the infected red blood cell population to achieve our goal. It is suggested in [39, 104] that CD8 cells may not function optimally in individuals suffering from chronic illnesses, we have investigate this scenario and accordingly have made a recommendation regarding the treatment of malaria for individuals suffering from chronic infections.

Despite a large area in research on malaria pathogenesis (within-host mechanisms through which plasmodium parasite causes disease) [5, 23, 55, 58] many questions remain unanswered. Issues in pathogenesis need to be explored to develop better treatment [58, 60]. It is known that most of the drugs act best against replicating pathogens in combination with effective immunological responses [5]. There is a need also to better understand effector cell mechanism in the development of immunity to malaria [1].

Chapter 3

Mathematical tools

3.1 The definition and computation of R_0

Definition 3.1.1 *The basic reproduction number (R_0), sometimes called the basic reproductive rate or the basic reproductive ratio of an infection is the average number of secondary cases caused by an infected individual introduced in a completely susceptible population [20].*

For the case of a single infected compartment, R_0 is simply the product of the infection rate and the mean duration of the infection [93]. But for models with several infected compartments, this definition is not sufficient. That is a more sophisticated technique is required as reviewed below. In this thesis, we only give a brief overview of the calculation of the basic reproduction number R_0, using the next generation method discussed by Diekmann [20] and van den Driessche *et. al* [93]. Let $x = (x_1, \ldots, x_n)^t$ with $x_i \geq 0$, be the number of individuals in each compartment $(i = 1, \ldots, n)$. We sort the compartments so that the first m compartments correspond to infected individuals and then, define the parasite free equilibria as $x_0 = \{x \geq 0 \mid x_i = 0, i = 1, \ldots, m\}$.

For the computation of R_0, it is important to distinguish new infections from all other changes in the population. As illustrated in figure (3.1), we let: $\mathcal{F}_i(x)$ be the rate of appearance of new infections in compartment i, $\mathcal{V}_i^+$ be the rate of transfer of individuals into compartment i and $\mathcal{V}_i^-(x)$ be the rate of transfer of individuals out of compartment i.

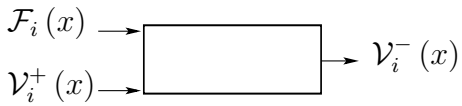

FIG. 3.1. Representation of $\mathcal{F}$ and $\mathcal{V}$

$\mathcal{F}_i(x), \mathcal{V}_i^+(x)$, and $\mathcal{V}_i^-(x)$ are differentiable continuous functions. In general, we can express a system of differential equations of the form $\dot{x} = f_i(x)$ in the form that accounts for inflow and outflow (3.1) as:

$$\dot{x}(t) = \mathcal{F}_i(x) - \mathcal{V}_i(x), \quad \text{and} \mathcal{V}_i(x) = \mathcal{V}_i^-(x) - \mathcal{V}_i^+(x), \quad \text{for } i = 1, ..., n.$$

Let the functions $\mathcal{F}_i(x), \mathcal{V}_i^+(x)$, and $\mathcal{V}_i^-(x)$ satisfy the following conditions.

(A1) : If $x \geq 0$, then $\mathcal{F}_i, \mathcal{V}_i^+, \mathcal{V}_i^- \geq 0$.

(A2) : If $x_i = 0$, then $\mathcal{V}_i^- = 0$. In particular, if $x \in x_0$, then $\mathcal{V}_i^- = 0$, for $i = 1, ..., m$.

(A3) : If $i > m, \mathcal{F}_i = 0$.

(A4) : If $x \in x_0$, then $\mathcal{F}_i(x) = 0$, and $\mathcal{V}_i^+(x) = 0$.

(A5) : If $f(x) = 0$, then the eigenvalues of $Df(x_0)$ have negative real parts and x_0 is the parasite free equilibrium.

The conditions listed above allow us to partition the matrix $\mathcal{D}\mathcal{F}(x)$ as shown in Remark 1.

Remark 1 *$\mathcal{D}\mathcal{F}(x_0)$ is the derivative $\left[\frac{\partial f_i}{\partial x_j}\right]$ evaluated at DFE. The conditions $(A_1 - A_5)$ allow us to partition the matrix $\mathcal{D}\mathcal{F}(x_0)$ and $\mathcal{D}\mathcal{V}(x_0)$ as;*

$$\mathcal{D}\mathcal{F}(x_0) = \begin{pmatrix} \mathcal{F} & 0 \\ 0 & 0 \end{pmatrix} \quad \text{and} \quad \mathcal{D}\mathcal{V}(x_0) = \begin{pmatrix} \mathcal{V} & 0 \\ J_3 & J_4 \end{pmatrix},$$

where $\mathcal{F}$ and $\mathcal{V}$ are $m \times m$ matrices defined as $\mathcal{F} = \left[\frac{\partial \mathcal{F}_i}{\partial x_j}(x_0)\right]$, and $\mathcal{V} = \left[\frac{\partial \mathcal{V}_i}{\partial x_j}(x_0)\right]$. Since $\mathcal{F}$ is non-negative, $\mathcal{V}$ is a non-singular matrix and all eigenvalues of J_4 have positive real parts.

If $f(x)$ satisfies $(A_1 - A_5)$, then the reproductive ratio is defined as $R_0 = \eta\left(\mathcal{F}\mathcal{V}^{-1}\right)$, where η is the spectral radius [93].

When $R_0 < 1$, the infection dies out, except for a model which exhibits a backward bifurcation. For $R_0 > 1$, the infection spreads in a population. Thus R_0 is a threshold parameter such that when $R_0 < 1$, the population remains healthy because the disease fails to establish itself. The stability of the disease free equilibrium point (maintaining the conditions for absence of disease in a population) is discussed by Diekmann ([20]), and van den Driessche [93]. The stability of parasite free equilibrium point is stated in theorem 3.1.2.

Theorem 3.1.2 *The parasite free equilibrium point is locally asymptotically stable for* $R_0 < 1$ *and unstable for* $R_0 > 1$.

The proof of this theorem is given in several studies [16, 43, 44].

3.2 The Routh-Hurwitz criterion

Let

$$a_n S^n + a_{n-1} S^{n-1} + \cdots + a_1 S^0 + a_0 = 0, \tag{3.1}$$

be a characteristic equation of a given Jacobian matrix. The Routh-Hurwitz table [36, 62] for the characteristic equation (3.1) of degree n can be determined as illustrated in TABLE 3.1.

TABLE. 3.1. The Routh-Hurwitz table showing the characteristic equation

S^n	a_n	a_{n-2}	a_{n-4}	a_{n-6}
S^{n-1}	a_{n-1}	a_{n-3}	a_{n-5}	a_{n-7}
S^{n-2}	$b_1 = \dfrac{a_{n-1}a_{n-2} - a_n a_{n-3}}{a_{n-1}}$	$b_2 = \dfrac{a_{n-1}a_{n-4} - a_n a_{n-5}}{a_{n-1}}$	$b_3 = \dfrac{a_{n-1}a_{n-6} - a_n a_{n-7}}{a_{n-1}}$	
S^{n-3}	$\dfrac{b_1 a_{n-3} - b_2 a_{n-1}}{b_1}$	$\dfrac{b_1 a_{n-5} - b_3 a_{n-1}}{b_1}$		
$\vdots$	$\vdots$	$\vdots$	$\vdots$	$\vdots$
S^0				

This table can be used as follows:

- If there are sign changes in the first column, then the eigenvalues have positive real parts.
- The number of sign changes in the first column is equal to the number of positive real roots of the characteristic equation.
- If there exists a mixture of positive and negative signs, then the given system is *unstable*.
- If there are no sign changes in the first column, then all eigenvalues are either positive or negative. If there are negative signs only, then the eigenvalues have negative real parts and the system is *stable*.

3.3 Sensitivity analysis

The parameter values and assumptions of any model are subject to changes and errors. Sensitivity analysis is a technique for establishing the significance of a parameter and how it impacts the dynamics of the model. An independent variable will impact a particular dependent variable if the variable is a differentiable function of that parameter [12, 74].

Sensitivity analysis is a very useful tool for characterizing the uncertainty associated with a parameter with regard to model conclusions. Its importance is part and parcel of good modelling practice and requires a modeller to provide an evaluation of confidence in the model results. Furthermore, it validates the relevance of the inputs by determining the output of the model [74, 99].

Uncertainty analysis may be used to asses the variability in the outcome variable that is due to the uncertainty in estimating the input values. Sensitivity analysis can extend uncertainty analysis by identifying important parameters that yield reliable predictions [7].

An alternative sensitivity analysis design, for a K parameter model, is to fix the values

of $K-1$ parameters and then vary only the value of the K^{th} parameter over a specified range. This sensitivity analysis design has the advantage that it is simple and quick, but suffers from major disadvantages. That is only one parameter may be varied at a time, only a small region of a $K-$dimension parameter space can be explored and values of $K-1$ parameters have to be estimated [7].

Latin Hypercube Sampling (LHS) is the type of stratified Monte Carlo sampling and may be viewed as an extension of the Latin Square sampling. In LHS, the uncertainty estimation for each input parameter is modelled by treating each input parameter as a random variable. It is an extremely efficient sampling design because is used only once in the analysis. An input vector is generated for each computer simulation of the deterministic model and the model is then run N times [7, 74].

A distribution function for each of the outcome variable can be directly derived because of the probability selection technique. LHS enables the results of a deterministic model to be interpreted within a statistical framework. The distribution may be characterized by simple descriptive statistics. Sensitivity analysis may be then be performed by calculating the partial rank correlation coefficients (PRCC) for each input parameter and each outcome variable [7, 75].

The LHS/PRCC technique involves seven steps [7]:

(a) Defining the probability distribution function for parameters and state variables. A mathematical model contains a certain number of parameters and state variables, the estimated values for all or only a subset of these will be uncertain.

(b) Calculating the number of simulations (N). The LHS design involves sampling without replacement. Therefore if only k draws are made (where k equals the number of uncertain variables), the k^{th} draw would be predetermined. Hence the lower limit to the value of N (where N equals the number of simulations) should be at least $(k+1)$.

(c) Dividing the range of each of the K parameters into N equal probable intervals. The range of each parameter is divided into N non-overlaping equiprobable intervals (where N is the number of simulations) and each interval is sequentially assigned a sampling index.

(d) Creating the LHS table. The LHS design involves random sampling without replacement and every equiprobable interval of each input variable is sampled once.

(e) Sampling the values of the input parameters and performing the N simulations. The LHS table is used to generate for example 100 by 30 input matrix.

(f) Analysing model outcomes of uncertainty analysis. The results of the simulation runs of the model consist of N observations of each outcome variable. Distribution functions of each outcome variable can be directly derived and characterized by simple descriptive statistics.

(g) Analysing the model outcome with respect to the N observations of each outcome variable which may be used to assess the sensitivity of the outcome variables and to estimate the uncertainty of the input parameters.

Chapter 4

A within host model of blood stage malaria

4.1 Introduction

Malaria parasites are transmitted from a mosquito to a human host. Upon entering the human host, extracellular malaria sporozoites must first take up residence in the liver before initiating red blood cell infection. In the liver, the sporozoites undergo spectacular phenotypic changes prior to multiplication [37, 69]. The sporozoites mature into schizonts which rapture and release merozoites [11], which are fully competent to infect red blood cells and instigate the pathology associated with malaria [83].

Several studies on the innate immune response to malaria infection have been formulated [13, 65, 84, 89]. A study by Su *et. al* [84] on the synchronization of parasite replication in different red blood cells, considers an age-structural human malaria infection of red blood cells. The numerical simulation results in that study showed that synchronization with regular periodic oscillation occurs when the replication rates increase. A more recent study by Niger and Gumel [65] has investigated the innate immune response to malaria infection and the effect of imperfect vaccines assuming a scenario of parasite life cycles. The simulation results [65] showed that a vaccine efficacy of at least 87% is necessary to eliminate Infected Red Blood Cells (IRBCs)in vivo.

As a sequel to these studies [5, 55, 65], we consider two stages of the parasite cycle namely (i)

stage 1: A short stage when merozoites are released from the liver to initiate the red blood cell infection. It is estimated that a primary infusion of 10^4 to 10^5 parasites are released into the blood [55]. (ii) stage 2: The red blood stage during which asexual multiplication of merozoites and infection of red blood cells by the merozoites occurs concurrently. Our model does not include the early stages of the exo-erythrocytic cycle which is known to be a reservoir for the erythrocytic stage [59]. Despite this, the results of this model can still contribute towards understanding the replicative dynamics of the parasite and hence the development of clinical malaria.

In-host mathematical models are important and necessary to enhance our understanding of the dynamics of Malaria pathogenesis [58]. Such models can also be used to give insight into the effectiveness of drug treatment and other intervention strategies [65]. In this Chapter, we investigate the dynamics of the malaria parasite during the red blood cycle. Our model includes the red blood cells, extracellular parasites, intracellular parasites and effector cells. This model differs from the models in the earlier studies [5, 34, 55, 65] in that we introduce a class of intracellular parasites in the pathogenesis process. We believe it is important to include this process in the dynamics so that intervention strategies can be targeted at different stages of the replication process as is the case in HIV/AIDS treatment [38]. Our study addresses the following questions: (i) what replicative characteristics offer the parasite opportunities to evade the host immune system? (ii) A significant number of individuals in sub-Sahara Africa are co-infected with viral (for example HIV, simian immunodeficiency virus (SIV)), bacterial and parasitic infections other than malaria [38, 42, 88, 104], it is important to investigate how such individuals respond to a malaria infection. Studies by Kalia et el [39] and Zhang et el [104] have shown that in hosts suffering from chronic infections, CD8 T-cell functions are compromised and are dysfunctional . To give insight into what happens when CD8 T-cell responses have been altered and impaired, we shall consider a hypothetical situation where a host is infected with the malaria parasite which would clear if CD8 T-cell responses were normal. We shall then alter the CD8 T-cell response parameters m and k_{tp} at time $t < t_c$, where, t_c is the time of clearance of the malaria infection, and investigate the prognosis of the malaria disease by finding the critical effector cell killing rate which must be maintained (or exceeded) to ensure that the parasite does not establish itself within the host?

Malaria can be managed with proper diagnosis and prompt treatment . Early diagnosis and

prompt treatment are the principle technical components of the global strategy to control malaria. This strategy is highly dependent on the drug efficacy. Effective anti-malarial drugs not only reduce mortality and morbidity of malaria but also reduce the risk of drug resistance of the parasites toward available anti-malarial drugs [90].

Our model includes the replication of the parasite within the infected red blood cells. While the process of entry into the red blood cells by the merozoites has been extensively studied, the replication process of the parasite within an infected red blood cell is not well understood. In this study, we have assumed a replication law for intracellular parasite similar to that of the tuberculosis bacteria in macrophages [25]. This assumption may not be an accurate representation of the malaria parasite replication law, however, we have utilized the available data [18] to ensure that parasite replication in a red blood cell produces between 8 to 32 merozoites. Using this information, we have determined the rate of bursting, k_b, for infected red blood cells taking the cell's carrying capacity to be 32. Furthermore, we have assumed that the release of the merozoites is through bursting of the infected red blood cell as is the case for bacteria in macrophages [25]. We have made this assumption because very little is known about the actual parasite release mechanism involved. We believe, however, that this study will stimulate experimental biologists into investigating the reproductive law for intracellular malaria parasites and the release mechanism of parasites from infected red blood cells.

We also extend the model to investigate the efficacy level required to clear the parasites. We introduce treatment with a drug of constant efficacy ϵ_1 targeting the infection terms [71].

4.2 Methodology

4.2.1 Model formulation

The system of equations describing the dynamics of in-host malaria is given below: The model represents the human blood stage of the malaria disease called the erythrocytic cycle.

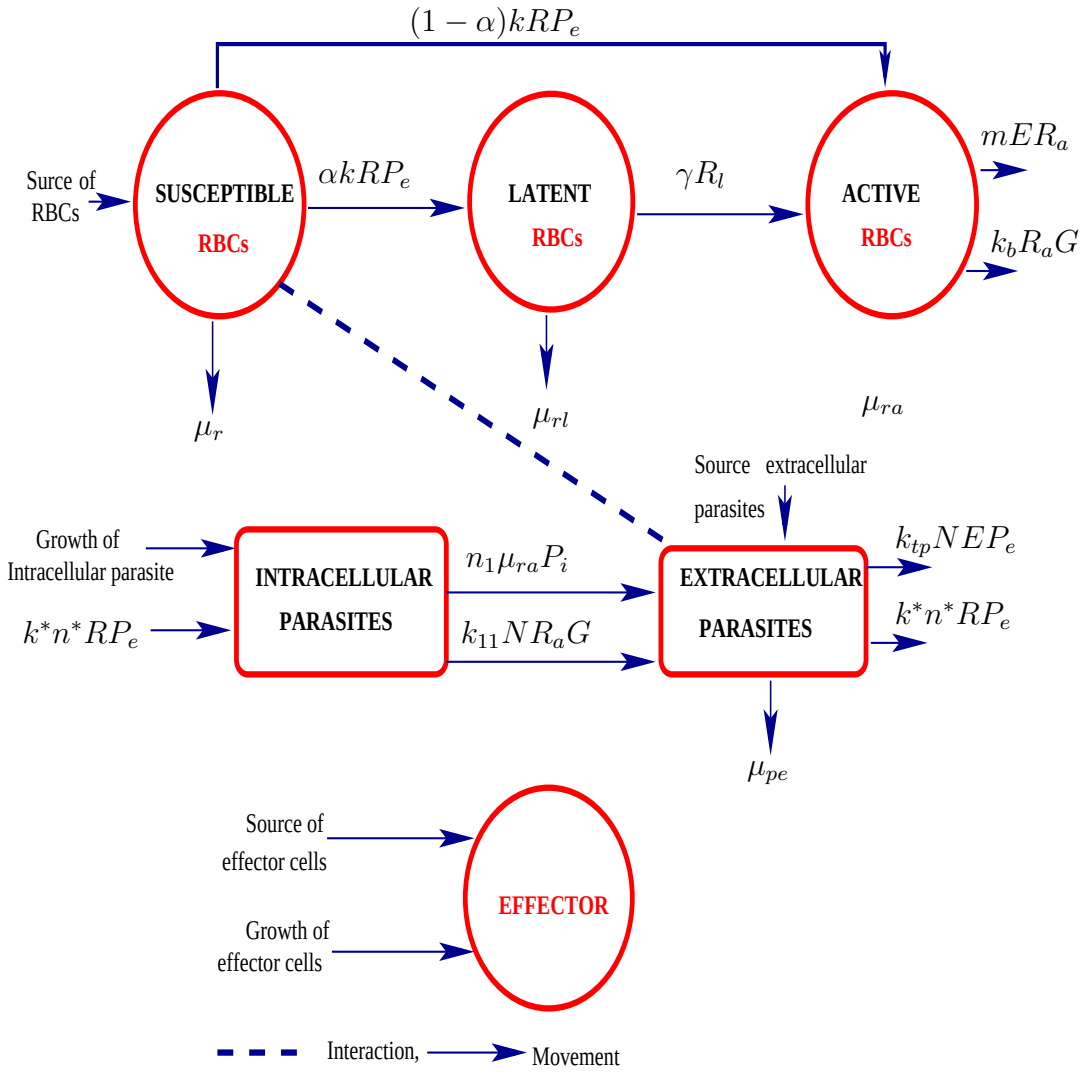

FIG. 4.1. A diagrammatic representation of within host malaria model.

TABLE. 4.1. The table with the variables, descriptions and units.

Variables	Descriptions	Units
R	Susceptible red blood cell	cell/ml
R_l	Latent red blood cell	cell/ml
R_a	Activated red blood cell	cell/ml
P_i	Intracellular parasites	cell/ml
P_e	Extracellular parasites	cell/ml
E	Effector cell	cell/ml

Red blood cells (RBCs)

$$\dot{R} = S_r - \mu_r R - kRP_e. \tag{4.1}$$

TABLE. 4.2. The table that shows parameters and their descriptions.

Parameter	Descriptions	Units
S_r	Constant sources of red blood cell	$cell/ml.day$
μ_r	Natural death rates of susceptible RBCs	day^{-1}
k	Infection rate	$ml/cell.day$
α	Proportion of RBCs	$dimensionless$
γ	Rate of activation	day^{-1}
μ_{rl}	Natural death rate of latent RBCs	day^{-1}
m	Rate of killing activated RBCs by effector cell	$ml/cell.day$
k_b	Rate of bursting	day^{-1}
μ_{ra}	Natural death rates of activated RBCs	day^{-1}
N	Number of parasites that fill the RBCs	$dimensionless$
k_{pi}	Rate of growth of intracellular parasites	day^{-1}
k_{11}	Rate of loss due to burst of activated cell	day^{-1}
n_1	A threshold number of intracellular parasites released as a results of the natural death of an activated RBC	$dimensionless$
k_{tp}	Rate of loss of extracellular parasites that are killed by effector cells	$ml/cell.day$
n^*k^*	Threshold number as a results of gain due to infection of susceptible RBC by extracellular parasites	$ml/cell.day$
μ_{pe}	Natural death rate of extracellular parasites	day^{-1}
ω_e	Growth rate of effector cells	day^{-1}
r_e	Carrying capacity of effector cell	$cell/ml$
S_{pe}	Source of extracellular parasites	$cell/ml.day$

During the human blood stage, the sporozoites injected into the human host by the female anopheles mosquito enter the blood stream and infect susceptible red blood cells (RBCs). The dynamics of the susceptible red blood cell (RBC) population are given in (4.1). The terms in this equation have the following meaning: The first term represents a constant natural source for the red blood cell population. The second term represents natural death of the susceptible red blood cells at a constant rate μ_r and the third term represents infection of RBCs by extracellular parasites (merozoites) at a constant rate k. The newly infected red blood cells may become latently infected with the malaria parasite, a state which inhibits parasite replication, or the RBCs may become actively infected, meaning that parasite replication persists in them. The rate of change for the latently infected red blood cell population, R_l, is given by equation (4.2)

$$\dot{R}_l = \alpha k R P_e - (\gamma + \mu_{rl}) R_l. \tag{4.2}$$

The terms in this equation have the following meaning: The first term represents a proportion of infected RBCs that have become latently infected, and the second term represents losses due to activation at a constant rate γ and due to natural death at a constant rate μ_{rl}. The actively infected red blood cell population evolves according to the following equation (4.3) below:

$$\dot{R}_a = (1-\alpha)kRP_e + \gamma R_l - mER_a - k_b R_a \left(\frac{P_i^2}{P_i^2 + (NR_a)^2}\right) - \mu_{ra}R_a. \qquad (4.3)$$

The first term in equation (4.3) represents the proportion of susceptible red blood cells that become actively infected, the second term represents gain due to activation of latently infected red blood cells, R_l, the third term represents the removal of activated infected RBCs due to killing by effector cells. When the merozoites infect red blood cells, they start to replicate within the infected red blood cells. This process can go on until the number of parasites within the infected red blood cell reaches 32 [55] causing it to burst. The fourth term measures an effective number of infected red blood cells that burst to release intracellular parasite. The bursting rate in this model is assumed to be dependent on the densities of intracellular parasites and infected red blood cells [25, 28]. This bursting law has been used for pathogens such as TB [25]. To the best of our knowledge this has not been used for malaria and is not supported by any literature. Not all infected red blood cells burst to release parasite. There is an effective number of infected red blood cells that burst to release parasite into the blood stream. The factor;

$$\frac{P_i^2}{P_i^2 + (NR_a)^2},$$

measures the proportion of infected red blood cells that burst to release parasite. **We have chosen this ratio so that the replication process has an upper bound. This law has revealed correct replicative dynamics for the TB bacteria [25] and is adopted in this study.** The fifth term accounts for natural death of infected red blood cells at a constant rate μ_{ra}.

Parasites

Intracellular parasites replicate inside an infected red blood cell. It is assumed in this study that the intracellular parasite population grows according to a law similar to the growth of

TB bacteria in macrophages [25]. In the absence of experimentally or clinically determined growth law for the intracellular malaria parasite, we assume a growth law of intracellular parasites inside an infected red blood cell of the form.

$$\begin{aligned}\dot{P}_i &= k_{pi}P_i\left(1-\frac{{P_i}^2}{{P_i}^2+(NR_a)^2}\right)+k^*n^*RP_e-k_{11}NR_a\left(\frac{{P_i}^2}{{P_i}^2+(NR_a)^2}\right)\\ &\quad -n_1\mu_{ra}P_i. \end{aligned} \tag{4.4}$$

In equation (4.4), the first term represents the growth of intracellular parasites. The second term represents gain of P_i due to infection of susceptible RBCs by extracellular parasites (merozoites), P_e, at a threshold n^*k^*, the third term represents an effective number of intracellular parasites lost due to bursting of activated RBCs and the forth term represents loss of intracellular parasites due to natural death of an infected red blood cell, R_a, where n_1 denotes a threshold number of intracellular parasites released. Upon bursting of an actively infected red blood cell, it releases the merozoites into the blood stream to continue the parasite cycle.

$$k_{pi}P_i\left(1-\frac{P_i^2}{P_i^2+(NR_a)^2}\right) = k_{pi}P_i\left(\frac{(NR_a)^2}{P_i^2+(NR_a)^2}\right).$$

This term has the following characteristics;

$$\lim_{R_a\to 0} k_{pi}P_i\left(\frac{(NR_a)^2}{P_i^2+(NR_a)^2}\right) = 0.$$

There is no growth of intracellular parasites.

$$\lim_{R_a\to\infty} k_{pi}P_i\left(\frac{1}{\left(\frac{P_i}{NR_a}\right)^2+1}\right) = k_{pi}P_i.$$

In this case the intracellular increases exponentially. As $P_i\to\infty$ the number of bursting infected red blood cells decreases and **the loss of infected red blood cells may be exponential.** The author is not aware of the replication law for malaria parasite hence, the replication law chosen here is similar to that for infection of macrophages by TB bacteria [25]. This is at best an approximation which needs further investigation. The fifth term represents loss due to natural death at a constant rate μ_{ra}.

Upon bursting of the actively infected red blood cells, the merozoites are released into the

blood stream to continue the parasite cycle. The rate of change of the merozoite population is described by equation by (4.5):

$$\begin{aligned}\dot{P}_e &= S_{pe}P_e + k_{11}NR_a\left(\frac{P_i^2}{P_i^2+(NR_a)^2}\right) + n_1\mu_{ra}P_i - k_{tp}NEP_e \\ &\quad -k^*n^*RP_e - \mu_{pe}P_e. \end{aligned} \tag{4.5}$$

The first term in (4.5) represents the amount of extracellular parasites present in the blood stream, the second and third terms in (4.5) represent gains of extracellular parasite population due to bursting of activated RBCs and natural death of activated infected red blood cells, P_i, the forth term is the loss due to killing of extracellular parasites by effector cells, the fifth term is loss due to infection of susceptible RBCs by merozoites and the sixth term is the natural death of merozoites at a constant rate μ_{pe}.

Effector cells

Effector cells are fully differentiated structural lymphocyte cells that are specialized in initiating and effecting an immune response. This population includes CD4+ T-cells, and CD8+ T-cells and is assumed to grow logistically [9] as shown in equation (4.6)

$$\dot{E} = \omega_e\left(1-\frac{E}{r_e}\right)E, \tag{4.6}$$

where ω_e denotes the constant growth rate of this population and r_e is the carrying capacity of the effector cells per millilitre of blood. We have simplified the dynamics of this population but we believe we have captured the biological role of these cells.

Positivity of the solutions

Lemma 1 *Let $R(0) \geq 0$, $R_l(0) \geq 0$, $R_a(0) \geq 0$ $P_i(0) \geq 0$, $P_e(0) \geq 0$ and $E(0) \geq 0$. Then, the solution $(R(t), R_l(t), R_a(t), P_i(t), P_e(t), E(t))$ are all non negative for all time $t > 0$ in the region*

$$\Gamma_6 = (R, R_l, R_a, P_i, P_e, E)\epsilon\ \mathbb{R}^6_+. \tag{4.7}$$

Proof 1 *Consider the susceptible RBCs dynamics given by equation (4.1):*

$$\frac{dR}{dt} = S_r - \mu_r R - kRP_e.$$

Multiplying equation (4.1) by the integration factor $e^{\left(k\int_0^t P_e(s)\mathrm{d}s+\mu_r t\right)}$, *and rearranging, we obtain*

$$\begin{aligned}
\frac{d}{dt}\left(R(t)e^{\left(k\int_0^t P_e(s)\mathrm{d}s+\mu_r t\right)}\right) &= S_r e^{\left(k\int_0^t P_e(s)\mathrm{d}s+\mu_r t\right)},\\
R(t_1) &= \underbrace{e^{\left(-k\int_0^{t_1} P_e(s)\mathrm{d}s-\mu_r t\right)}}_{\geq 0}\left(\underbrace{R(0)}_{\geq 0}+\underbrace{S_r\times\int_0^{t_1} e^{\left(k\int_0^t P_e(s)\mathrm{d}s+\mu_r t\right)}\mathrm{d}s}_{\geq 0}\right)\\
&\geq 0, \qquad As\ t\longrightarrow\infty
\end{aligned}$$

Now, consider the dynamics of the latently infected RBCs;

$$\frac{dR_l}{dt} = \alpha k R P_e-(\gamma+\mu_{rl})R_l.$$

Multiplying equation (4.2)the integrating factor $e^{(\gamma+\mu_{rl})t}$, *we obtain;*

$$\begin{aligned}
\frac{d}{dt}\left(R_l\left(e^{(\gamma+\mu_{rl})t}\right)\right) &= \alpha k R(t)P_e(t)e^{(\gamma+\mu_{rl})t},\\
R_l(t_1) &= e^{(-(\gamma+\mu_{rl})t_1)}\left(R_l(0)+\alpha k\int_0^{t_1} R_l(s)P_e(s)e^{(\gamma+\mu_{rl})s}\mathrm{d}s\right)\\
&\geq 0 \qquad As\ t_1\longrightarrow\infty.
\end{aligned}$$

The equation for activated infected RBCs gives;

$$\begin{aligned}
\frac{dR_a}{dt} &= (1-\alpha)kRP_e+\gamma R_l-mER_a-k_bR_a\left(\frac{P_i^2}{P_i^2+(NR_a)^2}\right)-\mu_{ra}R_a,\\
&\geq (1-\alpha)kRP_e+\gamma R_l-(mE+\mu_{ra}+k_b)R_a,\\
&= (1-\alpha)kRP_e+\gamma R_l-(mE+\mu_{ra}+k_b)R_a.
\end{aligned}$$

Multiplying through by the integrating factor $e^{\left(m\int_0^t E(s)\mathrm{d}s+(\mu_{ra}+k_b)t\right)}$, *gives:*

$$\begin{aligned}
\frac{d}{dt}\left(e^{m\int_0^t E(s)\mathrm{d}s+(\mu_{ra}+k_b)t}\right)R_a &\geq (1-\alpha)kR(t)P_e(t)e^{m\int_0^t E(s)\mathrm{d}s+(\mu_{ra}+k_b)t}.\\
R_a(t_1) &\geq R_a e^{\left(-m\left(\int_0^{t_1} E(s)\mathrm{d}s+(\mu_{ra}+k_b)t_1\right)\right)}\\
&+ (1-\alpha)ke^{\left(-\left(m\int_0^{t_1} E(s)\mathrm{d}s+(\mu_{ra}+k_b)t_1\right)\right)}\\
&\times \int_0^{t_1} R_a(v)P_e(v)e^{\left(m\int_0^v E(p)\mathrm{d}p+(\mu_{ra}+k_b)v\right)}\mathrm{d}v,\\
&\geq 0 \qquad As\ t_1\longrightarrow\infty.
\end{aligned}$$

A similar analysis for the intracellular parasite gives;

$$\begin{aligned}
\frac{dP_i}{dt} &= k_{pi}P_i\left(1-\frac{{P_i}^2}{{P_i}^2+(NR_a)^2}\right)+k^*n^*RP_e-k_{11}NR_a\left(\frac{{P_i}^2}{{P_i}^2+(NR_a)^2}\right)\\
&\quad -n_1\mu_{ra}P_i,\\
&\geq k^*n^*RP_e-k_{11}NR_a\frac{P_i^2}{P_i^2+(NR_a)^2}-n_1\mu_{ra}P_i,\\
&\geq k^*n^*RP_e-k_{11}NR_a-n_1\mu_{ra}P_i.\\
&= k^*n^*RP_e-\left(k_{11}+n_1\mu_{ra}P_i\right).
\end{aligned}$$

Multiplying through by the integrating factor is $e^{(k_{11}+n_1\mu_{ra})t}$*, we obtain;*

$$\begin{aligned}
\frac{d}{dt}\left(P_i(t)e^{(k_{11}+n_1\mu_{ra})t}\right) &\geq k^*n^*R(t)P_e(t)e^{(k_{11}+n_1\mu_{ra})t}\\
P_i(t_1) &\geq P_i(0)e^{(-(k_{11}+n_1\mu_{ra})t_1)}\\
&\quad +k^*n^*e^{(-(k_{11}+n_1\mu_{ra})t_1)}\int_0^{t_1}R(s)P_e(s)e^{(k_{11}+n_1\mu_{ra})}\mathrm{d}s,\\
&\geq 0 \qquad\qquad As\ t\longrightarrow\infty.
\end{aligned}$$

Lastly,

$$\begin{aligned}
\frac{d}{dt}\left(P_e(t)e^{\left(k_{tp}N\int_0^t E(s)\mathrm{d}s+k^*n^*\int_0^t R(s)\mathrm{d}s+\mu_{pe}t\right)}\right) &\geq n_1\mu_{ra}P_i(t)e^{\left(k_{tp}N\int_0^t E(s)\mathrm{d}s+k^*n^*\int_0^t R(s)\mathrm{d}s+\mu_{pe}t\right)}\\
P_e(t_1) &\geq P_e(0)e^{-k_{tp}\int_0^{t_1}E(s)\mathrm{d}s-k^*n^*\int_0^t R(s)\mathrm{d}s-\mu_{pe}t}\\
&\quad +n_1\mu_{ra}e^{\left(-k_{tp}\int_0^{t_1}E(s)\mathrm{d}s-k^*n^*\int_0^t R(s)\mathrm{d}s-\mu_{pe}t\right)}\\
&\quad \times\int_0^{t_1}P_i(t)e^{\left(k_{tp}N\int_0^{t_1}E(s)\mathrm{d}s+k^*n^*\int_0^t R(s)\mathrm{d}s+\mu_{pe}t\right)}\mathrm{d}t,\\
&\geq 0 \qquad\qquad As\ t\longrightarrow\infty.
\end{aligned}$$

The effector cells equation is logistic, and so its solution is

$$E=\frac{r_e}{1+Ce^{-\omega_e t}} \qquad As\ t\longrightarrow\infty \quad E\longrightarrow r_e$$

then $E(0)\geq 0$.

The model equation (4.1) - (4.6) is mathematically and epidemiologically well-posed and we proceed to consider the dynamics of the flow generated by it in Γ_6.

4.2.2 Mathematical analysis of the model

Local Stability of the parasite-free equilibrium point

The system of equations (4.1) - (4.6) has equilibrium points namely the parasite-free and the parasite-present equilibrium points. The parasite-free equilibrium point, obtained by setting the infected states and the parasite states to zero, that is, $R_l = R_a = P_i = P_e = 0$, is given by;

$$x_{02} = \left(\frac{S_r}{\mu_r}, 0, 0, 0, 0, r_e\right). \tag{4.8}$$

The model equations (4.1) to (4.6), depending on parameter values, can process either a unique parasite-present equilibrium point or multiple parasite-present equilibrium point

$$x_{03} = (R^*, R_l^*, R_a^*, P_i^*, P_e^*, E^*),$$

but analytical determination of such points is too cumbersome for a large model. Our numerical simulation, however, will demonstrate the existence and stability of these points. We have determined the model reproduction number by rearranging the system (4.1) to (4.6) as in the previous model (see [93] for details). We have:

$$\left.\begin{aligned}
\dot{R}_l &= \alpha k R P_e - (\gamma + \mu_{rl}) R_l, \\
\dot{R}_a &= (1-\alpha) k R P_e + \gamma R_l - m E R_a - k_b R_a \left(\tfrac{{P_i}^2}{{P_i}^2 + (N R_a)^2}\right) - \mu_{ra} R_a, \\
\dot{P}_i &= k_{pi} P_i \left(1 - \tfrac{{P_i}^2}{{P_i}^2 + (N R_a)^2}\right) + k^* n^* R P_e - k_{11} N R_a \left(\tfrac{{P_i}^2}{{P_i}^2 + (N R_a)^2}\right) \\
&\quad - n_1 \mu_{ra} P_i, \\
\dot{P}_e &= S_{pe} P_e + k_{11} N R_a \left(\tfrac{{P_i}^2}{{P_i}^2 + (N R_a)^2}\right) + n_1 \mu_{ra} P_i - k_{tp} N E P_e - k^* n^* R P_e \\
&\quad - \mu_{pe} P_e, \\
\dot{R} &= S_r - \mu_r R - k R P_e, \\
\dot{E} &= \omega_e \left(1 - \tfrac{E}{r_e}\right) E.
\end{aligned}\right\} \tag{4.9}$$

New infections occur in the four infected classes namely the class of intracellular parasites, extracellular parasites, latently infected red blood cells and actively infected red blood cells. The new infections are given in the matrix below:

$$F = \begin{pmatrix} \alpha k R P_e \\ (1-\alpha) k R P_e \\ k^* n^* R P_e \\ k_{11} N R_a \left(\frac{{P_i}^2}{{P_i}^2 + (NR_a)^2} \right) + n_1 \mu_{ra} P_i \end{pmatrix}.$$

The Jacobian $\mathcal{DF}|(x_{02})$ of F is given by

$$\mathcal{F} = J(F)|(x_{02}) = \begin{pmatrix} 0 & 0 & 0 & \frac{\alpha k S_r}{\mu_r} \\ 0 & 0 & 0 & \frac{(1-\alpha) k S_r}{\mu_r} \\ 0 & 0 & 0 & \frac{k^* n^* S_r}{\mu_r} \\ 0 & 0 & n_1 \mu_{ra} & 0 \end{pmatrix}.$$

The other transitions among the states are given by

$$V = \begin{pmatrix} (\gamma + \mu_{rl}) R_l \\ -\gamma R_l + mER_a + k_b R_a \left(\frac{{P_i}^2}{{P_i}^2 + (NR_a)^2} \right) + \mu_{ra} R_a \\ -k_{pi} P_i \left(1 - \frac{{P_i}^2}{{P_i}^2 + (NR_a)^2} \right) + k_{11} N R_a \left(\frac{{P_i}^2}{{P_i}^2 + (NR_a)^2} \right) + n_1 \mu_{ra} P_i \\ -S_{pe} + k_{tp} N E P_e + k^* n^* R P_e + \mu_{pe} P_e \end{pmatrix},$$

and the associated Jacobian is

$$\mathcal{V} = J(V)|(x_{02}) = \begin{pmatrix} (\gamma + \mu_{rl}) & 0 & 0 & 0 \\ -\gamma & m r_e + \mu_{ra} & 0 & 0 \\ 0 & 0 & -k_{pi} + n_1 \mu_{ra} & 0 \\ 0 & 0 & 0 & k_{tp} N r_e + \frac{k^* n^* S_r}{\mu_r} + \mu_{pe} - S_{pe} \end{pmatrix}.$$

The product $\mathcal{F}\mathcal{V}^{-1}$ is given by

$$\mathcal{F}\mathcal{V}^{-1} = \begin{pmatrix} 0 & 0 & 0 & \frac{k \alpha S_r}{\mu_r \left(N k_{tp} r_e + \mu_{pe} + \frac{k^* n^* S_r}{\mu_r} - S_{pe} \right)} \\ 0 & 0 & 0 & \frac{k(1-\alpha) S_r}{\mu_r \left(N k_{tp} r_e + \mu_{pe} + \frac{k^* n^* S_r}{\mu_r} - S_{pe} \right)} \\ 0 & 0 & 0 & \frac{k^* n^* S_r}{\mu_r \left(N k_{tp} r_e + \mu_{pe} + \frac{k^* n^* S_r}{\mu_r} - S_{pe} \right)} \\ 0 & 0 & \frac{n_1 \mu_{ra}}{n_1 \mu_{ra} - k_{pi}} & 0 \end{pmatrix}.$$

The reproduction number is defined as the largest absolute eigenvalue of the matrix $\mathcal{F}\mathcal{V}^{-1}$

and is given by

$$\begin{aligned} R_{02} &= \sqrt{\frac{k^*n^*n_1S_r\mu_{ra}}{(n_1\mu_{ra}-k_{pi})\left(\mu_{pe}\mu_r+k^*n^*S_r+Nk_{tp}r_e\mu_r-S_{pe}\mu_r\right)}} \\ &= \sqrt{\left(\frac{n_1\mu_{ra}}{(n_1\mu_{ra}-k_{pi})}\right)\left(\frac{k^*n^*S_r}{(\mu_{pe}\mu_r+k^*n^*S_r+Nk_{tp}r_e\mu_r-S_{pe}\mu_r)}\right)} = \sqrt{R_{02}^*}, \end{aligned} \tag{4.10}$$

where

$$R_{02}^* = R_{om}R_{op} \tag{4.11}$$

$$R_{om} = \frac{n_1\mu_{ra}}{n_1\mu_{ra}-k_{pi}}, n_1\mu_{ra}-k_{pi}>0. \tag{4.12}$$

$$R_{op} = \frac{k^*n^*S_r}{(\mu_{pe}\mu_r+k^*n^*S_r+Nk_{tp}r_e\mu_r-S_{pe}\mu_r)}. \tag{4.13}$$

The number R_{op} is positive if the inequality

$$\mu_{pe}\mu_r+Nk_{tp}r_e\mu_r-S_{pe}\mu_r\geq 0, n_1\mu_{ra}-k_{pi}\geq 0, \tag{4.14}$$

is satisfied. This simplifies to $\mu_{pe}+Nk_{tp}r_e\geq S_{pe}$. We can summarize this information as follows:

1. The positivity of the number R_{02}^* requires that $n_1\mu_{ra}-k_{pi}>0$ and $\mu_{pe}+Nk_{tp}r_e\geq S_{pe}$.

2. The number R_{02}^* is a product of two numbers, R_{op} and R_{om}, representing two processes of the red blood cycle, the infection of red blood cells by extracellular parasites and the asexual replication of parasites within an infected red blood cell respectively. This product describes a host-vector nature of the process whereby an extracellular parasite must infect a susceptible red blood cell first, multiply asexually within the infected red blood cell before the parasites are released to continue the red blood cycle.

Hence, from the numbers (1, 2), we conclude that, based on the model reproduction number, clinical malaria is caused mainly by the asexual reproduction of the parasite ($R_{om}>1$). According to our model, although a high number of susceptible red blood cells may be infected by extracellular parasites, this process alone does not generate enough secondary

infections ($R_{op} \leq 1$) to cause clinical malaria but the high number of merozoites released into the blood stream by the efficient asexual process is responsible for rapid depletion of the red blood cell population resulting in anaemia. One may ask the following questions " For what values of n_1 is the model reproduction number R_{02} greater than one and for what numbers n_1 is it less than one? Can we find the threshold n_1^* which determines the prognosis of the disease? We address these questions in detail in the section (4.2.4) on simulation. We can state the following stability theorem for the parasite-free equilibrium point.

Theorem 4.2.1 *The parasite-free equilibrium of the system (4.1) - (4.6) is locally stable if* $\mu_{pe}\mu_r + Nk_{tp}r_e\mu_r - S_{pe}\mu_r \geq 0$, $n_1\mu_{ra} - k_{pi} \geq 0$, *and* $R_{02}^* < 1$.

From the local stability condition we have calculated the threshold killing rate of merozoites by the effector cells and is given by

$$\hat{k_{tp}} = \frac{k_{pi}k^*n^*S_r}{Nr_e\mu_r\left(n_1\mu_{ra} - k_{pi}\right)} - \frac{\mu_{p_e}}{Nr_e}.$$

If $k_{tp} > \hat{k_{tp}}$, the immune cells manage to control the parasite population. In malaria endemic areas of the developing countries where many individuals suffer from chronic infections and their effector cell responses can be altered and impaired, the effector cells killing rate for some patients may be below $\hat{k_{tp}}$ as a results of cell fatigue [94]. This situation may be responsible for the recurrence of malaria. Note that the threshold killing rate, $\hat{m}$, of actively infected red blood cells by effector cells cannot be determined from the stability conditions of the parasite-free equilibrium point. We investigate the impact of the parameter m in section (4.2.4) on simulation.

4.2.3 A within host treatment model of blood stage malaria

Treatment with a drug of constant efficacy (ϵ_1) can be incorporated in the model (4.1) - (4.6) by inserting the factor $(1-\epsilon_1)$ next to the infection terms as shown below:

$$\left.\begin{aligned}
\dot{R} &= S_r - \mu_r R - k(1-\epsilon_1)RP_e, \\
\dot{R}_l &= \alpha k R(1-\epsilon_1)P_e - (\gamma+\mu_{rl})R_l, \\
\dot{R}_a &= (1-\alpha)kR(1-\epsilon_1)P_e + \gamma R_l - mER_a - k_b R_a\left(\tfrac{{P_i}^2}{{P_i}^2+(NR_a)^2}\right) - \mu_{ra}R_a, \\
\dot{P}_i &= k_{pi}P_i\left(1-\tfrac{{P_i}^2}{{P_i}^2+(NR_a)^2}\right) + k^*n^*R(1-\epsilon_1)P_e - k_{11}NR_a\left(\tfrac{{P_i}^2}{{P_i}^2+(NR_a)^2}\right) \\
&\quad -n_1\mu_{ra}P_i, \\
\dot{P}_e &= S_{pe}P_e + k_{11}NR_a\left(\tfrac{{P_i}^2}{{P_i}^2+(NR_a)^2}\right) + n_1\mu_{ra}P_i - k_{tp}\left(1+\tfrac{\epsilon_1}{1+\epsilon_1}\right)NEP_e \\
&\quad -k^*n^*R(1-\epsilon_1)P_e - \mu_{pe}P_e, \\
\dot{E} &= \omega_e\left(1-\tfrac{E}{r_e}\right)E.
\end{aligned}\right\} \tag{4.15}$$

The reproduction number calculated as in [93] is given by

$$\begin{aligned}
R_{04} &= \sqrt{\tfrac{k^*n^*n_1(1-\epsilon_1)S_r\mu_{ra}}{(n_1\mu_{ra}-k_{pi})(H_3\mu_r)}} \\
&= \sqrt{\left(\tfrac{n_1\mu_{ra}}{(n_1\mu_{ra}-k_{pi})}\right)\left(\tfrac{k^*n^*(1-\epsilon_1)S_r}{(H_3\mu_r)}\right)} = \sqrt{R^*_{04}}.
\end{aligned}$$

where

$$H_3 = k_{tp}\left(1+\frac{\epsilon_1}{1+\epsilon_1}\right)Nr_e + \frac{k^*n^*(1-\epsilon_1)S_r}{\mu_r} + \mu_{pe} - S_{pe}. \tag{4.16}$$

and

$$R^*_{04} = \left(\frac{n_1\mu_{ra}}{n_1\mu_{ra}-k_{pi}}\right)\left(\frac{k^*n^*(1-\epsilon_1)S_r}{(H_3\mu_r)}\right). \tag{4.17}$$

The number R^*_{04} consists of two parts, $\left(\frac{n_1\mu_{ra}}{(n_1\mu_{ra}-k_{pi})}\right)$ and $\left(\frac{k^*n^*(1-\epsilon_1)S_r}{H_3\mu_r}\right)$. These parts define the infection process which starts with the infection of red blood cells (the part $\left(\frac{k^*n^*(1-\epsilon_1)S_r}{H_3\mu_r}\right)$) and the asexual reproduction of the parasite ($\left(\frac{n_1\mu_{ra}}{(n_1\mu_{ra}-k_{pi})}\right)$).
Note that;

$$\left(\frac{k^*n^*(1-\epsilon_1)S_r}{H_3\mu}\right) < 1, \qquad \left(\frac{n_1\mu_{ra}}{(n_1\mu_{ra}-k_{pi})}\right) > 1. \tag{4.18}$$

The efficacy parameter ϵ_1 ranges between 0 and 1. As $\epsilon_1 \longrightarrow 1$, $R^*_{04} \longrightarrow 0$, and as $\epsilon_1 \longrightarrow 0$, $R^*_{04} = R^*_{02}$. We want to determine, in the section on simulation, the least efficacy level $\epsilon^*_1 < 1$ for which the disease clears. We can summarize the local stability of the parasite-

free equilibrium point in the following theorem:

Theorem 4.2.2 *The model (4.15) is stable for* $R_{04}^{*} < 1$, *implying that treatment maintains the stability of the model.*

4.2.4 Simulations of the within host model of blood stage malaria

Sensitivity and uncertainty analysis of R_{02} and parameter estimation

The model (4.1) - (4.6) requires several input parameter values, which can be divided into three sets, namely (i) those that have been measured clinically or experimentally [TABLE 4.3], (ii) those that have been estimated by other researchers [TABLE 4.3] and (iii) those that have been estimated by us using the parameters in (i) and (ii) above. Since a number of parameters are not known [TABLE 4.3], we begin by investigating the level of uncertainties

TABLE. 4.3. The table that shows the parameter values of the model.

Parameter	Value	Source
S_r	$2.5 * 10^8 < S_r < 2.5 * 10^9$	Estimated [89, 101]
μ_r	0.01	[101]
k	$2 * 10^{-9}$	[89]
μ_{rl}	$0.022 < \mu_{rl} < 0.01$	Estimated [5, 101]
μ_{ra}	$0.014 < \mu_{ra} < 0.02$	[101]
N	32	[55]
n_1	$12 < n_1 < 32$	Estimated [55]
n^*k^*	10^{-8}	Estimated
k_{11}	0.01	Estimated
k_b	$0.05 < k_b < 0.4$	Estimated
μ_{pe}	0.0208	[89]
γ	$0.0001 < \gamma < 0.04$	Estimated
α	0.2	Estimated
m	10^{-8}	[5, 89]
k_{pi}	0.08745	Estimated
k_{tp}	0.01	Estimated
r_e	$4000 < r_e < 15000$	[100]
ω_e	0.04	Estimated
S_{pe}	$0 < S_{pe} < 50$	Estimated [78]

in the model parameters and their sensitivity using Latin Hypercube Sampling Techniques

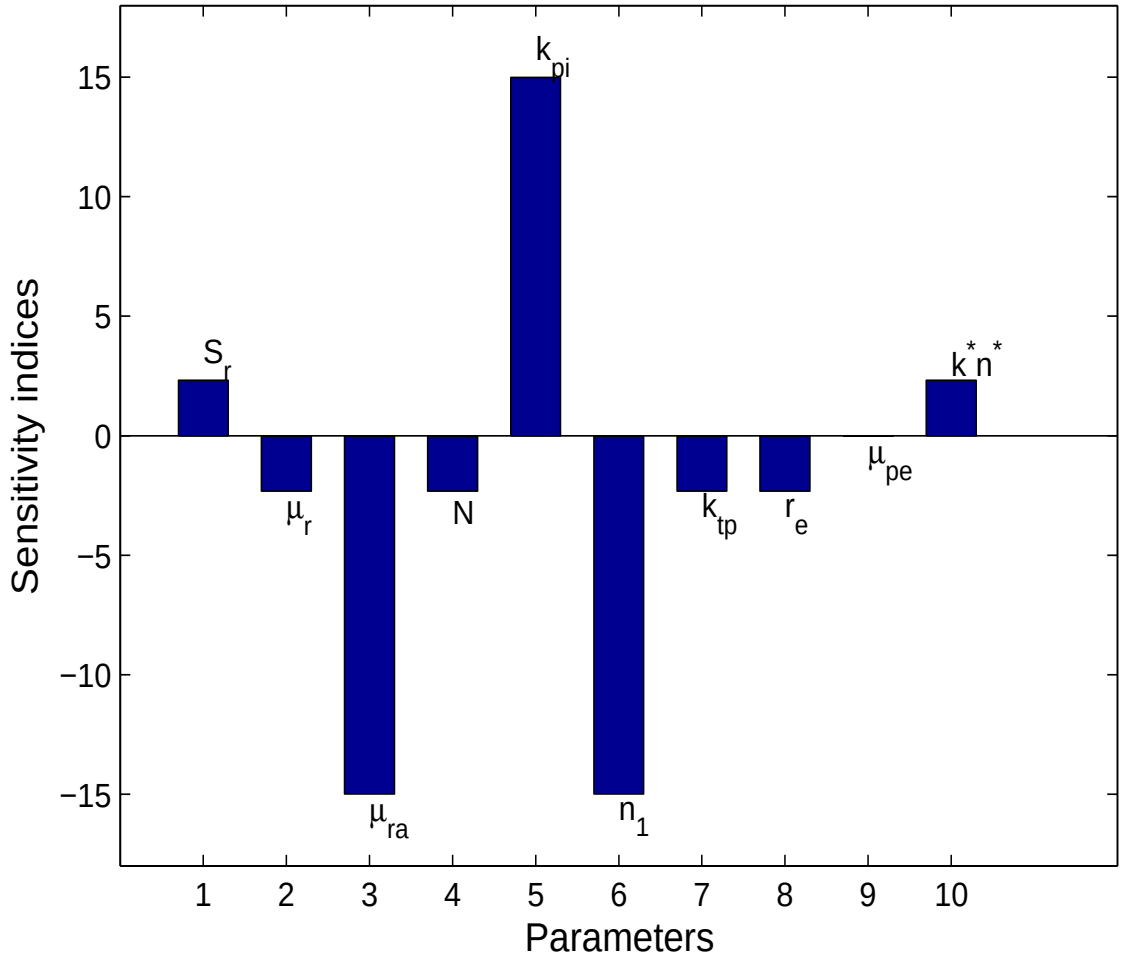

FIG. 4.2. A diagram showing sensitivity of various parameters on the reproduction number.

[32]. The partial rank correlation coefficients plotted in FIG. 4.2 show the impact of the various parameters on the reproduction number R_{02}. We can see that the reproduction number is highly positively correlated to k_{p_i}, the rate of growth of intracellular parasites, and highly negatively correlated to μ_{ra}, the natural death rate of intracellular parasites and n_1 another intracellular parasite related parameter. The range of the parameter n_1 is known and is given in [55]. The parameter μ_{ra} is also known and is given in [101]. The parameter k_{p_i} has not been estimated clinically or experimentally and is estimated in this study using the parameters from McQueen and McKenzie [55] and the references therein. Using the values in [TABLE 4.3], we have found using an iterative procedure that

$n_1 = 16$ is the threshold value for which $R_{02} = 1$. Using this value of n_1 and the parameter values in [TABLE 4.3], we have estimated the value of the growth rate of parasites to be $k_{pi} = 0.08745$.

We want to use the parameters in [TABLE 4.3] to study the following hypothetical problems: (a) First, from the model equations (4.1) - (4.6), we want to determine the number, n_1, of merozoites in an infected red blood cell at the time of its natural death for which $R_{02} < 1$, and for which $R_{02} > 1$. In other words, we want to use the threshold value $n_1^* = 16$ ($R_{02} = 1$), to determine the prognosis of the malaria disease. (b) Secondly, while acute infections usually result in effective immune responses, chronic infections are associated with suboptimal effector cell responses [94]. To illustrate this, we consider a hypothetical situation where a host has malaria infection which would clear if CD8 T-cell responses were normal (that is $R_{02} < 1$). We then alter the CD8 T-cell response parameters m and k_{tp} at time $t < t_c$, where t_c is the time of clearance of the malaria infection, and investigate the prognosis of the disease. (iii) The malaria extracellular parasites are generated either by bursting of infected RBCs or by natural death of infected red blood cells. We investigate which of these replication mechanisms is responsible for the development of clinical malaria.

4.2.5 Simulations of the within host treatment model of blood stage malaria

The models equations (4.15) require several input parameter values, which can be divided into three sets, namely (i) those that have been measured clinically or experimentally [TABLE 4.4], (ii) those that have been estimated by other researchers [TABLE 4.4], and (iii) those that have been estimated by us using the parameters in (i) and (ii) above. We used MATLAB routines ODE45, ODE15s etc, to analyse our system and the sensitivity analysis for estimation of parameter on [TABLE 4.4] was done in section 4.2.4 and is not repeated here. We have included [TABLE 4.4] here to make referencing easier. The time used from simulations is zero to 60 days, which, clinically, is the time for an infected person to shows symptoms of malaria. In this example, we have started treatment on 32 day after

TABLE. 4.4. The table that shows the parameter values of the model.

Parameter	Value	Units	Source
S_r	$2.5 * 10^{7.2}$	$cell/ml.day$	Estimated [5, 55]
μ_r	0.01	day^{-1}	[101]
k	$2 * 10^{-9.5}$	$ml/cell.day$	[5, 89]
μ_{rl}	0.008	day^{-1}	Estimated [5, 101]
μ_{ra}	0.014	day^{-1}	[101]
N	32	$dimensionless$	[55]
n_1	12	$dimensionless$	Estimated [55]
n^*k^*	10^{-8}	$ml/cell.day$	Estimated
k_{11}	0.01	day^{-1}	Estimated
k_b	0.4	day^{-1}	Estimated
μ_{pe}	0.0208	day^{-1}	[89]
γ	0.0001	day^{-1}	Estimated
α	0.2	$dimensionless$	Estimated
m	10^{-8}	$ml/cell.day$	[5]
k_{pi}	0.08745	day^{-1}	Estimated
k_{tp}	0.0009	$ml/cell.day$	Estimated
μ_{pe}	0.0208	day^{-1}	[89]
r_e	880	$cell/ml$	[100]
ω_e	0.05	day^{-1}	Estimated
S_{pe}	20	$cell/ml.day$	Estimated [78]
ϵ_1	$0 < \epsilon_1 < 0.95$	$dimensionless$	Estimated

initial infection. This is because, the average time for clinical symptoms to appear is between $(8 - 25)$ days but it can take longer depending on the immune system of the host [48].

4.3 Results of the within host model of blood stage malaria

Dynamics of the system

FIG. (4.3) shows the time plots for the various classes of human cells and parasite classes for $R_{02} = 0.8327$ As expected the susceptible red blood cell drops initially but settles at a stead state level which is high enough to sustain life. All the infected states tend to zero and the disease does not establish itself. FIG. 4.4 shows a time plot for all the human cell populations and the parasite populations for $R_{02} = 1.3165$. It is clear that the disease establishes itself. The level of red blood cells falls rapidly below a level sufficient to support life.

Figures 4.5 and 4.6 show the evolution of the intracellular (FIG. 4.5) and extracellular (FIG. 4.6) parasites for various values of the parameter n_1 ($8 \leq n_1 \leq 32$) and the corresponding reproduction numbers. These figures, surprisingly, show that the replication of intracellular and extracellular parasites in the host is fastest for $n_1 = 8$. At this level of replication, each merozoite released from an infected red blood cell generates on average 1.6679 secondary infections. The replication of extracellular and intracellular parasites decreases as n_1 increases. Likewise, the reproduction number decreases as n_1 increases (FIG. 4.5 and FIG. 4.6). We can see from these plots that the parasite persists for $n_1 < 16$ possibly resulting in clinical malaria but fails to invade the host for $n_1 \geq 16$ provided the effector cell functions are normal. The fact that the parasite persists for small values n_1 suggests that the increase in the merozoite population within the host does not depend on the bursting of the infected red blood cells (filled to cell capacity, that is, $N = 32$) but on the natural death of infected red blood cells. FIG. 4.7, which is typical for other values of n_1, illustrates the relative impact of the two merozoite replication mechanisms namely, replication by bursting of infected red blood cells, P_1, for $N = 32$ and replication by natural death of infected red blood cells, P_2, for the case $n_1 = 12$. It is clear from (FIG. 4.7) that replication by natural death of infected red blood cells contributes significantly more than replication from bursting of infected red blood cells thereby confirming our earlier assertion. We are led to conclude that the merozoites may have preference for infecting older susceptible red blood cells that do not have a long time left to live. Figures (4.8 and 4.9)

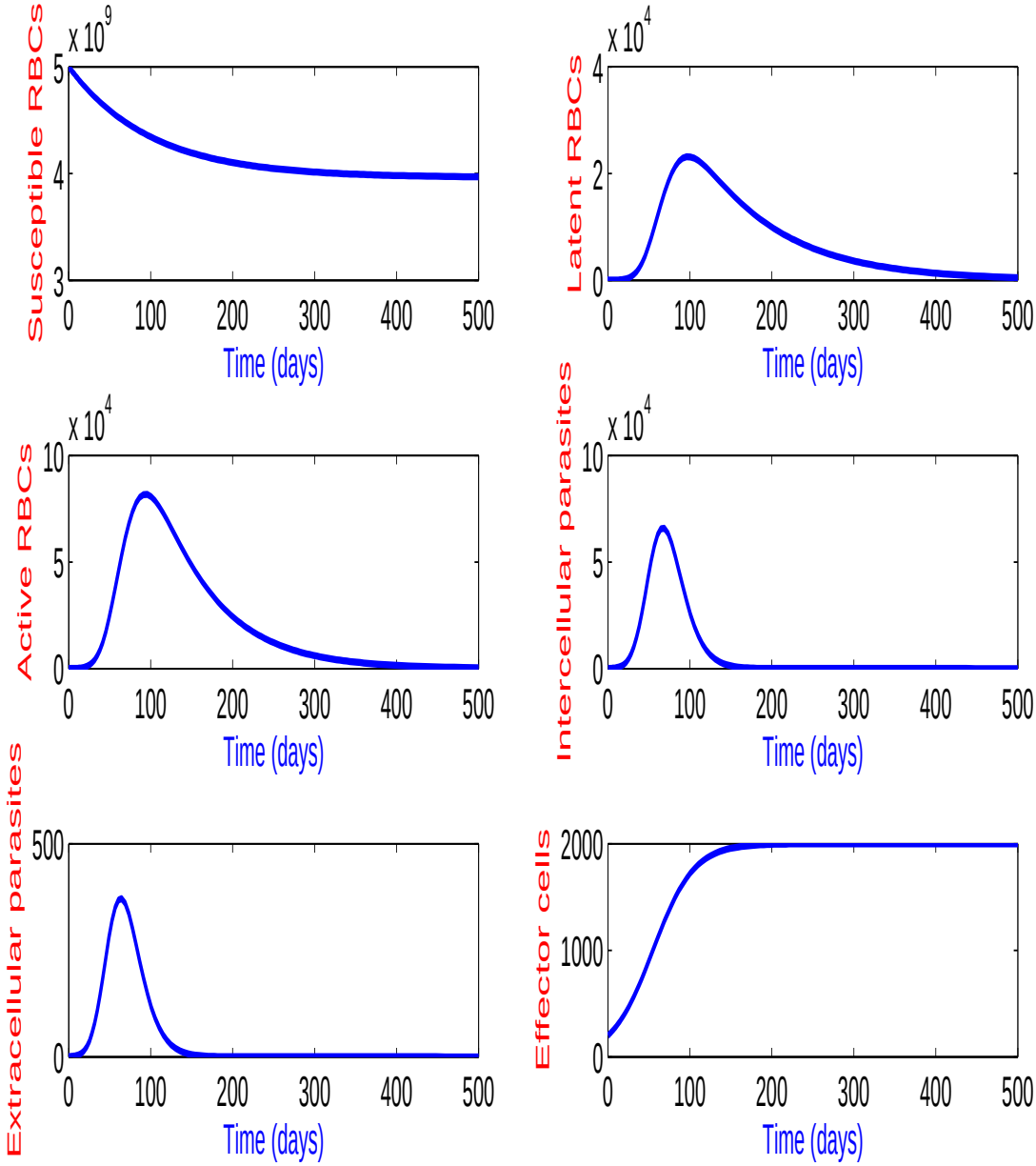

FIG. 4.3. Shows a diagram of parasite-free equilibrium with $R_{02} = 0.8327$.

show the evolution of red blood cell and infected red blood cell populations respectively. The population of red blood cells declines rapidly while the infected red blood cell population increases to a peak before going down. The peak of the infection, measured by the

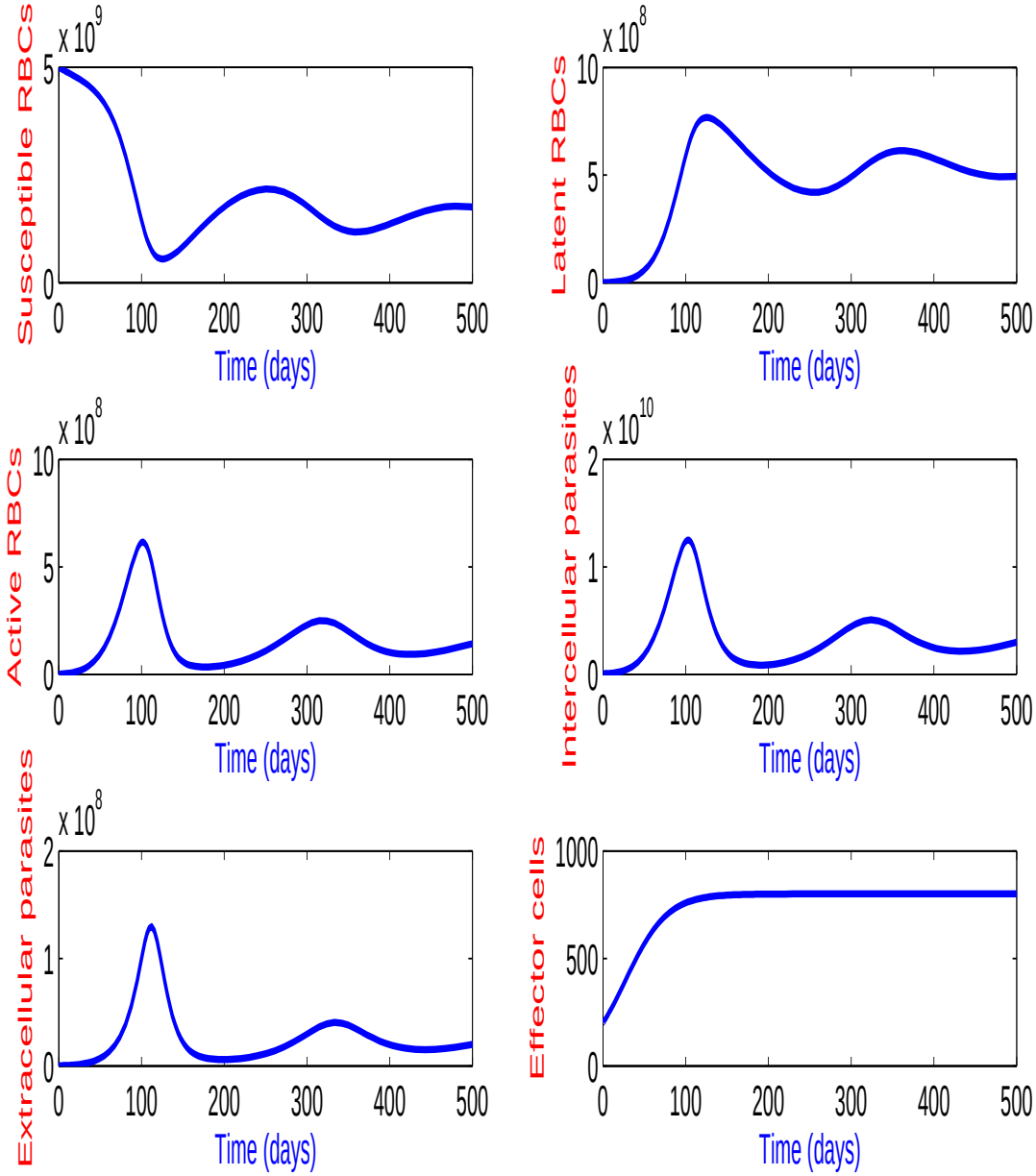

FIG. 4.4. A diagram of parasite-present equilibrium with $R_{02} = 1.3165$.

level of infected red blood cells, occurs approximately 37 days after the infection started, which agrees with clinical data [91, 96]. For $n_1 < 16$ the infection never clears and the red cell steady state level is only $25\% - 40\%$ (FIG. 4.10) of the parasite-free level,a which

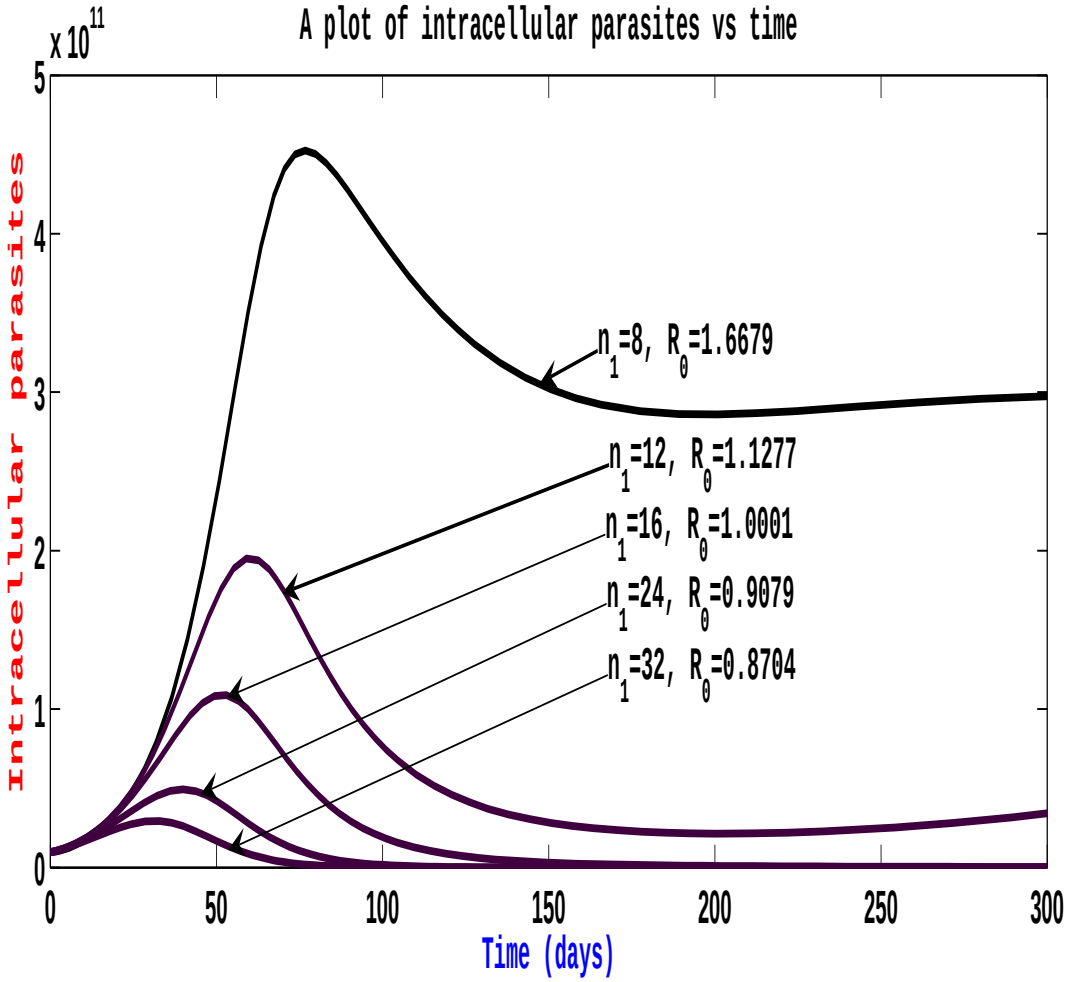

FIG. 4.5. A diagram showing population of intracellular parasites for $n_1 < 16$ the parasite-present equilibrium cases and $n_1 \geq 16$ the parasite-free equilibrium cases.

is too low to sustain life. Clearly, for $n_1 < 16$ treatment with malaria drugs is the only means of controlling the malaria parasite. The results for $n_1 \geq 16$ show that the parasite clears from the host as illustrated in FIG. 4.11 and FIG. 4.12. These figures show that the activated and latently infected red blood cell populations become extinct. For $n_1 = 16$, FIG. 4.10 shows that after the infection has cleared the red cell steady state level is 80% of the parasite-free level which is high enough to sustain life. However, for individuals with chronic illnesses [22, 72, 81, 104], the effector cell functions can be compromised. To illustrate this, we consider a malaria infection which under normal effector cell function would lead to a parasite-free equilibrium state and investigate the effect of reducing the role of effector cells by decreasing the parameters k_{tp} and m. Taking the state variables at

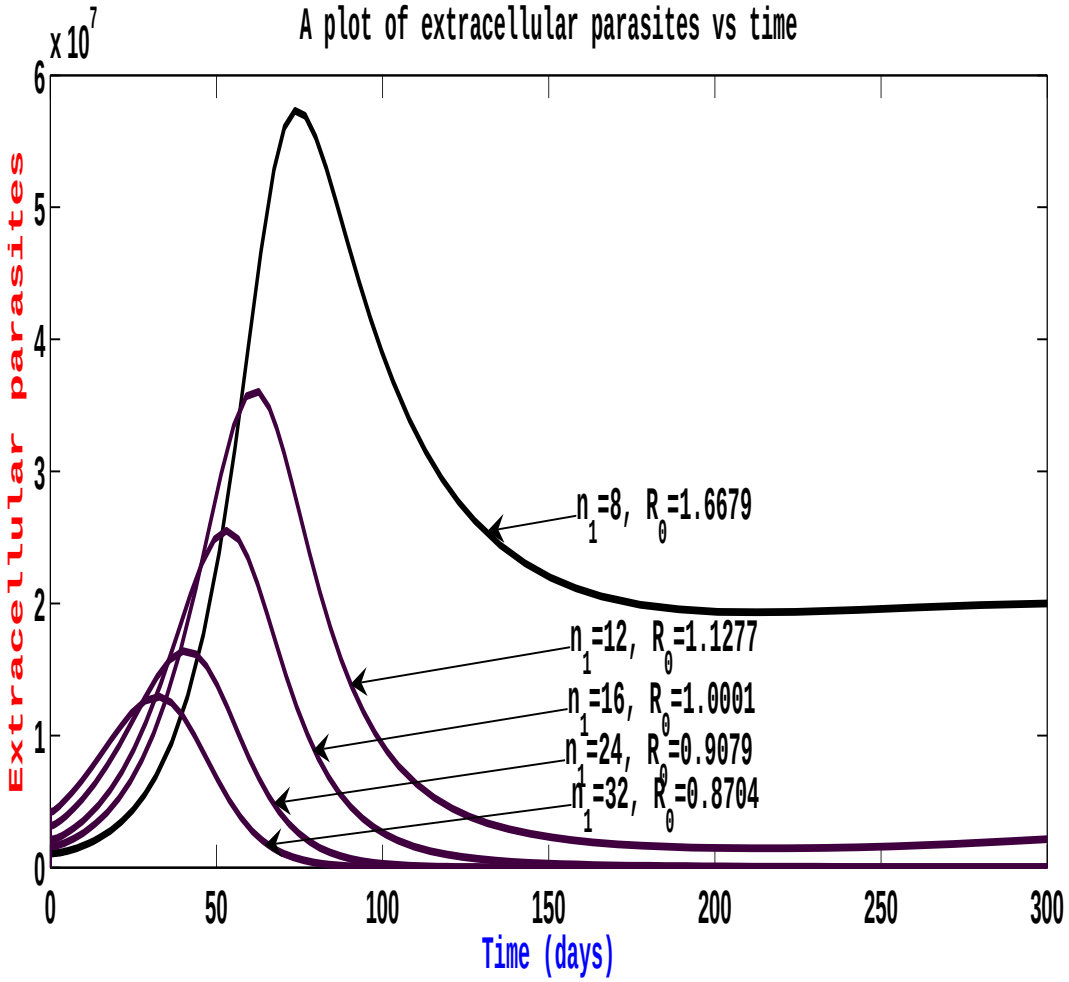

FIG. 4.6. A diagram showing population of extracellular parasites for $n_1 < 16$ the parasite-present equilibrium cases and $n_1 \geq 16$ the parasite-free equilibrium cases.

time $t = 350$ and decreasing the parameters k_{tp} and m, we notice that the population of activated red blood cells (FIG. 4.13) immediately increases while the susceptible red cell population (FIG. 4.14) declines. We conclude that if the role of the effector cells is reduced even for the case $n_1 = 24$ the host would develop malaria.

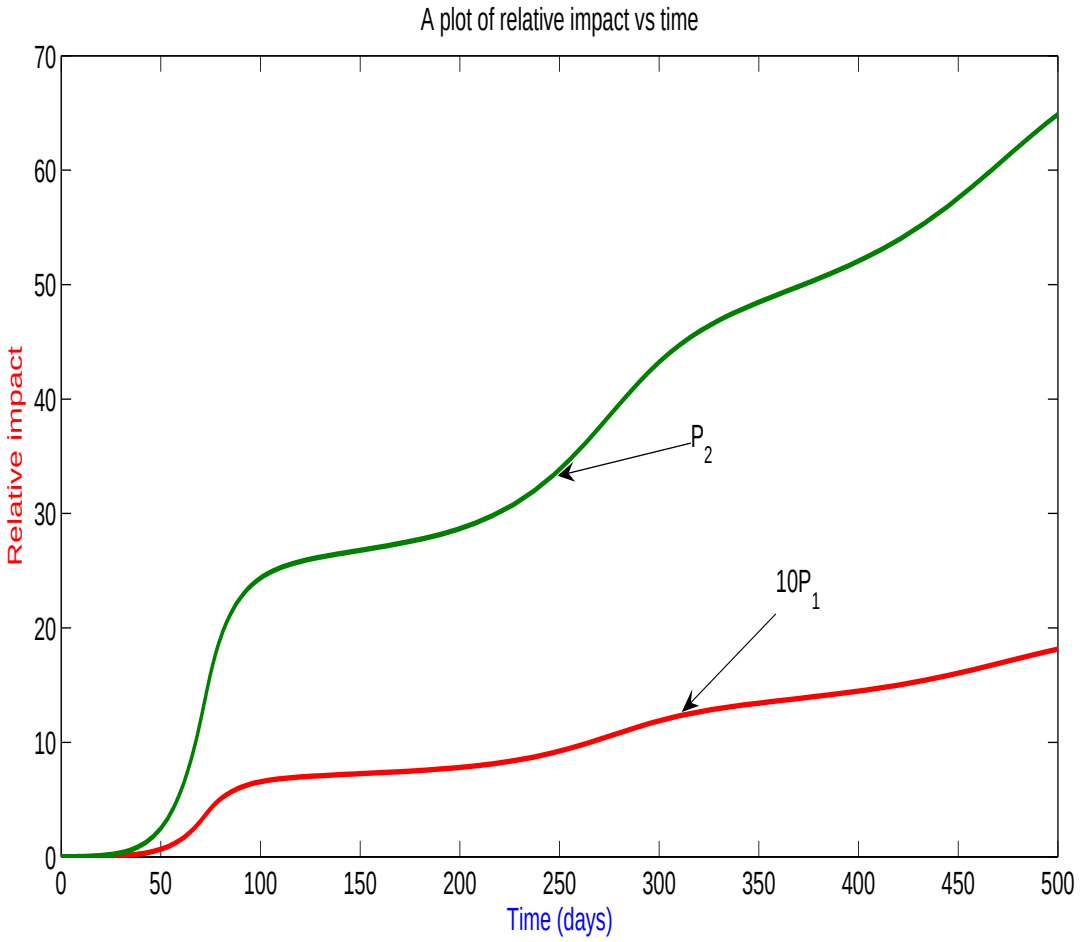

FIG. 4.7. Represents relative impact of the two parasite production mechanisms $10 * P_1$ and (P_2) for $n_1 = 12$ and $R_{02} = 1.1277$.

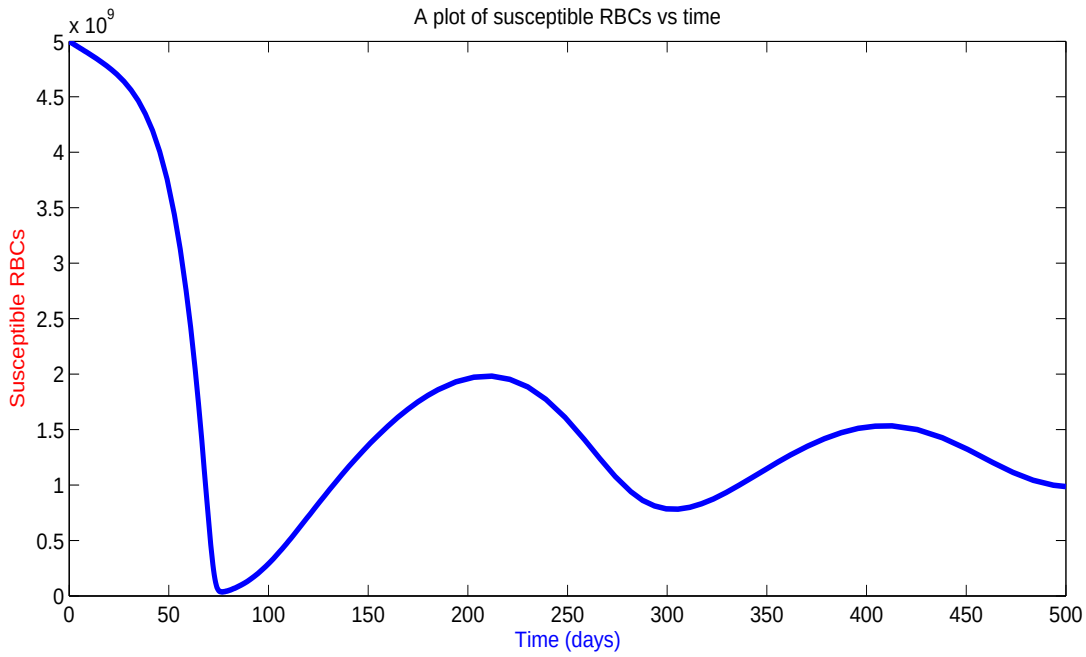

FIG. 4.8. A diagram showing the evolution of RBCs with time.

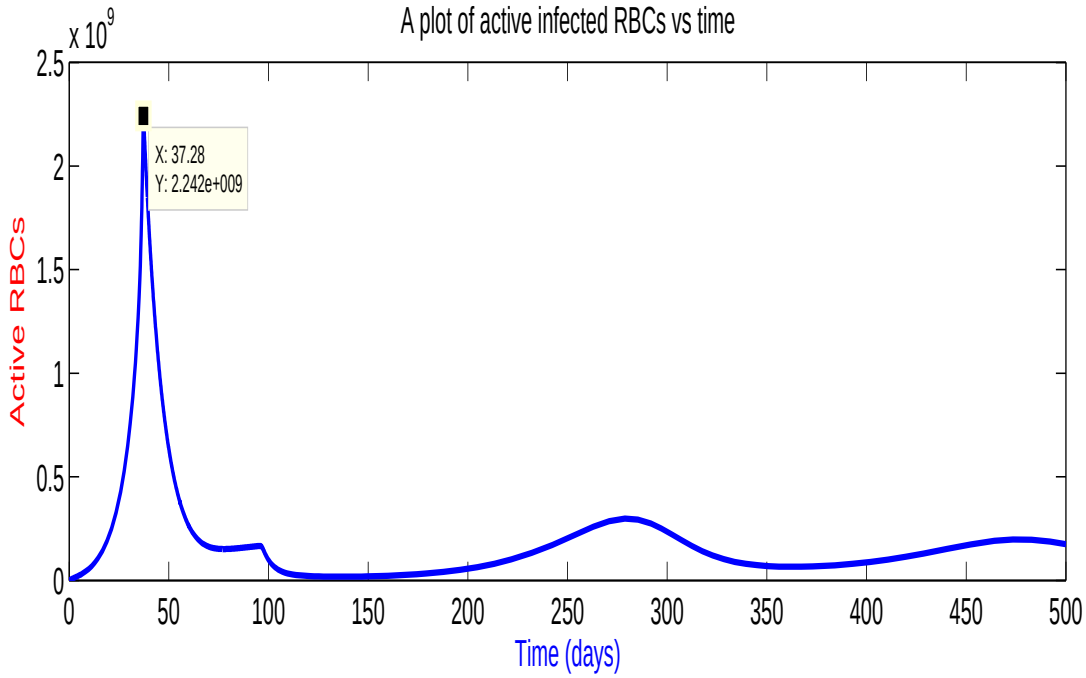

FIG. 4.9. A diagram showing the evolution of active infected RBCs with time.

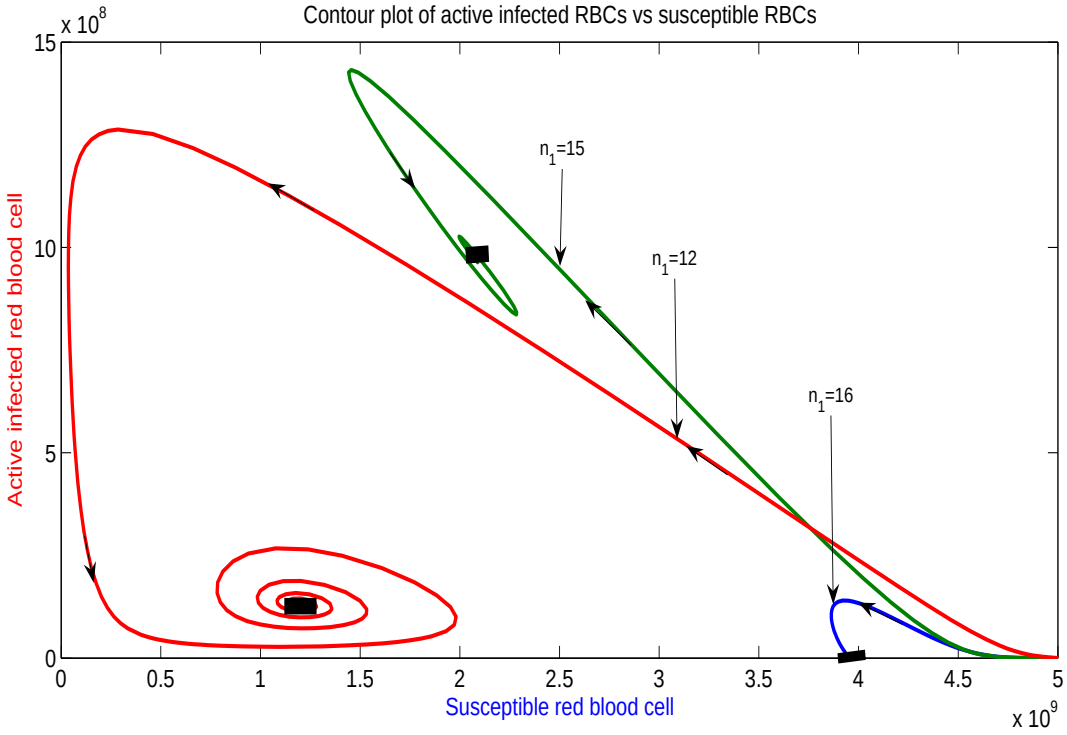

FIG. 4.10. Contour plots for $n_1 = 12$ and $n_1 = 15$ and $n_1 = 16$.

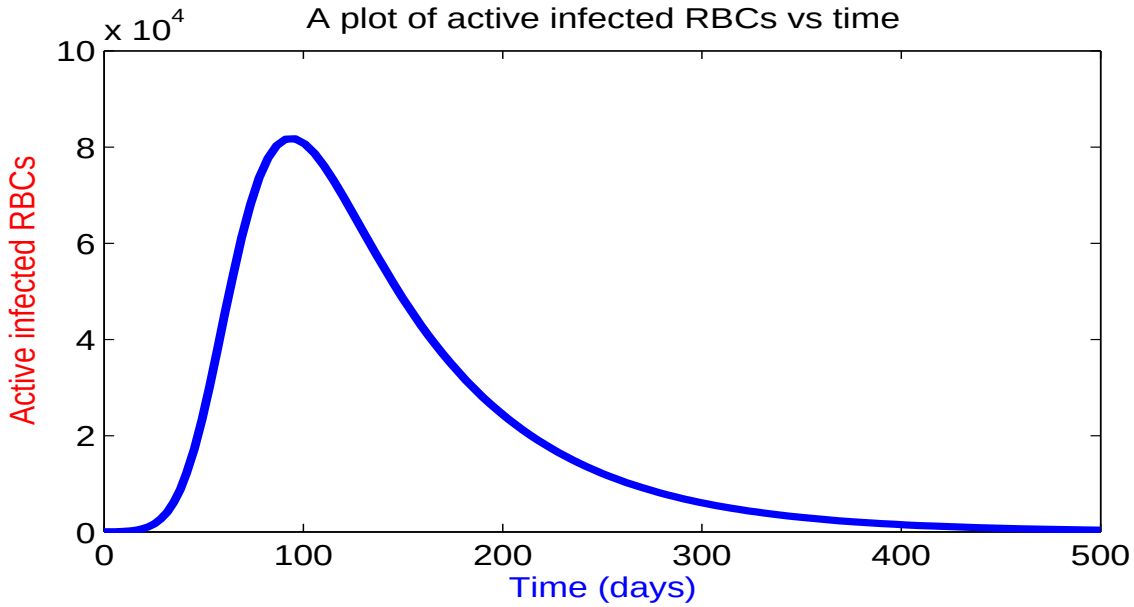

FIG. 4.11. Shows the population of actively infected RBCs at for $n_1 = 24$.

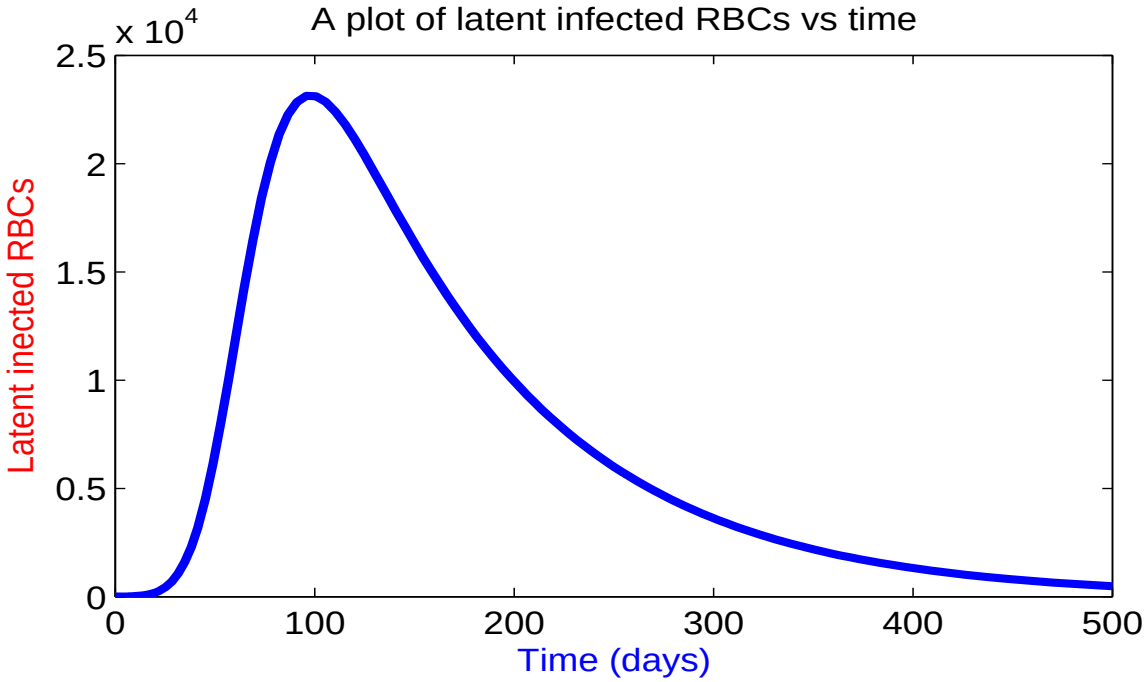

FIG. 4.12. Shows the population of latently infected RBCs at for $n_1 = 24$.

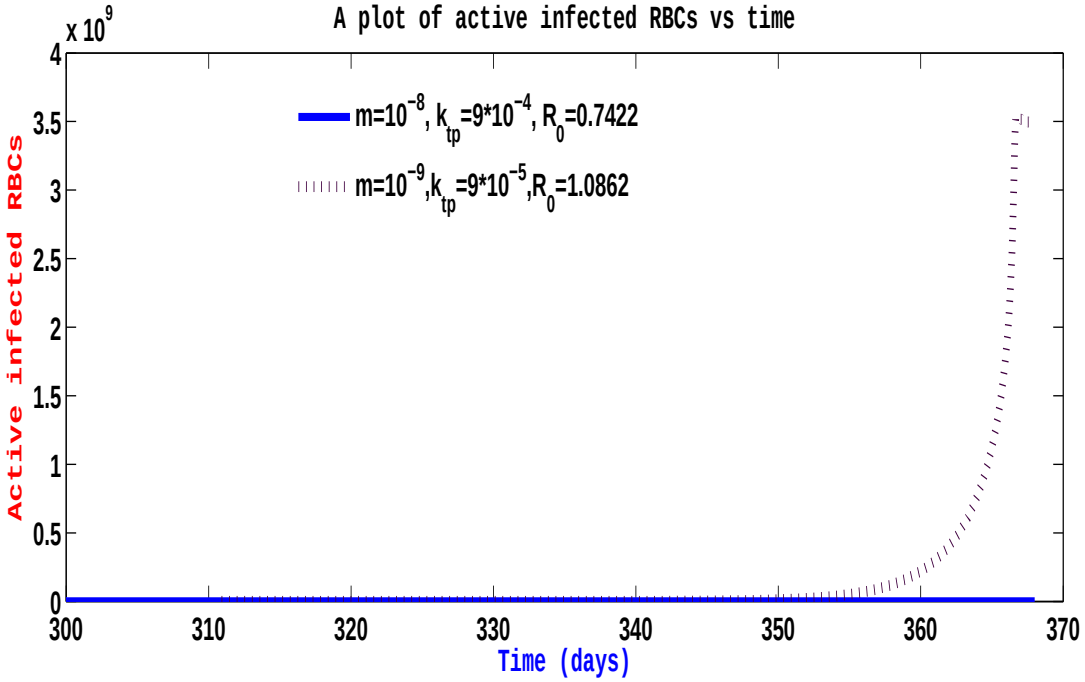

FIG. 4.13. Diagram showing the population of actively infected RBCs population for different values of m and k_{tp}.

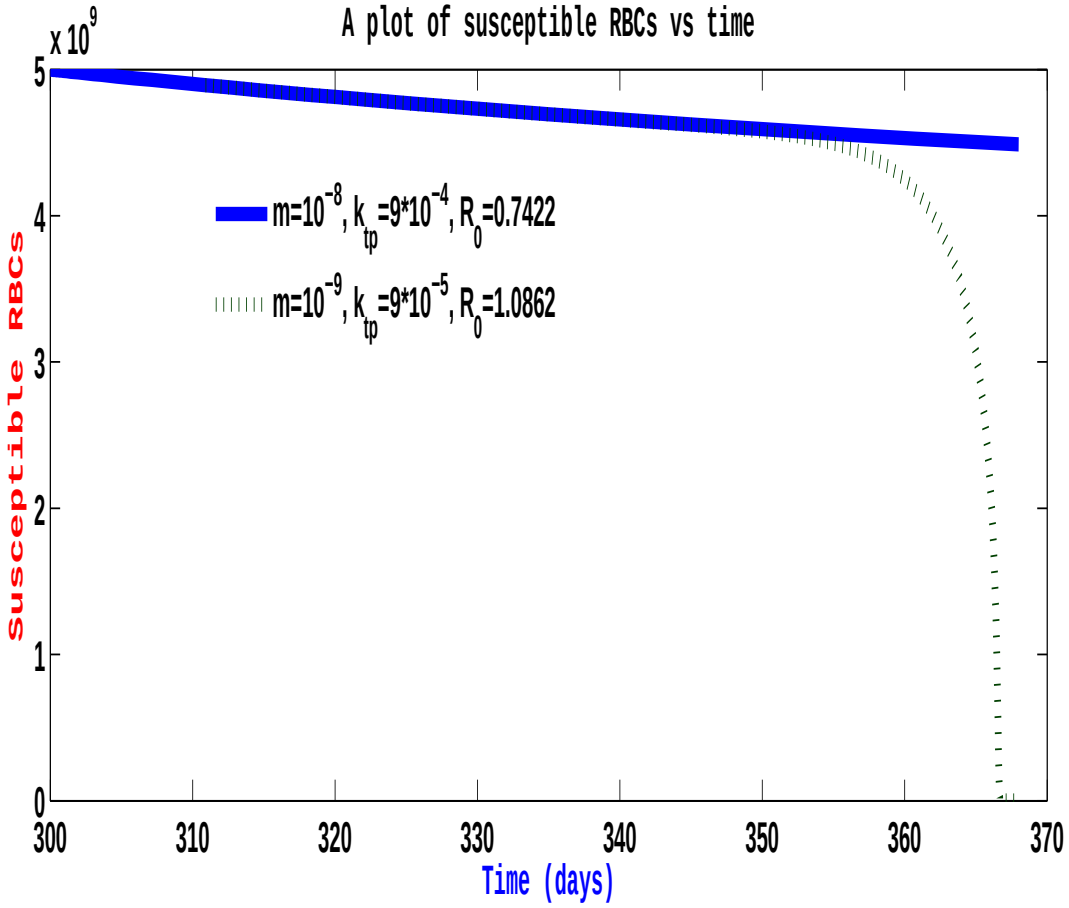

FIG. 4.14. Diagram showing the population of susceptible RBCs population for different values of m and k_{tp}.

4.4 Results of within host treatment model of blood stage malaria

FIG. (4.15) shows that susceptible red blood cell population decreases between day 20 and day 50 in the absence of treatment. The latently and actively infected red blood cell population increase during the same period.

The FIG. 4.16 shows plots when treatment is administered for drug efficacies ranging from ($\epsilon_1 = 0$) to ($\epsilon_1 = 0.95$). the figure shows that the depletion of the susceptible red blood cell population decreases with increasing efficacy. On the other hand the latently and actively infected red blood cell populations decrease with increasing efficacy. Intracellular parasites decrease with increasing efficacy while extracellular parasites increase and show the same characteristic as time increases. the reproduction number is a decreasing function of efficacy from $R_{04} = 1.3723$ for $\epsilon_1 = 0$ to $R_{04} = 0.5074$ for $\epsilon_1 = 0.95$. .

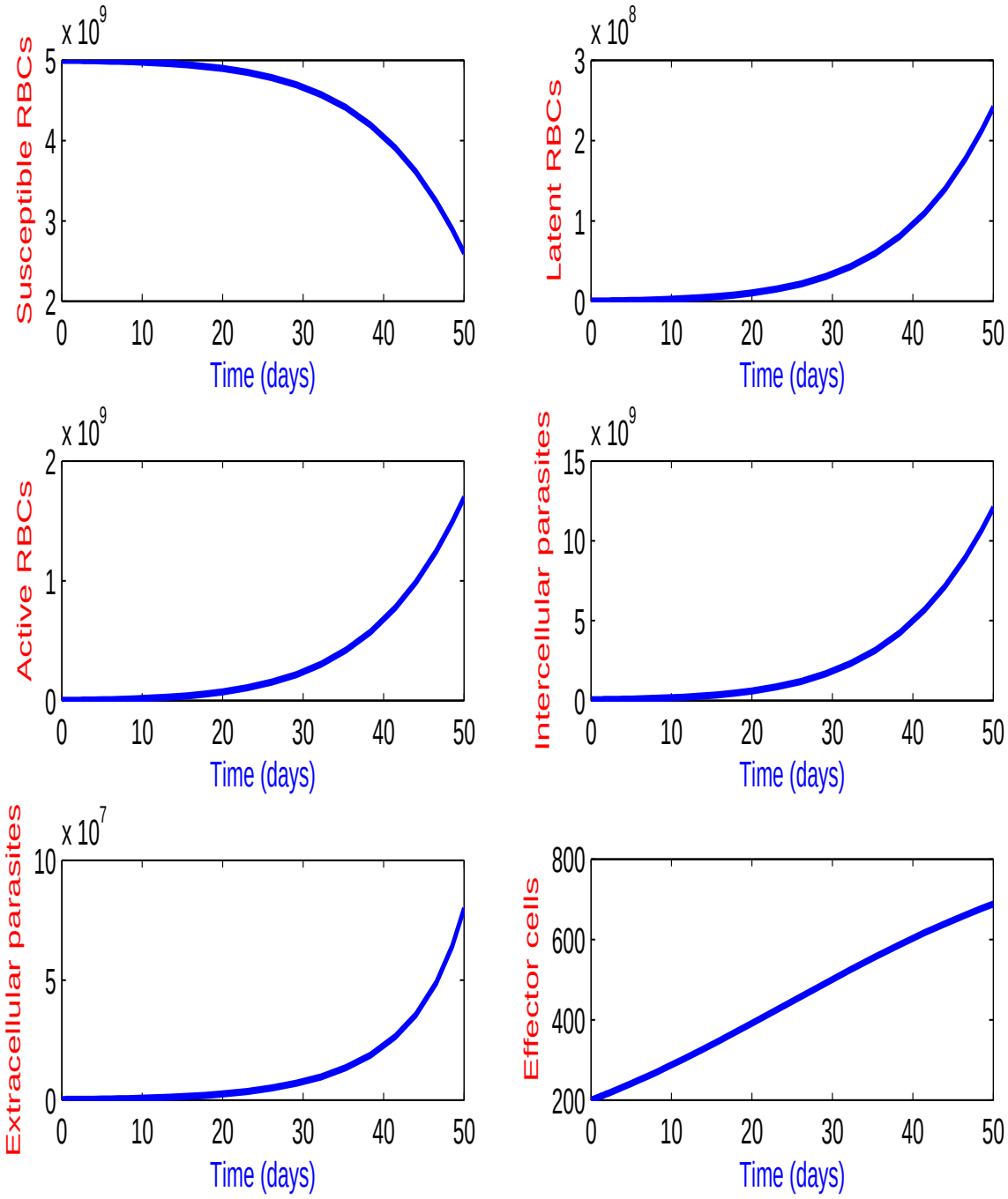

FIG. 4.15. A diagram shows malaria without treatment.

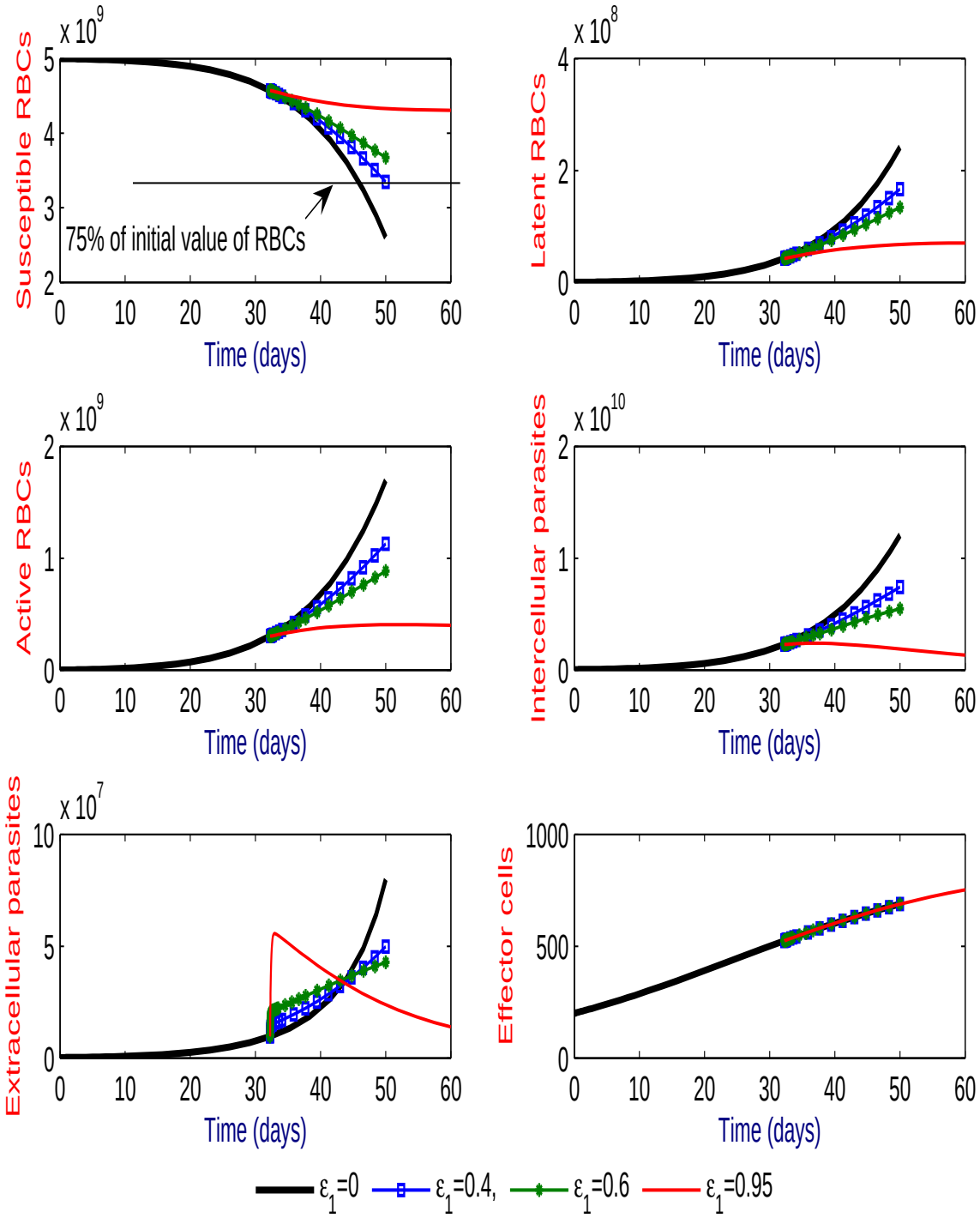

FIG. 4.16. Diagram showing one type of drug in treatment of malaria after 32 days and $\epsilon_1 = 0 \implies R_{04} = 1.3723$, $\epsilon_1 = 0.4 \implies R_{04} = 1.2114$, $\epsilon_1 = 0.6 \implies R_{04} = 1.0932$, $\epsilon_1 = 0.95 \implies R_{04} = 0.5074$.

4.5 Discussion

Sensitivity and uncertainty analysis has shown that the reproduction number is highly sensitive to the rate of growth of intracellular parasites (k_{pi}). An overestimate or underestimate of this parameter has serious implications regarding the prognosis of the disease. Therefore, there is need for a clinical or experimental determination of this parameter in particular but also a number of other parameters, such as rate of loss of extracellular parasites that are killed by effector cells (k_{tp}), threshold number as a results of gain due to infection of susceptible RBC by extracellular parasites (n^*k^*), rate of loss due to burst of activated cell (k_{11}), rate of bursting (k_b), rate of activation (γ), proportion of RBCs (α), to enhance the understanding of malaria.

We have found that parasites are replicated in two ways: (i) from naturally dying infected red blood cells and (ii) from bursting of infected red blood cells filled to carrying capacity N. Of the two mechanisms, we have found that natural death of infected red blood cells contributes more to the population of extracellular parasites. Interestingly, the number of parasites in a dying infected red blood cell need not be high for clinical malaria to develop. In fact the larger the number of parasites in a dying infected cell the smaller the chances of clinical malaria developing. Furthermore, we have found the following link between a threshold number of intracellular parasites released as a results of the natural death of an activated RBC (n_1) and the reproduction number R_{02} : For $n_1 < 16$, $R_{02} > 1$ and for $n_1 \geq 16$, $R_{02} \leq 1$. This result suggests that the larger n_1 is, the longer it takes to produce the parasites and the higher the chance of an infected red blood cell being identified and apoptosised by the effector cells. This has led us to conclude that in order to minimize the possibility of infected red blood cells being detected and eliminated by the immune cells, the parasite has a strategy of infecting older red blood cells whose life expectancy is much shorter than the younger cells [55] and in this way avoid the infected red blood cell being detected and apoptosised.

The reproduction number (4.10) is a product of two reproduction numbers R_{op} and R_{om} that reveal the host-vector infection nature of the process during the erythrocytic stages. Of the two processes namely infection of susceptible red blood cells by extracellular parasites and asexual production of parasites, it is the asexual replication process, measured by R_{om}, which is responsible for the pathology of clinical malaria as the reproductive rate for this process is greater than one per merozoite. To prevent clinical malaria from developing, it is important to administer highly efficacious drugs to stop the erythrocytic stage of the parasite cycle. However, the fact that the major source of parasite production is from naturally dying infected red blood cells has implications regarding the control of malaria as even treatment with highly efficacious drugs could generate drug resistant malaria strains if some infected red blood cells died before the drug chemodynamic effects are completed. We believe that only a malaria vaccine can reliably protect against blood stage malaria infection.

We have also shown that chronic infections can transform manageable malaria into a more active disease. The recommendation from our study is that in malaria endemic areas, *individuals with malaria or showing malaria symptoms should be tested for chronic infections and those who test positive for any chronic infection should be treated for both malaria and the chronic infection.*

We have investigated the effects of treatment on parasite depletion of susceptible red blood cells by introducing a drug of efficacy ϵ_1. As a first step, we determined the reproduction number which is now dependent on the drug efficacy. Taking $\epsilon = 0$ in the formula for R_0 gives the reproduction number obtained in the model without treatment. Clearly, the effect of the drug is apparent on the population sizes of red cells. It is found that the population of susceptible red blood cells increases with increasing efficacy (FIG. 4.16). The infected red blood cell populations on the other hand decrease with increasing efficacy. A drug of efficacy of at least 0.6 is capable of clearing the parasites (FIG. 4.16). Most malaria treatment drugs are of higher efficacy than 0.6. It is possible to combat malaria with treatment drugs but the administration of drugs should be done at health centres or hospitals to ensure that patients complete their treatment. This will go a long way towards reducing the rate of drug resistance to current malaria drugs.

Chapter 5

A within host treatment model with three stages of malaria life cycle

5.1 Introduction

Malaria remains one of the most serious global health problems and it is one of the leading causes of death and illness in children and adults in tropical countries [6, 91, 95]. Malaria control requires an integrated approach, such as prevention which includes vector control and treatment with effective anti-malarial drugs. The once affordable and widely available anti-malarial treatment drug, chloroquine, that was used from the 1950's to the 1970's is now totally ineffective [6, 102, 103]. The use of ACTs is the best current treatment strategy; unfortunately the implementation of this treatment strategy has lagged behind due to various factors such as high cost of the drugs [95].

The malaria life cycle (FIG. 2.2), involves two hosts namely an infected female anopheles mosquito which inoculates sporozoites into the blood circulation of a human host during a blood meal, and the human host. Initial replication of the parasite starts in the liver with the sporozoites infecting and invading liver cells (hepatocytes). The sporozoites then mature into schizonts which rupture to release merozoites into the blood stream. In the blood stream, the merozoites infect the red blood cells (RBCs) within which they undergo asexual multiplication (erythrocytic schizogony). This stage is responsible for the development of clinical malaria [2, 11, 41, 45, 101].

The sporogonic cycle (mosquito cycle) starts when the gametocytes (micro-gametes and macro-gametes) are ingested by a female anopheles mosquito during a blood meal. While in the mosquito stomach, fertilization occurs and to form zygotes. The zygotes transform into ookinetes which invade the midgut wall of the mosquito where they transform into oocysts. Oocysts grow, rupture and release sporozoites which invade mosquito sali-

vary glands. When the mosquito bites a susceptible human, the mosquito life cycle starts [11, 45, 50]. Mathematical models have been valuable decision-making tools for vaccination and treatment strategies against infectious diseases. Many mathematical models of malaria parasite pathogenesis and its transmission continue to be constructed by researchers [52, 55–57, 65, 84]. Most of these models focus on within-host dynamics of blood stage malaria or cell-mediated immune response to pathogenesis. Very few researchers, among them Miranda [87], have considered the within-mosquito parasite replication cycle.

The study by Iggidr *et. al* [35] considers a malaria within host model with k stages of age for the parasitized red blood cells and n strains for the parasite. A study by Niger and Gumel [65] has investigated the innate immune response to malaria infection and the effect of imperfect vaccines assuming a scenario of parasite life cycles. The simulation results [65] showed that a vaccine efficacy of at least 87% is necessary to eliminate Infected Red Blood Cells (IRBCs)in vivo. Our model will include three stages of the parasite life cycle namely: the exo-erythrocytic schizogony, which includes susceptible liver cells (S_l), infected liver cells (I_l), Sporozoites (P) and Schizonts (C_l), the erythrocytic schizogony, which includes susceptible red blood cells (R), infected red blood cells (R_i), merozoites (M_r), trophozoites (T), and schizonts (C_r) and the sporogonic cycle, include susceptible midgut cells (S_{mc}), infected midgut cells (I_{mc}) and gametocytes (G). We shall also introduce treatment with a drug of constant efficacy ϵ_1, and the immune response represented by the effector cells.

Despite vast clinical and experimental knowledge of the immunology of the malaria parasite life cycle [11, 26, 45, 50], development of the vaccine for malaria is still elusive. The development of the vaccine is as much immunological as it is epidemiological. The epidemiology of malaria guides the processes of development of new vaccines and treatments [79] and implementation of the vaccine and treatment trials. Needless to say, the effective and affordable drug that will treat all the three stages of the malaria cycle will have major impact on global public health.

In this chapter, we formulate a model based on the schemata of the parasite life cycle presented on the Center for Disease Control Website (FIG. 2.2).

5.2 Methodology

5.2.1 Model development

We shall use the following variables

TABLE. 5.1. The table describing the variables and units of variables

Variables	Descriptions	Units
S_l	Susceptible liver cells	cell/ml
I_l	Infected liver cells	cell/ml
P	Sporozoites	cell/ml
C_l	Schizonts inside liver cells	cell/ml
R	Susceptible red blood cell	cell/ml
R_i	Activated red blood cell	cell/ml
M_r	Merozoites	cell/ml
T	Trophozoites	cell/ml
C_r	Schizonts inside red blood cells	cell/ml
S_{mc}	Susceptible midgut cells	cell/ml
I_l	Infected liver cells	cell/ml
G	Gametocytes	cell/ml
E	Effector cells	cell/ml

TABLE. 5.2. The table describing the parameters and units of parameters

Parameter	Descriptions	Units
Π_l	Constant source of liver cells	$cell/ml.day$
β_l	Infection rate	$ml/cell.day$
μ_{sl}	Natural death rate of susceptible liver cells	day^{-1}
k_l	Rate of bursting of infected liver cells	day^{-1}
N	Cell carrying capacity	$dimensionless$
m	Rate of killing of infected cell by effector cells	$ml/cell.day$
μ_{il}	Natural death of an infected liver cells	day^{-1}
Π_p	Source of sporozoites	day^{-1}
β_p	Infection rate	$ml/cell.day$
α_p	Rate of gain/loss of sporozoites	day^{-1}
k_{12}	Rate of bursting of infected midgut cells	day^{-1}
n_3	Average number of sporozoites release from an infected midgut cells that dies naturally	$dimensionless$
μ_{imc}	Natural death of an infected midgut cells	day^{-1}
μ_p	Natural death of sporozoites	day^{-1}
k_{cl}	Growth rate of schizonts	day^{-1}
k_{tp}	Rate of loss of schizonts inside the liver cells that are killed by effector cells	$ml/cell.day$
n_1	Average number of schizonts release from an infected liver cells that dies naturally	$dimensionless$
μ_{cl}	Natural death of schizonts inside the liver cells	day^{-1}
S_r	Constant source of red blood cells (RBCs)	$cell/ml.day$
k	Infection rate	$ml/cell.day$

TABLE. 5.3. The table describing the parameters and units of parameters

Parameter	Descriptions	Units
μ_r	Natural death of susceptible RBCs	day^{-1}
k_b	Rate of loss of infected RBCs due to bursting of infected RBCs	day^{-1}
μ_{ri}	Natural death of infected RBCs	day^{-1}
k_r	Growth rate due to infection of RBCs	day^{-1}
k_7	Rate of killing of merozoites by effector cells	$ml/cell.day$
k_{13}	Rate of loss of merozoites	day^{-1}
μ_{mr}	Natural death of merozoites	day^{-1}
γ	Proportion of merozoites	$dimensionless$
ω	Rate of gain/loss of trophozoites	day^{-1}
μ_t	Natural death of trophozoites	day^{-1}
k_{11}	Rate of loss of schizonts due to bursting of infected RBCs	day^{-1}
μ_{cr}	Natural death of schizonts inside RBCs	day^{-1}
Π_{mc}	Constant source of midgut cells	$cell/ml.day$
β_{mc}	Infection rate	$ml/cell.day$
μ_{mc}	Natural death of susceptible midgut cells	day^{-1}
μ_{imc}	Natural death of infected midgut cells	day^{-1}
μ_g	Natural death of gametocytes	day^{-1}
ω_e	Growth rate of effector cells	day^{-1}
r_e	Carrying capacity of effector cell	$cell/ml$

Liver stage (exo-erythrocytic schizogony)

From FIG. 2.2, it is easy to see that, the model for the liver stages (exo-erythrocytic schizogony) must include susceptible liver cells (S_l), infected liver cells (I_l), Sporozoites (P) and Schizonts (C_l). We also introduce treatment with a drug of constant efficacy ϵ_1. The dynamics for the susceptible liver cells is given by:

$$\dot{S}_l = \Pi_l - \beta_l(1-\epsilon_1)S_l P - \mu_{sl} S_l. \tag{5.1}$$

The first term of equation (5.1) is a source for the susceptible liver cells, the second term represents loss due to infection of susceptible liver cells by sporozoites [85] and the third term represents natural death of susceptible liver cell at constant rate μ_{sl} . The rate of change of the population of infected liver cells is given by:

$$\dot{I}_l = \beta_l(1-\epsilon_1)S_l P - k_l I_l \left(\frac{{C_l}^2}{{C_l}^2 + (NI_l)^2}\right) - mEI_l - \mu_{il} I_l. \tag{5.2}$$

The first term in equation (5.2) is due to infection of liver cells, the second term represents loss due to bursting of infected liver cells which is assumed to be dependent on the densities of gametocytes and infected liver cells [28], the third and fourth terms represent losses due lysing of infected cells by effector cells and natural death at a constant rate μ_{il} respectively. We have assumed a bursting rate similar to that of bacteria in infected macrophages [25, 28], an assumption which has not been confirmed clinically or experimentally for malaria.

$$\begin{aligned}\dot{P} &= \Pi_p P - \beta_p S_l P - \alpha_p P + k_{12} I_{mc}\left(\frac{G^2}{G^2 + (NI_{mc})^2}\right) \\ &\quad + n_3 \mu_{imc} I_{mc} - \mu_p P.\end{aligned} \tag{5.3}$$

Sporozoites enter the susceptible liver cells immediately after being inoculated into the blood stream by the mosquito (FIG. 2.2). Within the liver cells the sporozoites develop into schizonts [26, 45]. In equation (5.3) the first term represents a source of sporozoites, the second term is loss of sporozoites due to infection of liver cells, the third term is loss due to maturity of sporozoites into schizonts, the fourth term measures the number of infected midgut cells that burst to release gametocytes. The fifth term is the gain due to natural death of midgut cells, and the sixth term is the natural death of the sporozoites.

$$\dot{C}_l = \alpha_p P + k_{cl} S_l \left(1 - \frac{{C_l}^2}{{C_l}^2 + (NI_l)^2}\right) - k_{tp} NEC_l - n_1 \mu_{cl} C_l. \tag{5.4}$$

Equation (5.4) represents the evolution of liver schizonts. The first term of the equation represents the maturation of sporozoites into the liver schizonts [50], the second term is growth of schizonts by an assumed law [25, 26, 28]. The third term is the loss of schizonts lysis by effector cells, the forth term is the loss due to death of infected liver cell.

Blood stages (erythrocytic schizogony)

Erythrocytic schizogony [45] is the blood stage of the malaria infection described in an earlier chapter and it involves susceptible red blood cells (R), infected red blood cells (R_i), merozoites (M_r), trophozoites (T), and schizonts (C_r). Schizonts here are a result of the asexual reproduction during the blood stage of the infection. The red blood cell population evolves according to the equation below:

$$\dot{R} = S_r - k(1-\epsilon_1)RM_r - \mu_r R. \tag{5.5}$$

The terms in equation 5.5 can be explained as follows: The first term represents a source of health red blood cells from bone marrow [55] and the second term represents infection of healthy red blood cells by merozoites. The third term represents natural death of healthy red blood cell at a constant rate μ_r. An infected red blood cell is an incubator of the parasite and as such is targeted by the effector cells as explained in equation (5.6). The dynamics if the infected red cells is given by:

$$\dot{R}_i = k(1-\epsilon)RM_r - mER_i - k_b R_i \left(\frac{{C_r}^2}{{C_r}^2 + (NR_i)^2}\right) - \mu_{ri}R_i, \tag{5.6}$$

The first term of equation (5.6) represents gain by the population of infected red blood cells due to infection of susceptible red blood cells by merozoites [26], the second term is loss as a results of the immune response which triggers the effector cells to remove the infected red blood cells assumed here to be at a constant rate m, the third term is loss due to bursting of infected red blood cells. The fourth term represents natural death of infected red blood cell at a constant rate μ_{ri}. Within an infected red blood cell, we assume a law for the evolution of the merozoites population given in equation (5.7) below:

$$\begin{aligned}\dot{M}_r = {} & n_1\mu_{il}C_l + k_r M_r\left(1 - \frac{{M_r}^2}{{M_r}^2 + (NR_i)^2}\right) - k_7 E M_r \\ & -k_{13}M_r - \mu_{mr}M_r,\end{aligned} \tag{5.7}$$

In equation (5.7) which represents the merozoite dynamics, the first term represents merozoites released from dying infected liver cells, the second term is logistic growth of the merozoite population, the third term is loss due lysing of merozoites by effector cells, the fourth term is loss as merozoites mature into trophozoites and the fifth term is the natural death of merozoites at constant rate μ_{mr}. The rate of change of the trophozoites and schizonts populations are described by equation (5.8) and (5.9)

$$\dot{T} = \gamma k_{13} M_r - \omega T - \mu_t T. \tag{5.8}$$

In equation (5.8) which represents the trophozoites dynamics, the first term represents a proportion of trophozoites that mature into merozoites, the second term is loss as tropho-

zoites mature into schizonts and the third term is the natural death of trophozoites at a constant rate μ_t.

$$\dot{C_r} = \omega T - k_{11} N R_i \left(\frac{{C_r}^2}{{C_r}^2 + (NR_i)^2} \right) - \mu_{cr} C_r. \tag{5.9}$$

The mature trophozoites asexually divide to form schizonts [26]. In equation (5.9) which represents the evolution of blood schizonts, the first term represents gain due to maturity of trophozoite, the second term is loss due to bursting of infected red blood cells, and the third term is the natural death of schizonts at a constant rate μ_{cr}.

Mosquito stages (sporogony)

The mosquito stages (sporogonic) consist of three classes namely, susceptible midgut cells (S_{mc}), infected midgut cells (I_{mc}) and gametocytes (G). The dynamics of the midgut cells is given by:

$$\dot{S_{mc}} = \Pi_{mc} - \beta_{mc} G S_{mc} - \mu_{mc} S_{mc}. \tag{5.10}$$

The first term of equation (5.10) represents a constant source of midgut cells, the second term represents infection of susceptible midgut cells by gametocytes at a constant rate β_{mc}, and the third term is natural death of susceptible midgut cells at a constant rate μ_{mc}.

$$\dot{I_{mc}} = \beta_{mc} G S_{mc} - n_3 \mu_{imc} I_{mc}. \tag{5.11}$$

The first term of equation (5.11) represents a gain due infection of susceptible midgut cells by gametocytes at a constant rate β_{mc}, the second term represents loss of infected midgut cells due to death of infected mid gut cells. The dynamics of the gametocytes are explained by equation (5.12) below:

$$\dot{G} = (1-\gamma) k_{13} M_r - k_{12} I_{mc} \left(\frac{G^2}{G^2 + (NI_{mc})^2} \right) - \mu_g G. \tag{5.12}$$

Gametocytes are taken by the susceptible mosquito as part of a blood meal. The gametocytes dynamics are represented by equation (5.12). The first term represents a proportion of merozoites that become gametocytes, the second term is loss due to bursting of infected midgut cells, and third term is natural death of gametocytes at constant rate μ_g.

Effector cells

The effector cells include CD4+ T-cells, and CD8+ T-cells. We have simplified the dynamics of this group of cells but we hope their biological role is adequately represented.

$$\dot{E} = \omega_e \left(1 - \frac{E}{r_e}\right) E. \tag{5.13}$$

In the equation (5.13), ω_e denotes the constant growth rate of this population and r_e is the carrying capacity of the effector cells per millilitre of blood.

Positivity of solutions

Lemma 2 *Let* $S_l(0) \geq 0$, $I_l(0) \geq 0$, $P(0) \geq 0$, $C_l(0) \geq 0$, $R(0) \geq 0$, $R_i(0) \geq 0$, $M_r(0) \geq 0$, $T(0) \geq 0$. $C_r(0) \geq 0$, $S_{mc}(0) \geq 0$, $I_{mc}(0) \geq 0$, $G(0) \geq 0$, $E(0) \geq 0$. *Then, the state variables in the solution* $(S_l(t),\ I_l(t),\ P(t),\ C_l(t),\ R(t),\ R_i(t),\ M_r(t),\ T(t),\ C_r(t),\ S_{mc}(t),\ I_{mc}(t),\ G(t),\ E(t))$ *are all non negative for all time* $t > 0$ *in the region.*

$$\Gamma_e = (S_l,\ I_l,\ P,\ C_l,\ R,\ R_i,\ M_r,\ T,\ C_r,\ S_{mc},\ I_{mc},\ G,\ E)\, \epsilon\, \mathbb{R}^{13}_{+}. \tag{5.14}$$

Proof 2 *Consider the susceptible liver cells;*

$$\frac{dS_l}{dt} = \Pi_l - (\beta_l(1-\epsilon_1)P - \mu_{sl})\, S_l.$$

Multiplying both sides by the integration factor $\left(e^{\beta_l(1-\epsilon_1)\int_0^t P(s)\mathrm{d}s + \mu_{sl}t}\right)$, *we obtain:*

$$\frac{d}{dt}\left(S_l(t)e^{\beta_l(1-\epsilon_1)\int_0^t P(s)\mathrm{d}s + \mu_{sl}t}\right) = \Pi_l e^{\left(\beta_l(1-\epsilon_1)\int_0^t P(s)\mathrm{d}s + \mu_{sl}t\right)}$$

$$\begin{aligned}
S_l(t_1) &= S_l(0)e^{\left(-\beta_l(1-\epsilon_1)\int_0^{t_1} P(s)\mathrm{d}s - \mu_{sl}t\right)} \\
&\quad + \Pi_l e^{\left(-\beta_l(1-\epsilon_1)\int_0^{t1} P(s)\mathrm{d}s - \mu_{sl}t\right)} \int_0^{t_1} e^{\left(\beta_l(1-\epsilon_1)\int_0^t P(s)\mathrm{d}s + \mu_{sl}t\right)}\mathrm{d}t \\
&\quad \geq 0. \\
At\ t &= 0, S_l(t) = S_l(0) \geq 0. \\
As\ t_1 &\longrightarrow \infty, S_l(t) \geq 0.
\end{aligned}$$

Similarly, we can show that

$$\begin{aligned} &I_l(t_1) \longrightarrow 0, \quad P(t_1) \longrightarrow 0, \quad C_l(t_1) \longrightarrow 0, \quad R(t_1) \longrightarrow 0 \\ &R_i(t_1) \longrightarrow 0, \quad M_r(t_1) \longrightarrow 0, \quad T(t_1) \longrightarrow 0, \quad C_r(t_1) \longrightarrow 0 \\ &S_{mc}(t_1) \longrightarrow 0, \quad I_{mc}(t_1) \longrightarrow 0, \quad G(t_1) \longrightarrow 0, \quad R(t_1) \longrightarrow 0 \\ &E(t_1) \longrightarrow 0 \end{aligned}$$

As $t_1 \longrightarrow \infty$. The system (5.1) to (5.13) is mathematically and immunologically well-posed and we proceed to consider the dynamics of the flow generated by it in Γ_e.

5.2.2 Mathematical Analysis of the model

The analysis that follows involves deriving the equilibrium points, the reproduction number, and establishing the stability of the equilibrium points.

Stability of parasite-free equilibrium and the reproduction number

We derive the parasite-free equilibrium points by putting the variables for infected states equal to zero, giving;

$$\begin{aligned} x_{06} &= (S_l, I_l, P, C_l, R, R_i, M_r, T, C_r, S_{mc}, I_{mc}, G, E) \\ &= \left(\frac{\Pi_l}{\mu_{sl}}, 0, 0, 0, \frac{S_r}{\mu_r}, 0, 0, 0, 0, \frac{\Pi_{mc}}{\mu_{mc}}, 0, 0, r_e\right). \end{aligned}$$

The model equations (5.1 - 5.13), depending on parameter values, can possess a unique parasite present equilibrium point or multiple parasite-present equilibrium points

$$\begin{aligned} x_{07} &= (S_l, I_l, P, C_l, R, R_i, M_r, T, C_r, S_{mc}, I_{mc}, G, E) \\ &= (S_l^*, I_l^*, P^*, C_l^*, R^*, R_i^*, M_r^*, T^*, C_r^*, S_{mc}^*, I_{mc}^*, G^*, E^*), \end{aligned}$$

which algebraically are too complicated to calculate for a large model. Our numerical simulation, however, will demonstrate the existence of these points. The reproduction

number is computed by considering the infectious states only as in the previous chapters:

$$\left.\begin{array}{rcl}
\dot{I}_l &=& \beta_l(1-\epsilon_1)S_lP - k_lI_l\left(\frac{{C_l}^2}{{C_l}^2+(NI_l)^2}\right) - mEI_l - \mu_{il}I_l,\\
\dot{P} &=& \Pi_pP - \beta_pS_lP - \alpha_pP + k_{12}I_{mc}\left(\frac{G^2}{G^2+(NI_{mc})^2}\right)\\
&& +n_3\mu_{imc}I_{mc} - \mu_pP,\\
\dot{C}_l &=& \alpha_pP + k_{cl}S_l\left(1-\frac{{C_l}^2}{{C_l}^2+(NI_l)^2}\right) - k_{tp}NEC_l - n_1\mu_{cl}C_l,\\
\dot{R}_i &=& k(1-\epsilon_1)RM_r - mER_i - k_bR_i\left(\frac{{C_r}^2}{{C_r}^2+(NR_i)^2}\right) - \mu_{ri}R_i,\\
\dot{M}_r &=& n_1\mu_{il}C_l + k_rM_r\left(1-\frac{{M_r}^2}{{M_r}^2+(NR_i)^2}\right) - k_7EM_r\\
&& -k_{13}M_r - \mu_{mr}M_r,\\
\dot{T} &=& \gamma k_{13}M_r - \omega T - \mu_tT,\\
\dot{C}_r &=& \omega T - k_{11}NR_i\left(\frac{{C_r}^2}{{C_r}^2+(NR_i)^2}\right) - \mu_{cr}C_r,\\
\dot{I_{mc}} &=& \beta_{mc}GS_{mc} - n_3\mu_{imc}I_{mc},\\
\dot{G} &=& (1-\gamma)k_{13}M_r - k_{12}I_{mc}\left(\frac{G^2}{G^2+(NI_{mc})^2}\right) - \mu_gG.
\end{array}\right\} \tag{5.15}$$

From the model(5.15), the new infections are given by

$$F = \begin{pmatrix}
\beta_l(1-\epsilon_1)S_lP\\
k_{12}I_{mc}\frac{G^2}{G^2+(NI_{mc})^2} + n_3\mu_{imc}I_{mc}\\
\alpha_pP\\
k(1-\epsilon_1)RM_r\\
n_1\mu_{il}C_l\\
\gamma k_{13}\mu_r\\
\omega T\\
\beta_{mc}GS_{mc}\\
(1-\gamma)k_{13}M_r
\end{pmatrix},$$

and its Jacobian matrix at the parasite-free equilibrium is given by

$$\mathcal{F} = \mathcal{D}\mathcal{F}|(x_{06}) = \begin{pmatrix}
0 & \frac{\beta_l(1-\epsilon_1)\Pi_l}{\mu_{sl}} & 0 & 0 & 0 & 0 & 0 & 0 & 0\\
0 & 0 & 0 & 0 & 0 & 0 & 0 & n_3\mu_{imc} & 0\\
0 & \alpha_p & 0 & 0 & 0 & 0 & 0 & 0 & 0\\
0 & 0 & 0 & 0 & \frac{k(1-\epsilon_1)S_r}{\mu_r} & 0 & 0 & 0 & 0\\
0 & 0 & n_1\mu_{il} & 0 & 0 & 0 & 0 & 0 & 0\\
0 & 0 & 0 & 0 & \gamma k_{13} & 0 & 0 & 0 & 0\\
0 & 0 & 0 & 0 & 0 & \omega & 0 & 0 & 0\\
0 & 0 & 0 & 0 & 0 & 0 & 0 & 0 & \frac{\beta_{mc}\Pi_{mc}}{\mu_{mc}}\\
0 & 0 & 0 & 0 & (1-\gamma)k_{13} & 0 & 0 & 0 & 0
\end{pmatrix}.$$

The other transitions among the states are given by

$$V = \begin{pmatrix} k_l I_l \left(\frac{C_l^2}{C_l^2+(NI_l)^2}\right) + mEI_l + \mu_{il} I_l \\ -\Pi_p P + \beta_p S_l P + \alpha_p P + \mu_p P \\ -k_{cl} S_l \left(1 - \frac{C_l^2}{C_l^2+(NI_l)^2}\right) + k_{tp} NEC_l + n_1 \mu_{cl} C_l \\ mER_i + k_b R_i \left(\frac{C_r^2}{C_r^2+(NR_i)^2}\right) + \mu_{ri} R_i \\ -k_r M_r \left(1 - \frac{M_r^2}{M_r^2+(NR_i)^2}\right) + k_7 EM_r + k_{13} M_r + \mu_{mr} M_r \\ \omega T + \mu_t T \\ k_{11} NR_i \left(\frac{C_r^2}{C_r^2+(NR_i)^2}\right) + \mu_{cr} C_r \\ n_3 \mu_{imc} I_{mc} \\ k_{12} I_{mc} \left(\frac{G^2}{G^2+(NI_mc)^2}\right) \end{pmatrix},$$

with its Jacobian matrix at the parasite-free equilibrium given by

$$\mathcal{V} = \mathcal{D}\mathcal{V}|(x_{06}) = \begin{pmatrix} Q_1 & 0 & 0 & 0 & 0 & 0 & 0 & 0 & 0 \\ 0 & Q_2 & 0 & 0 & 0 & 0 & 0 & 0 & 0 \\ 0 & 0 & Q_3 & 0 & 0 & 0 & 0 & 0 & 0 \\ 0 & 0 & 0 & Q_4 & 0 & 0 & 0 & 0 & 0 \\ 0 & 0 & 0 & 0 & Q_5 & 0 & 0 & 0 & 0 \\ 0 & 0 & 0 & 0 & 0 & Q_6 & 0 & 0 & 0 \\ 0 & 0 & 0 & 0 & 0 & 0 & \mu_{cr} & 0 & 0 \\ 0 & 0 & 0 & 0 & 0 & 0 & 0 & n_3\mu_{imc} & 0 \\ 0 & 0 & 0 & 0 & 0 & 0 & 0 & 0 & \mu_g \end{pmatrix}.$$

Where

$$Q_1 = mr_e + \mu_{il}, \quad Q_2 = \left(\frac{\Pi_l \beta_p}{\mu_{sl}} + \alpha_p + \mu_p - \Pi_p\right),$$
$$Q_3 = Nk_{tp} r_e + n_1 \mu_{cl}, \quad Q_4 = mr_e + \mu_{ri},$$
$$Q_5 = k_{13} - k_r + \mu_{mr} + k_7 r_e, \quad Q_6 = \omega + \mu_t.$$

The product $\mathcal{FV}^{-1}$ is given by

$$\mathcal{FV}^{-1} = \begin{pmatrix} 0 & \frac{\Pi_l(1-\epsilon_1)\beta_l}{Q_2} & 0 & 0 & 0 & 0 & 0 & 0 & 0 \\ 0 & 0 & 0 & 0 & 0 & 0 & 0 & 1 & 0 \\ 0 & \frac{\alpha_p}{Q_2} & Q_3 & 0 & 0 & 0 & 0 & 0 & 0 \\ 0 & 0 & 0 & 0 & \frac{k(1-\epsilon_1)S_r}{\mu_r Q_5} & 0 & 0 & 0 & 0 \\ 0 & 0 & \frac{n_1\mu_{il}}{Q_3} & 0 & 0 & 0 & 0 & 0 & 0 \\ 0 & 0 & 0 & 0 & \frac{\gamma k_{13}}{Q_5} & 0 & 0 & 0 & 0 \\ 0 & 0 & 0 & 0 & 0 & \frac{\omega}{\omega+\mu_t} & 0 & 0 & 0 \\ 0 & 0 & 0 & 0 & 0 & 0 & 0 & 0 & \frac{\Pi_{mc}\beta_{mc}}{\mu_g\mu_{mc}} \\ 0 & 0 & 0 & 0 & \frac{(1-\gamma)k_{13}}{Q_5} & 0 & 0 & 0 & 0 \end{pmatrix},$$

The largest eigenvalue of $\mathcal{FV}^{-1}$ is called the reproduction number and is given by;

$$R_{06} = \sqrt[5]{\left(\frac{\Pi_{mc}(1-\epsilon_1)\beta_{mc}}{\mu_g\mu_{mc}}\right)\left(\frac{\Pi_l\beta_l}{Q_2}\right)\left(\frac{k(1-\epsilon_1)S_r}{\mu_r Q_5}\right)\left(\frac{n_1\mu_{il}}{Q_3}\right)\left(\frac{\omega}{\omega+\mu_t}\right)} \quad (5.16)$$

$$R^*_{06} = \left(\frac{\Pi_{mc}(1-\epsilon_1)\beta_{mc}}{\mu_g\mu_{mc}}\right)\left(\frac{\Pi_l\beta_l}{Q_2}\right)\left(\frac{k(1-\epsilon_1)S_r}{\mu_r Q_5}\right)\left(\frac{n_1\mu_{il}}{Q_3}\right)\left(\frac{\omega}{\omega+\mu_t}\right) \quad (5.17)$$

Since ϵ_1 ranges between 0 and 1. We see that as $\epsilon_1 \longrightarrow 1$, $R^*_{06} \longrightarrow 0$ and as $\epsilon_1 \longrightarrow 0$,

$$R^*_{06} = R^*_{07} = \left(\frac{\Pi_{mc}\beta_{mc}}{\mu_g\mu_{mc}}\right)\left(\frac{\Pi_l\beta_l}{Q_2}\right)\left(\frac{kS_r}{\mu_r Q_5}\right)\left(\frac{n_1\mu_{il}}{Q_3}\right)\left(\frac{\omega}{\omega+\mu_t}\right), \quad (5.18)$$

where

$$R_{07} = \sqrt[5]{R_{07^*}} = \sqrt[5]{\left(\frac{\Pi_{mc}\beta_{mc}}{\mu_g\mu_{mc}}\right)\left(\frac{\Pi_l\beta_l}{Q_2}\right)\left(\frac{kS_r}{\mu_r Q_5}\right)\left(\frac{n_1\mu_{il}}{Q_3}\right)\left(\frac{\omega}{\omega+\mu_t}\right)}. \quad (5.19)$$

We want to determine, in the section on simulation, the least efficacy $\epsilon_1^* < 1$ for which the disease clears. The reproduction numbers R_{06} and R_{07} are positive if
$k_{13} + \mu_{mr} + k_7 r_e > k_r$ and $\frac{\Pi_l\beta_p}{\mu_{sl}} + \alpha_p + \mu_p > \Pi_p$
We can explain R^*_{06} in terms of the three stages of the malaria life cycle as follows; The contribution to the reproduction number R_{06} by each stage is explained below: $R_{0L} = \left(\frac{\Pi_l\beta_l}{Q_2}\right)$ defines the reproductive ratio for the liver stage. $R_{0B} = \left(\frac{kS_r}{\mu_r Q_5}\right)\left(\frac{n_1\mu_{il}}{Q_3}\right)\left(\frac{\omega}{\omega+\mu_t}\right)$ defines the reproduction ratio for the red blood stage and $R_{0M} = \left(\frac{\Pi_{mc}\beta_{mc}}{\mu_g\mu_{mc}}\right)$ defines the reproduction ratio for the mosquito stage. The fifth root of the reproduction number R_{06} indicates the path the parasite undergoes through from the mosquito through the liver, the blood stream before starting another cycle in the mosquito. We can state the following

stability theorem for the parasite-free equilibrium point.

Theorem 5.2.1 *The parasite-free equilibrium is locally asymptotically stable if* $R_{06} < 1$, *otherwise it is unstable.*

5.2.3 Simulations

The model equations (5.1) to (5.13) require several input parameter values, which can be divided into three sets, namely (i) those that have been measured clinically or experimentally [TABLE 5.4] and [TABLE 5.5], (ii) those that have been estimated by other researchers [TABLE 5.4] and [TABLE 5.5], (iii) those that have been estimated by us [TABLE 5.4] and [TABLE 5.5].

TABLE. 5.4. The table with the parameters, values and source

Parameter	Value/range of values	Source
Π_l	$9.9 * 10^5 < \Pi_l < 2 * 10^{11}$	Estimated [15, 19, 68]
β_l	$4 * 10^{(-10)}$	[19]
μ_{sl}	$0.004 < \mu_{sl} < 0.01$	Estimated[19]
k_l	0.2	Estimated
N	32	[55]
m	$10^{(-8)}$	[5]
μ_{il}	$0.01 < \mu_{il} < 0.1$	[19]
Π_p	$0 < \Pi_p < 10^5$	Estimated [47, 87]
β_p	$4 * 10^{(-10)} < \beta_p < 4 * 10^{(-9)}$	Estimated
α_p	$0.2 < \alpha_p < 0.5$	Estimated
k_{12}	$0.2 < k_{12} < 0.3$	Estimated
n_3	$5 < n_3 < 30$	Estimated
μ_{imc}	$0.01 < \mu_{imc} < 0.2$	Estimated
μ_p	$0.001 < \mu_p < 0.01$	Estimated
k_{cl}	0.02	Estimated
k_{tp}	$0.0001 < k_{tp} < 0.25$	Estimated
n_1	$12 < n_1 < 32$	[55]
μ_{cl}	0.01	Estimated
S_r	$2.5 * 10^8 < S_r < 2.5 * 10^9$	Estimated [89, 101]
k	$2 * 10^{(-9.25)} < k < 2 * 10^{(-8)}$	Estimated [89]

Sensitivity analysis

FIG. 5.1 shows how some parameters are correlated to R_{07}, and how sensitive R_{07} is to changes in these parameters. Knowledge of how these parameters affect R_{07} helps to determine whether the severity of the disease will be overestimated or underestimated as these parameters vary. If a parameter is positively correlated to R_{07} then increasing that parameter overestimates the severity of the disease. On the other hand, if a parameter is negatively correlated to R_{07} then changes in that parameter could underestimate the

TABLE. 5.5. The table with the parameters, values and source

Parameter	Value/range of values	Source
μ_r	0.01	[101]
k_b	0.4	Estimated
μ_{ri}	0.2	[101]
k_r	$0.001 < k_r < 0.01$	Estimated
k_7	$10^{(-8)}$	[5, 89]
k_{13}	0.6	Estimated
μ_{mr}	$0.0208 < \mu_{mr} < 0.1$	Estimated [89]
γ	$0.003 < \gamma < 0.4$	Estimated
ω	$10^{(-4)} < \omega < 0.01$	Estimated
μ_t	0.01	Estimated
k_{11}	0.02	Estimated
μ_{cr}	0.2	Estimated
Π_{mc}	$2.4 * 10^2 < \Pi_{mc} < 2.4 * 10^4$	[17]
β_{mc}	$10^{(-8)} < \beta_{mc} < 10^{(-7)}$	Estimated
μ_{mc}	$10^{(-10)} < \mu_{mc} < 0.025$	Estimated
μ_{imc}	$0.01 < \mu_{imc} < 0.2$	Estimated
μ_g	$0.04 < \mu_g < 0.4$	Estimated [89]
ω_e	0.04	Estimated
r_e	$2.1 * 10^5$	[97, 100]

severity of the disease.

The range of the parameter n_1 is known and is given in McQueen and McKenzie [55]. The parameter μ_{sl} is significantly positively correlated to R_{07}. This is an important parameter estimated in [19]. Parameters β_l and μ_{il} are given in [19] and parameter Π_{mc} is given in [17]. The parameters Π_l, S_r, k, which have not been estimated clinically or experimentally are estimated in [15, 19, 68, 89, 101] respectively. We can see from the sensitivity analysis that the reproduction number R_{07} is highly positively correlated to ω, rate of loss or gain of trophozoites, β_{mc}, infection rate and k_r, growth rate due to infection of RBCs. Parameters k_7,N, r_e, μ_r, are given/estimated in [5, 55, 89, 97, 100, 101] respectively. The parameters μ_g and μ_{mr} have not been determined clinically or experimentally but are estimated in [89]. We can also see that, the reproduction number is negatively correlated to k_{tp}, μ_p, μ_{cl}, μ_{mc}, α_p, k_{13}, β_p, μ_t. There is a need to determine these parameters either clinically or experimentally.

The time used in our simulations is from $t = 0$ days to 60 days, which, clinically, is the time for an infected person to show symptoms of malaria. In this example, we have started treatment on 30^{th} day after the initial infection. This is because, the average time for clinical symptoms to appear is estimated to be between $(8 - 25)$ days although this period

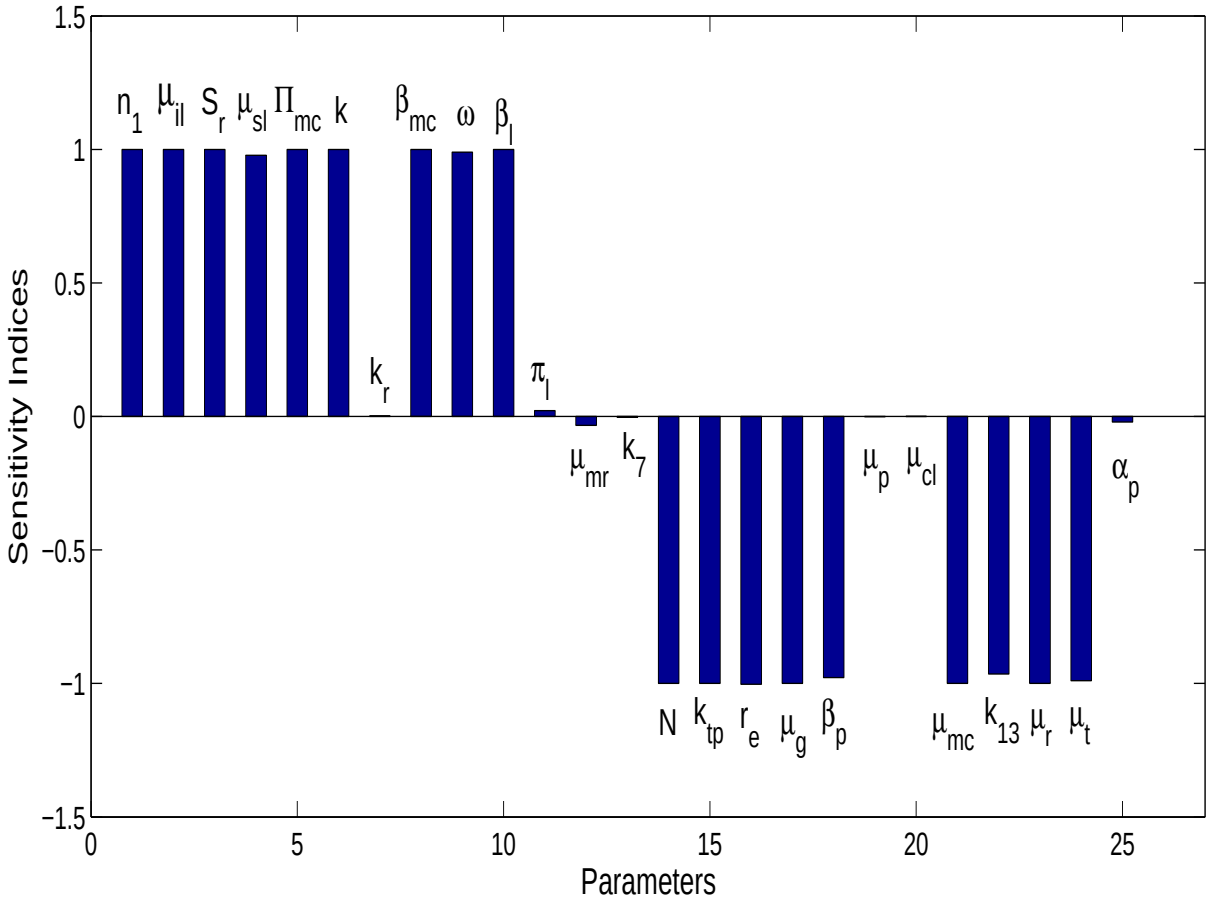

FIG. 5.1. Diagram shows sensitivity analysis of R_{07}.

can be much longer depending on the immune system of the host [48].

5.3 Results

The numerical simulation of the model equations (5.1) to (5.13) considers how changes in the parameters affect the dynamics of the disease and the role of treatment.

5.3.1 Dynamics of the system before treatment

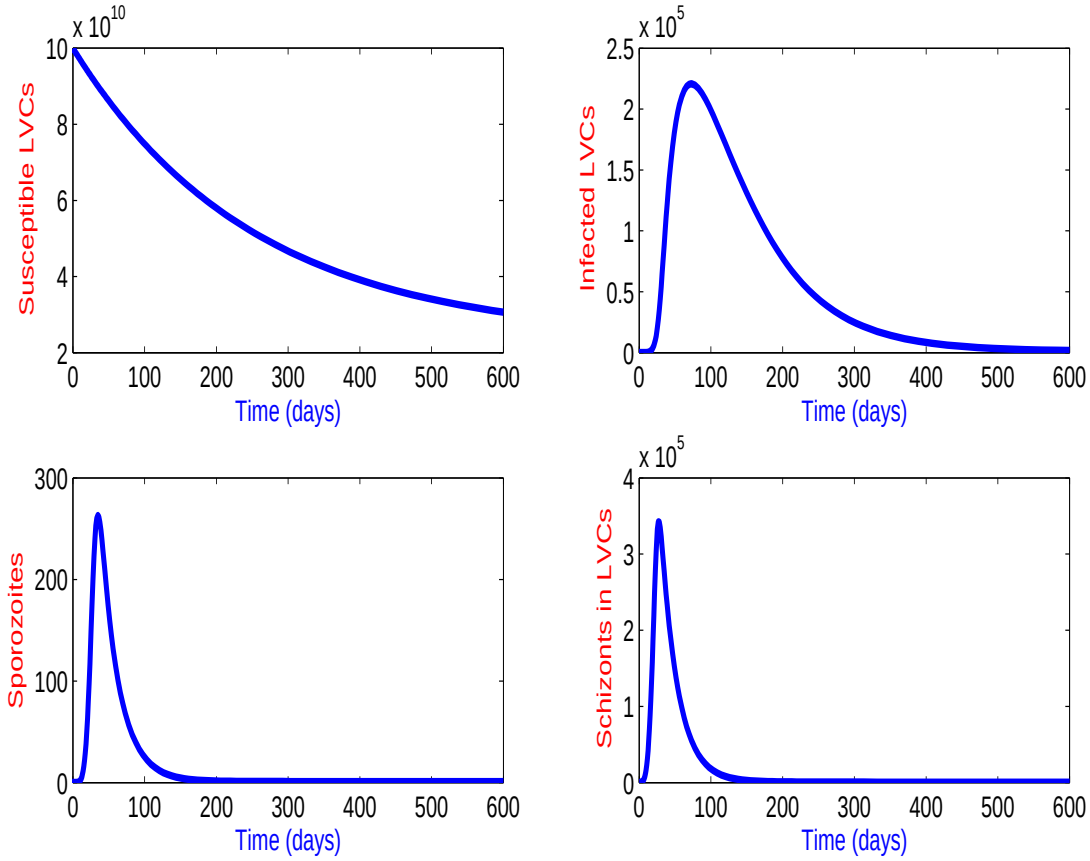

FIG. 5.2. Diagram shows the parasite-free equilibrium (DFE) at liver stage with $R_{07} = 0.0063$.

FIG. 5.2 shows the time plots for the various classes during the liver stage. Susceptible liver cells (LVCs) drop initially but eventually settle at parasite-free level. All the infected LVCs, sporozoites and schizonts inside LVCs tend to zero and the disease does not establish itself.

FIG. 5.3 shows the time plots for the various classes during the blood stage of the disease. The susceptible RBCs drop initially but eventually settle at parasite-free level which is

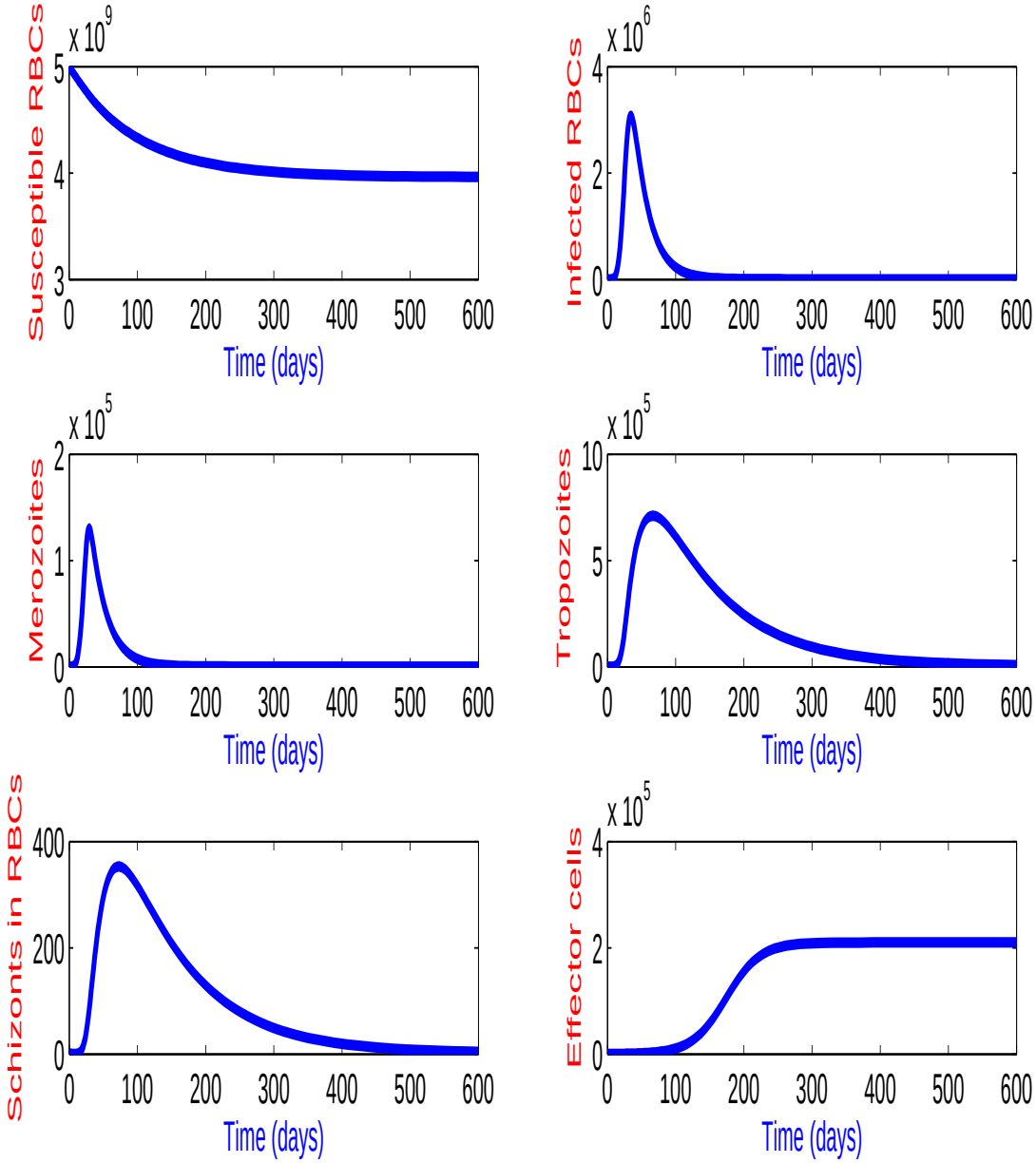

FIG. 5.3. Diagram shows the parasite-free equilibrium (DFE) at blood stage $R_{07} = 0.0063$.

high enough to sustain the life. All the infected classes tend to zero. The effector cells increase logistically.

FIG. 5.4 shows the various classes during the mosquito stage of the replication cycle. The

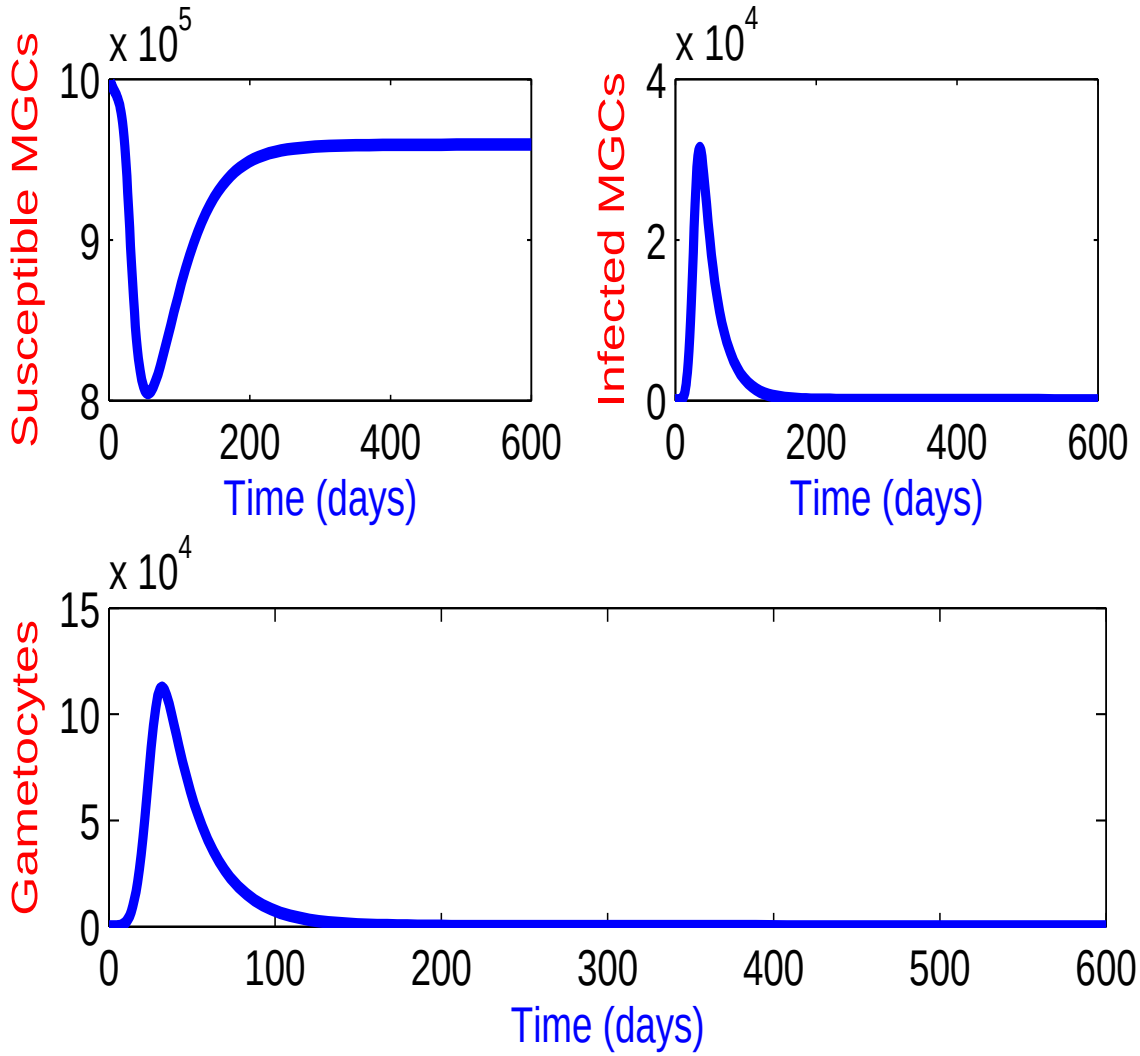

FIG. 5.4. Diagram shows the parasite-free equilibrium (DFE) at mosquito stage $R_{07} = 0.0063$.

susceptible MGCs drop initially and settle at parasite-free level. All the infected classes tend to zero.

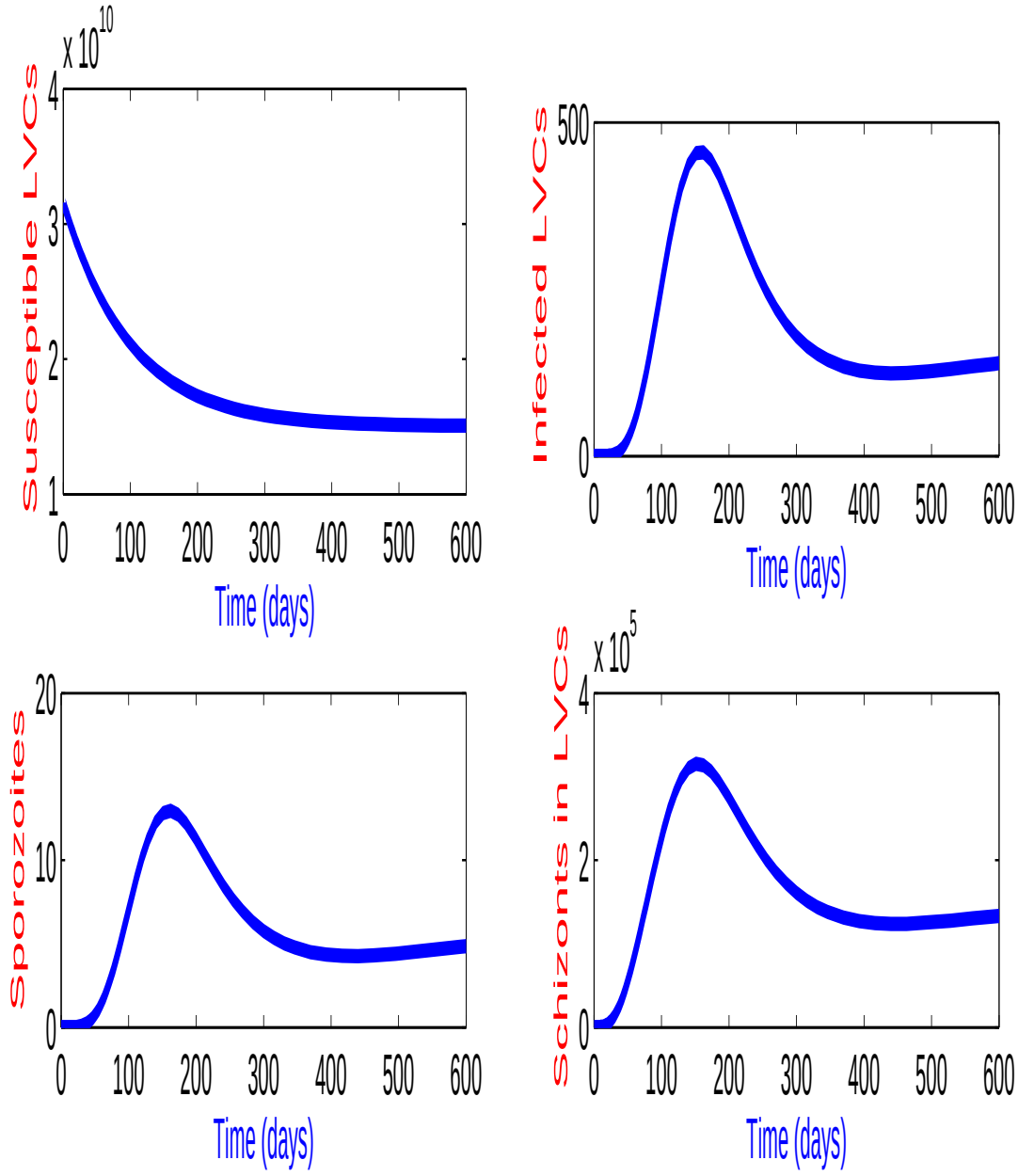

FIG. 5.5. Diagram shows the parasite-present equilibrium point (EEP) at liver stage $R_{07} = 4.7265$.

FIG. 5.5, FIG. 5.6 and FIG. 5.7 are time plot of various class during the liver, blood stage and mosquito stages respectively. It is clear that the disease establishes itself.

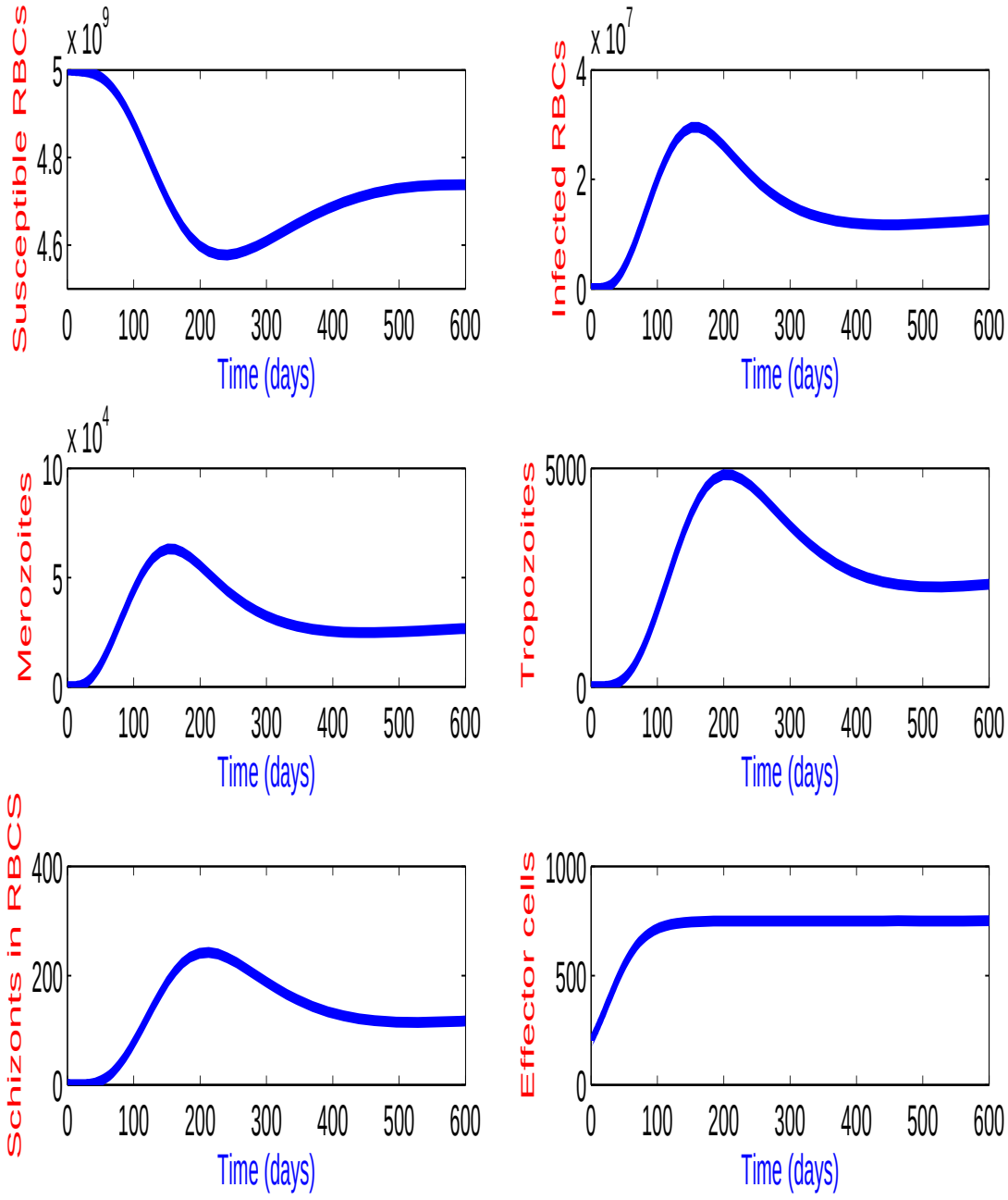

FIG. 5.6. Diagram shows the parasite-present equilibrium point (EEP) at blood stage $R_{07} = 4.7265$.

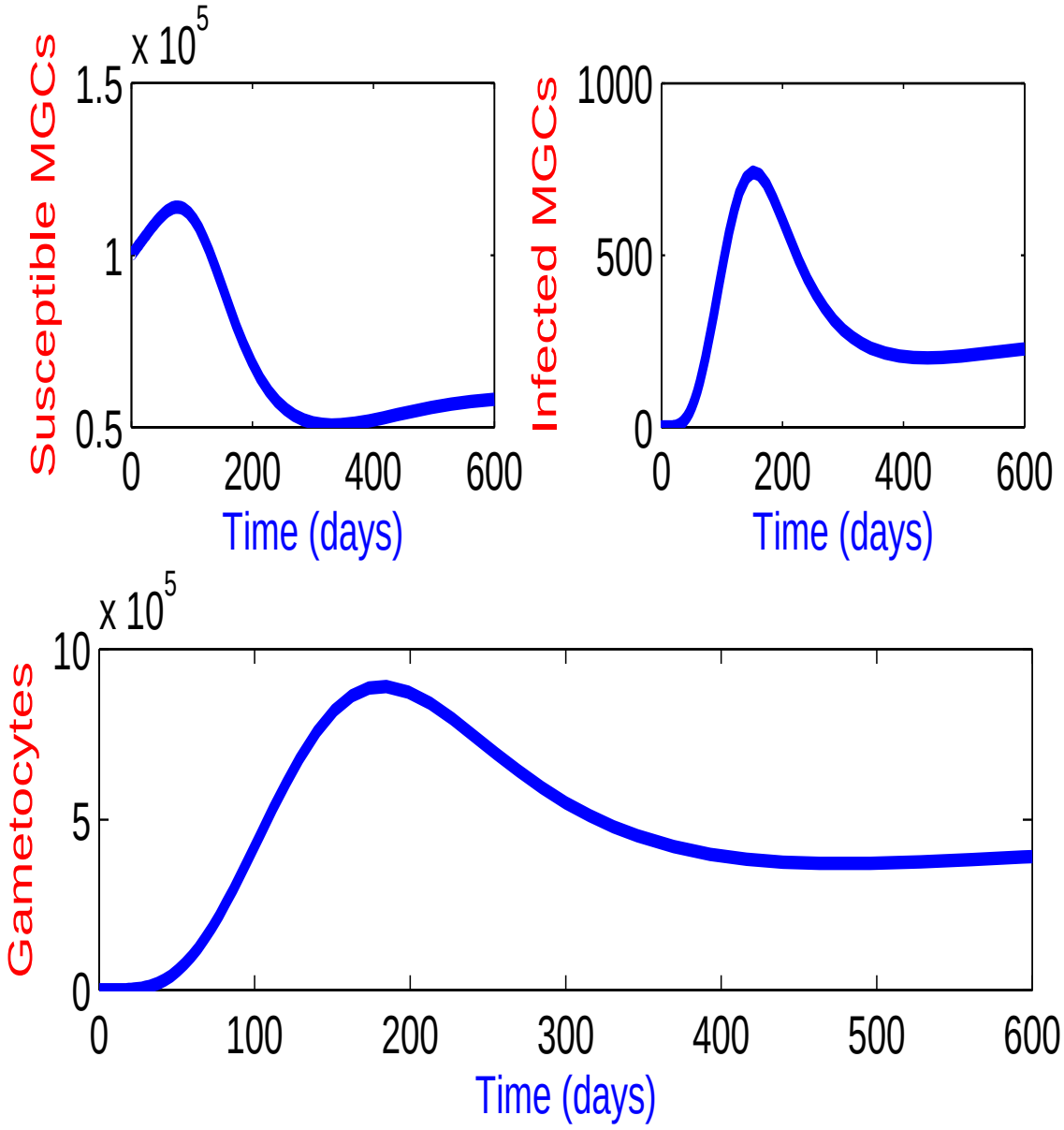

FIG. 5.7. Diagram shows the parasite-present equilibrium point (EEP) at mosquito stage $R_{07} = 4.7265$.

FIG. 5.8 shows the variation of k_{tp} and n_1 with R_{06}. As k_{tp} increases it reduces the reproduction number R_{07} in agreement the results of our sensitivity analysis. On the other hand, increasing μ_{il} increases R_{07} FIG. 5.9.

Increasing killing rate of merozoites by effector cells, reduces the disease manifestation in the blood as illustrated in the FIG. 5.10. Also increasing the growth rate of merozoites, increases the severity of the disease manifested by a sharp decline in population of RBCs.

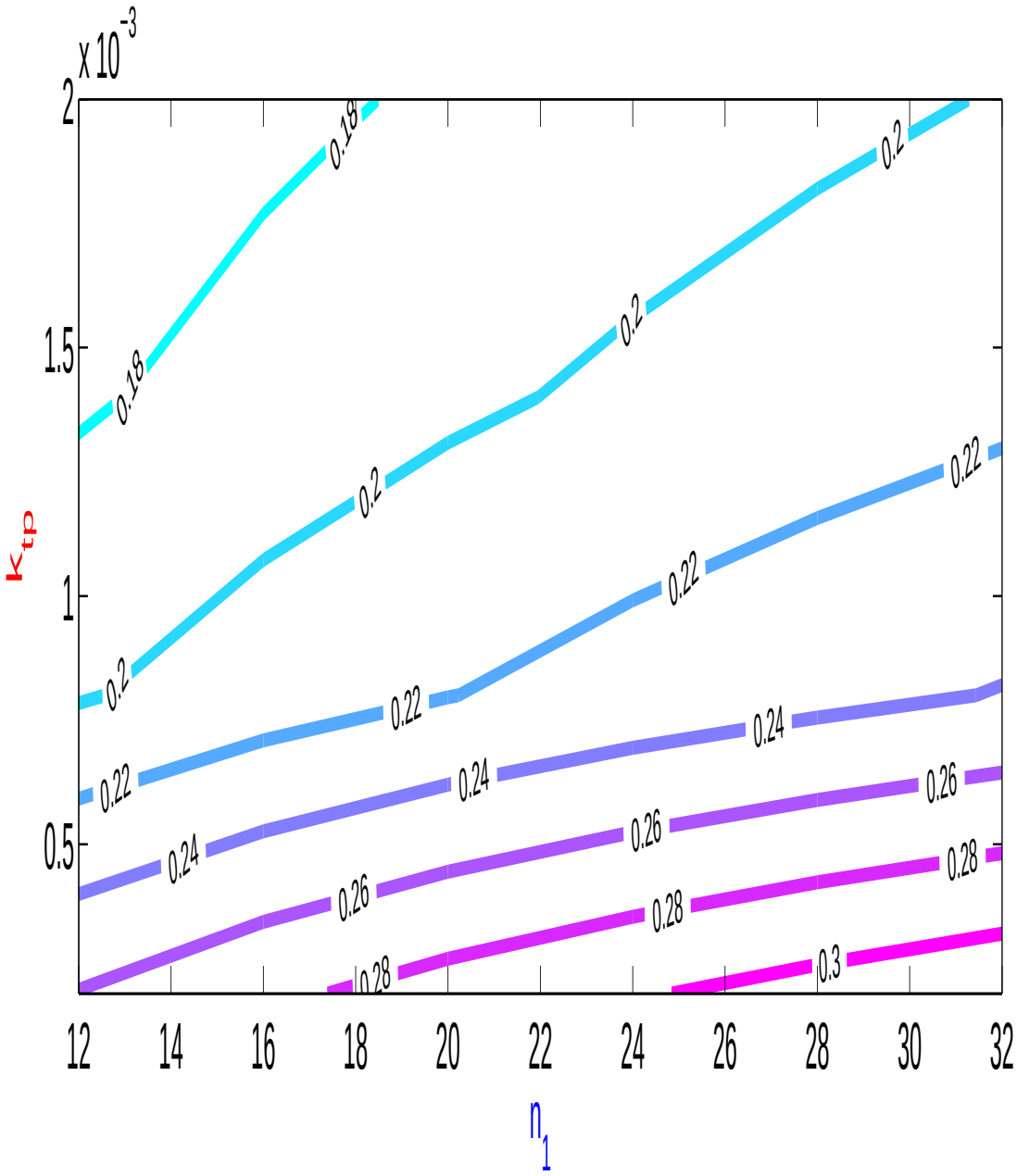

FIG. 5.8. Shows the contour plot of R_{07} as a function of an average number of schizonts release from an infected liver cells that die naturally (n_1) and the rate of loss of schizonts inside liver cells that are killed by effector cells (k_{tp}).

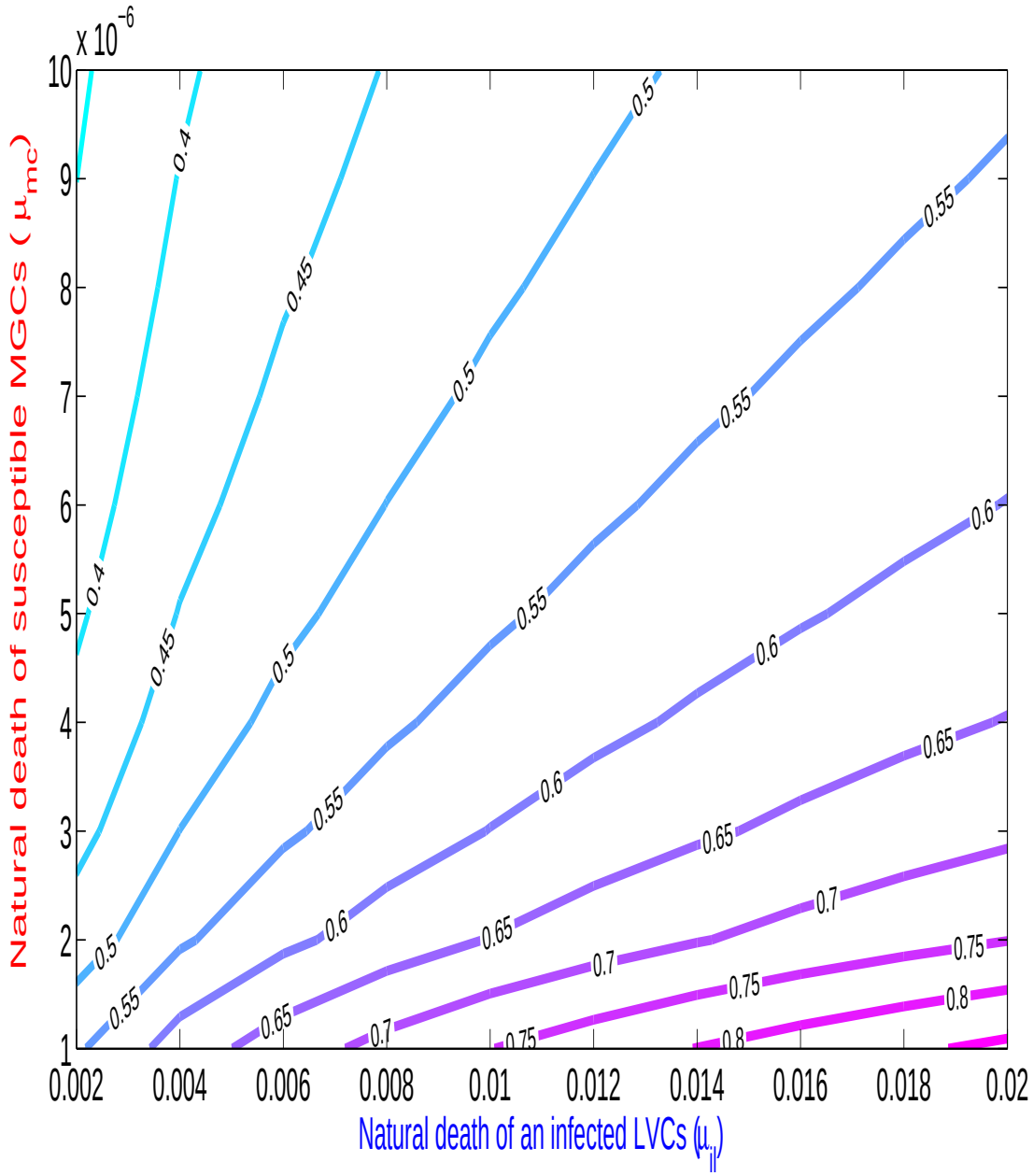

FIG. 5.9. Shows the contour plot of R_{07} as a function of the natural death of an infected liver cells (μ_{il}) and natural death of susceptible midgut cells (μ_{mc}).

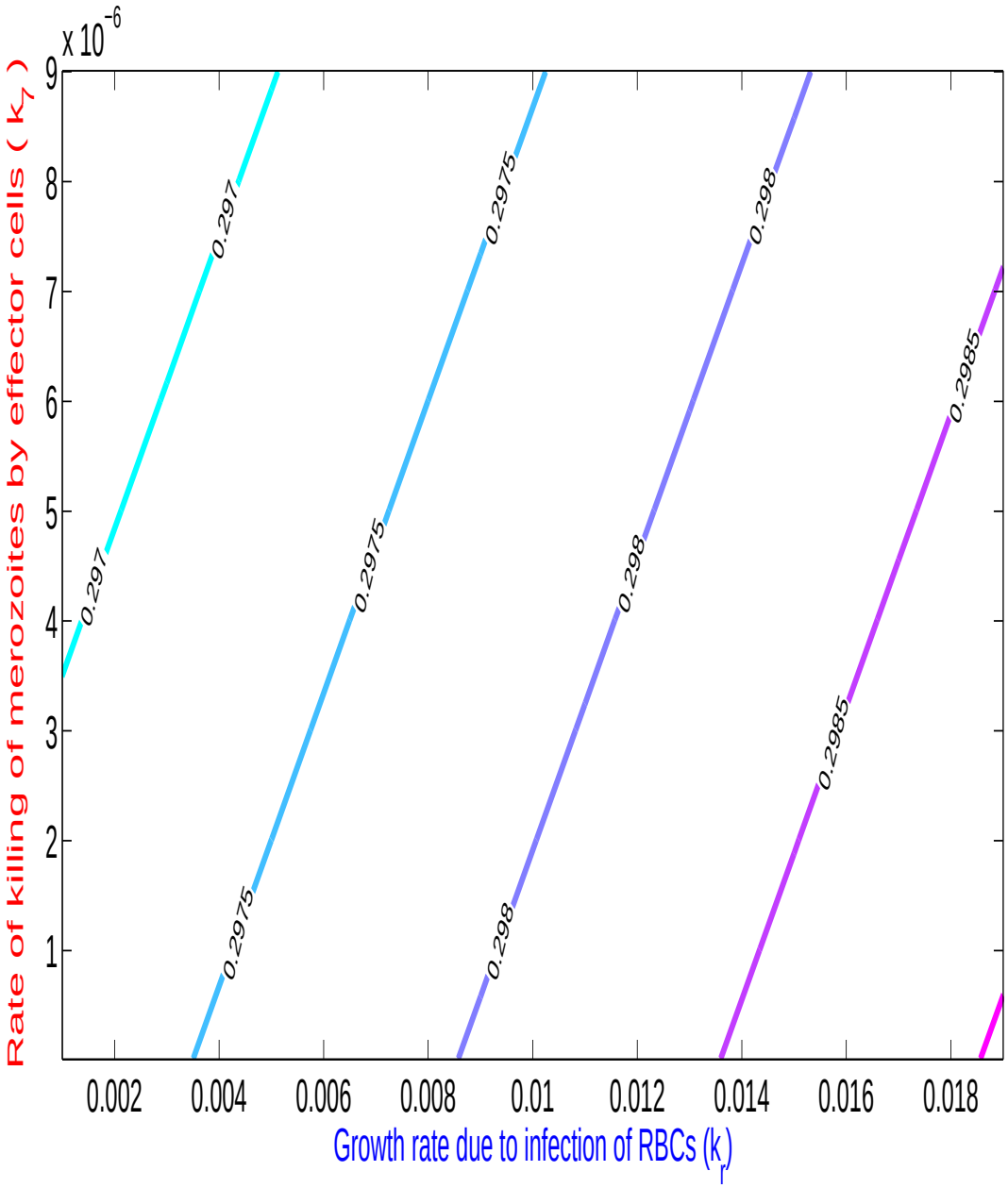

FIG. 5.10. Shows the contour plot of R_{07} as a function of the growth rate due to infection of RBCs (k_r) the rate of killing of merozoites by effector cells(k_7).

5.3.2 Treatment strategy

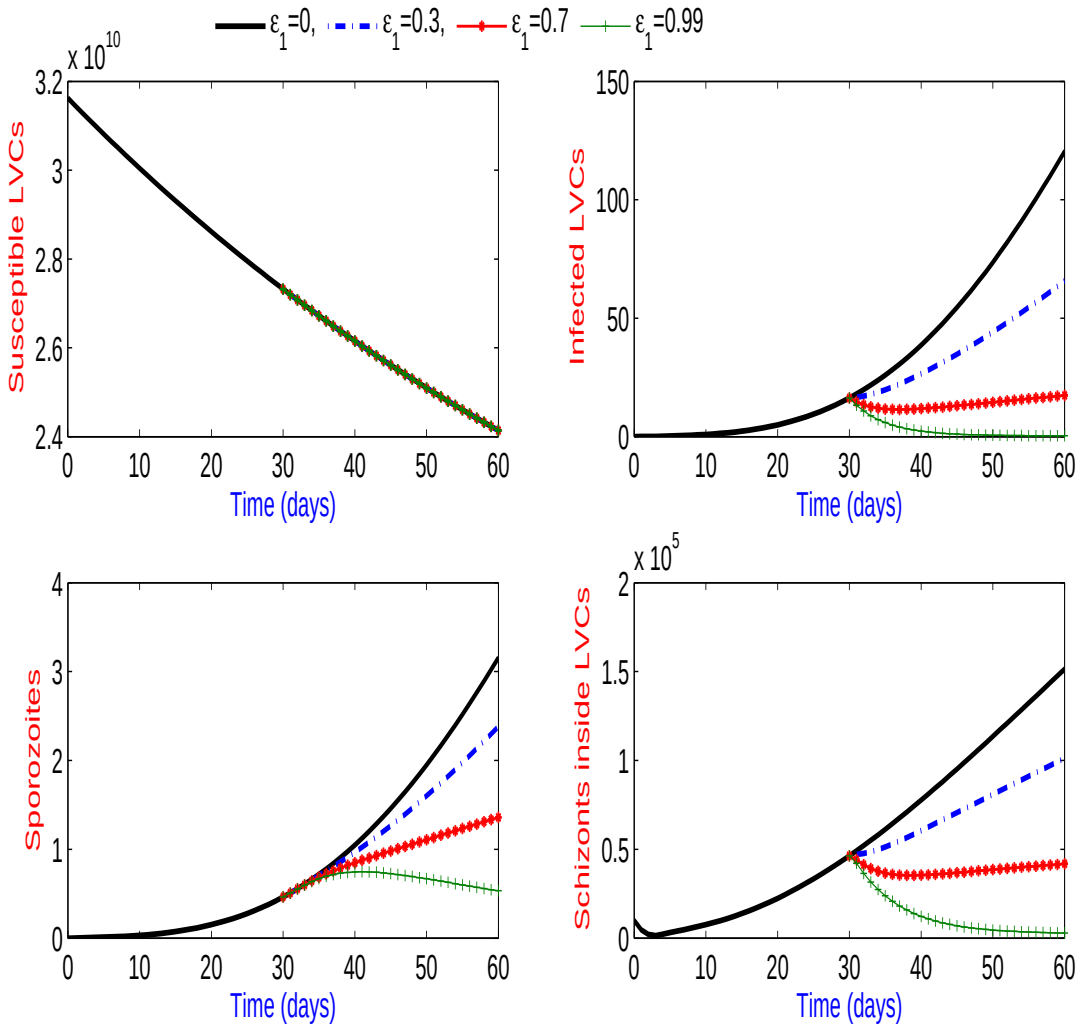

FIG. 5.11. Diagram shows an application of treatment after 30 days at liver stage and $\epsilon_1 = 0 \Longrightarrow R_{06} = 4.7265$, $\epsilon_1 = 0.3 \Longrightarrow R_{06} = 4.0980$, $\epsilon_1 = 0.7 \Longrightarrow R_{06} = 2.9200$, $\epsilon_1 = 0.99 \Longrightarrow R_{06} = 0.7491$.

FIG. 5.11 shows time plot of various classes during the liver stage as treatment is administered for drug efficacy ranging from $\epsilon_1 = 0$ to $\epsilon_1 = 0.99$. The susceptible liver cell populations do not change due to clearance of the pathogen as the drug efficacy increases. The infected liver cell populations, Sporozoites and schizonts decrease with increasing efficacy. The reproduction number is a decreasing function of efficacy, for example, $R_{06} = 4.0980$ for $\epsilon_1 = 0$ and $R_{06} = 0.7491$ for $\epsilon_1 = 0.99$.

FIG. 5.12 shows time plot of various classes during the blood stage of the disease in the

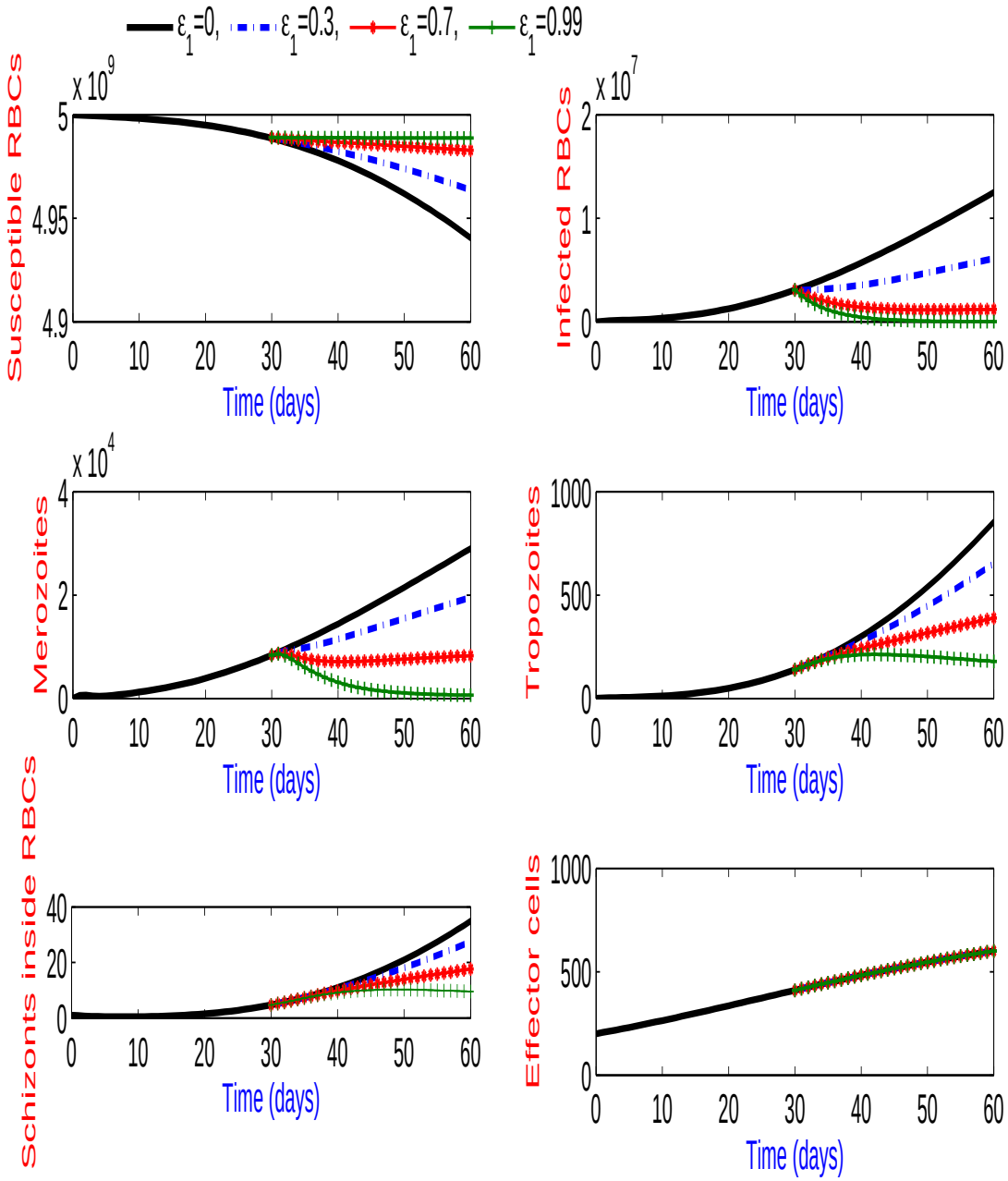

FIG. 5.12. Diagram shows an application of treatment after 30 days at blood stage and $\epsilon_1 = 0 \Longrightarrow R_{06} = 4.7265$, $\epsilon_1 = 0.3 \Longrightarrow R_{06} = 4.0980$, $\epsilon_1 = 0.7 \Longrightarrow R_{06} = 2.9200$, $\epsilon_1 = 0.99 \Longrightarrow R_{06} = 0.7491$.

presence of treatment. The susceptible RBCs population increases with increasing treatment efficacy. The infected classes decrease with increasing treatment efficacy.

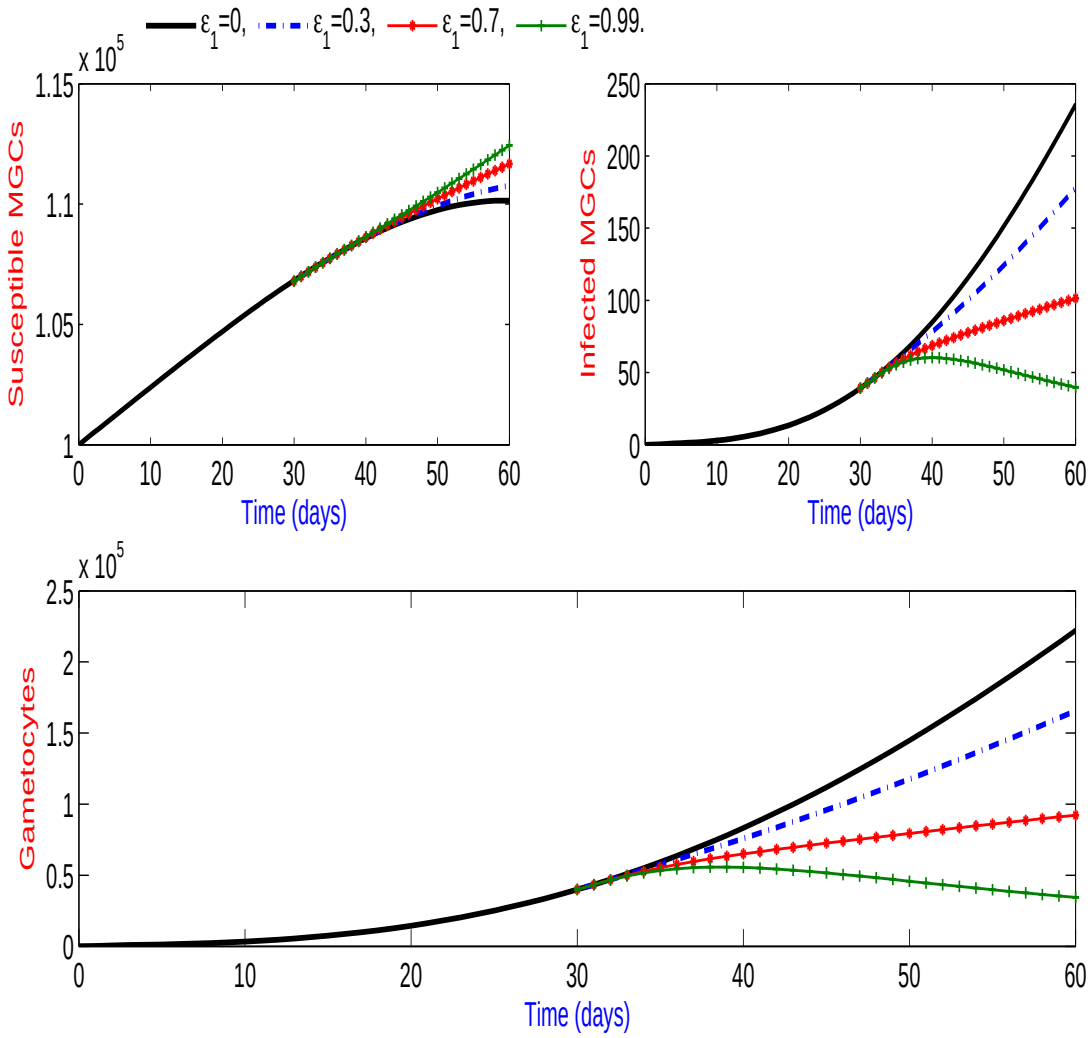

FIG. 5.13. Diagram shows an application of treatment after 30 days at mosquito stage and $\epsilon_1 = 0 \Longrightarrow R_{06} = 4.7265$, $\epsilon_1 = 0.3 \Longrightarrow R_{06} = 4.0980$, $\epsilon_1 = 0.7 \Longrightarrow R_{06} = 2.9200$, $\epsilon_1 = 0.99 \Longrightarrow R_{06} = 0.7491$.

5.4 Discussion

We investigated the interaction between the malaria parasites and the immune cells for all the three stages of malaria life cycle. The model has been studied and results were presented. The effect of treatment was discussed using numerical results with reasonable choices of parameter values. Therapy which was represented by drug efficacy ϵ_1 and targeted to kill sporozoites, merozoites and gemotocytes.

The model investigated the interaction between the malaria parasites and the immune cells for all three stages of the malaria life cycle. The three- stage malaria model presents many challenges in that there are many parameters that are not known clinically. However, using the known parameters, we have performed a sensitivity analysis ([7]) which has helped to determine the magnitude and range of our unknown parameters. This analysis has shown that the reproduction number R_{07} is positively correlated to the rate of gain/loss of trophozoites (ω), infection rate (β_{mc}), and growth rate due to infection of RBCs (k_r), and is negatively correlated to rate of loss of schizonts inside the liver cells that are killed by effector cells (k_{tp}), natural death of sporozoites (μ_p), natural death of schizonts inside the liver cells (μ_{cl}), natural death of susceptible midgut cells (μ_{mc}), rate of gain/loss of sporozoites (α_p), rate of loss of merozoites (k_{13}), infection rate (β_p) and natural death of trophozoites (μ_t). Overestimation of rate of gain/loss of trophozoites (ω), β_{mc}, and growth rate due to infection of RBCs (k_r) or underestimation of rate of loss of schizonts inside the liver cells that are killed by effector cells (k_{tp}), $\mu_p, \mu_{cl}, \mu_{mc}, \alpha_p, k_{13}, \beta_p$ and μ_t can have serious implications regarding the prognosis of the disease. There is a need for clinical or experimental determination of these parameters.

The contour plot results (FIG. 5.8, FIG. 5.9 and FIG. 5.10) have shown how changes in some parameters affected the reproduction number. The results are in agreement with the sensitivity and uncertainty analysis results. The graphs corresponding to $R_{07} < 1$ and those corresponding to $R_{07} > 1$ are in agreement with the predictions of (Theorem 5.2.1).

As in the previous chapter on treatment, treatment had the effect of slowing down the depletion of susceptible cells and clearance the parasite populations. Our results showed that when using therapy with an efficacy of $\epsilon_1 = 0.99$, the infected liver cells, and infected red blood cells take 10 days to revert to a parasite-free equilibrium state $R_{06} = 0.7494$.

As in the previous Chapter 4, we recommend a change in the manner treatment is administered. Specifically, malaria treatment should be administered at health centres like tuberculosis and in the presence of healthy workers. We believe that only a malaria vaccine can reliably protect against all stages of malaria infection.

Chapter 6

Conclusion

Mathematical models of interactions of malaria parasites and the host immune system have been presented in this study. We discussed the mathematical and numerical analysis of these models. We then introduced treatment efficacy (ϵ_1) to enable us explore the effect of treatment on the pathogenesis of malaria. The results obtained from the models presented in Chapters 4, and 5 are as follows:

1. The model of the blood stage in Chapter 4, revealed that parasite replicative characteristics allow the parasite to evade the immune response during the red blood stage of malaria infection. We found that, the larger a threshold number of intracellular parasites released as a results of the natural death of an activated RBC (n_1) is, the longer it takes to produce the parasites and the higher the chance of an infected red blood cell being identified and apoptosised by the effector cells. Hence we concluded that in order to minimize the possibility of infected red blood cells being detected and eliminated by the immune cells, the parasite infects older red blood cells whose life expectancy is much shorter than the younger cells thereby avoiding the infected red blood cell from being detected and apoptosised.

2. The effect of drug efficacy at blood stage cycle in Chapter 4 showed that, a high drug efficacy of $\epsilon_1 = 0.95$ could stop the development of the disease. Since most malaria treatment drugs are of higher efficacy than 0.6, it is possible to combat malaria with treatment drugs but the administration of drugs should be done at health centres or hospitals to ensure that patients complete their treatment.

3. The model with three stages of malaria life cycle in Chapter 5, showed that, as the drug efficacy increases up to $\epsilon_1 = 0.99$ and $R_{06} = 0.7494$, the populations of the infected LVC and infected RBC approach the parasite-free equilibrium after 10 days. Sporozoites, schizonts and gametocytes took more than 10 days to approach the disease free equilibrium with an efficacy of $\epsilon_1 = 0.99$. We found that, treatment had the

effect slowing down the depletion of susceptible cells and clearing the parasite populations. This showed that an effective drug treatment could stop the development of disease.

6.1 Limitations and recommendations

Due to the detailed nature of the models developed in this study, some of the parameters used have not been clinically or experimentally determined before. This has been the biggest challenge in our assessment. The models studied in this thesis lacked data sets that would be fitted on them so as to validate the predictions of the observed outputs. We therefore recommend that, the clinicians or experimentalists estimate the unknown and important parameters such as: rate of loss of schizonts inside the liver cells that are killed by effector cells (k_{tp}), threshold number as a results of gain due to infection of susceptible RBC by extracellular parasites (n^*k^*), rate of loss of schizonts due to bursting of infected RBCs (k_{11}), rate of loss of infected RBCs due to bursting of infected RBCs (k_b), proportion of merozoites (γ), proportion of RBCs (α), growth rate of effector cells (ω_e), natural death of infected midgut cells (μ_{imc}), natural death of schizonts inside RBCs (μ_{cr}), growth rate of schizonts (k_{cl}), natural death of sporozoites (μ_p), natural death of sporozoites (n_3), rate of bursting of infected midgut cells (k_{12}), rate of bursting of infected liver cells (k_l), that have been influential in the predictions of the models outputs. We recommend that therapy with highly efficacious drugs would be an effective control measure in eradicating malaria at all stages but we think that only a malaria vaccine could reliably protect against all stages malaria infection. We have also shown that chronic infections can transform manageable malaria into a more active disease. The recommendation from our study is that; in malaria endemic areas, individuals with malaria or showing malaria symptoms should be tested for chronic infections and those who test positive for any chronic infection should be treated for both malaria and the chronic infection. We also recommend a change in manner treatment is administered. Specifically, malaria treatment should be administered at health centres

6.2 Future work

The models analysed in this work could be extended as follows:

1. Since the model did not incorporate the effect of cytokines (how do cell communicate), we hope to extend the model by considering the effect of cytokines.
2. Since there is relationship between malaria and HIV/AIDS, we hope to include the model of co-infection of HIV and Malaria.

Appendix A

Parameters values and initial variables used in simulations

In this Appendix we will show some of the parameters used to draw the figures on our model.

TABLE. A.1. The table that shows the initial variables that used in FIG. (4.3,4.4)

Variables	$R(0)$	$R_l(0)$	$R_a(0)$	$P_i(0)$	$P_e(0)$	$E(0)$
Values(DFE)	$5 * 10^9$	0	0	50	0	200
Values(EEP)	$5 * 10^9$	0	0	10^7	0	200

TABLE. A.2. The table with parameters values used in FIG. (4.3)

Parameters	S_r	μ_r	k	α	γ	μ_{rl}	k_b
Values	$2.5 * 10^{(7.2)}$	0.01	$2 * 10^{(-9)}$	0.2	0.0001	0.01	0.4
Parameters	μ_{ra}	N	k_{11}	n^*k^*	μ_{pe}	ω	S_{pe}
Values	0.014	32	0.01	$10^{(-8)}$	0.0208	0.04	20
Parameters	k_{pi}	n_1	m	k_{tp}	r_e		
Values	0.08745	24	$10^{(-8)}$	0.0009	2000		

TABLE. A.3. The table with parameters values used in FIG. (4.4)

Parameters	S_r	μ_r	k	α	γ	μ_{rl}	k_b
Values	$2.5 * 10^{(7.2)}$	0.01	$2 * 10^{(-9.46)}$	0.2	0.001	0.008	0.4
Parameters	μ_{ra}	N	k_{11}	n^*k^*	μ_{pe}	ω	S_{pe}
Values	0.014	32	0.01	$10^{(-8)}$	0.0208	0.04	15
Parameters	k_{pi}	n_1	m	k_{tp}	r_e		
Values	0.08745	12	$10^{(-8)}$	0.0009	800		

TABLE. A.4. The table that shows the initial variables that used in FIG. (4.5,4.6)

Variables	$R(0)$	$R_l(0)$	$R_a(0)$	$P_i(0)$	$P_e(0)$	$E(0)$
Values(DFE)	10^{11}	0	0	$10^(10)$	0	200

TABLE. A.5. The table with parameters values used in FIG. (4.5,4.6)

Parameters	S_r	μ_r	k	α	γ	μ_{rl}	k_b
Values	$2 * 10^{(9)}$	0.01	$2 * 10^{(-9)}$	0.1	0.04	0.01	0.4
Parameters	μ_{ra}	N	k_{11}	n^*k^*	μ_{pe}	ω	S_{pe}
Values	0.014	32	0.01	$10^{(-8)}$	0.0208	0.04	10
Parameters	k_{pi}	m	k_{tp}	r_e			
Values	0.08745	$10^{(-8)}$	0.01	4000			

TABLE. A.6. The table that shows the initial variables that used in FIG. (4.7)

Variables	$R(0)$	$R_l(0)$	$R_a(0)$	$P_i(0)$	$P_e(0)$	$E(0)$			
Values(DFE)	$5 * 10^9$	0	0	$5 * 10^(7)$	0	200	1	1	1

TABLE. A.7. The table with parameters values used in FIG. (4.7)

Parameters	S_r	μ_r	k	α	γ	μ_{rl}	k_b
Values	$2.5 * 10^{(7.2)}$	0.01	$2 * 10^{(-9.46)}$	0.2	0.0001	0.008	0.4
Parameters	μ_{ra}	N	k_{11}	n^*k^*	μ_{pe}	ω	S_{pe}
Values	0.014	32	0.01	$10^{(-8)}$	0.0208	0.04	20
Parameters	k_{pi}	m	k_{tp}	r_e	n_1		
Values	0.08745	$10^{(-8)}$	0.008745	880	12		

TABLE. A.8. The table that shows the initial variables that used in FIG. (4.8,4.9, 4.10)

Variables	$R(0)$	$R_l(0)$	$R_a(0)$	$P_i(0)$	$P_e(0)$	$E(0)$
Values(4.8)	$5 * 10^9$	0	0	$5 * 10^(7)$	0	200
Values(4.9)	$5 * 10^9$	0	0	$5 * 10^(8)$	10	200

TABLE. A.9. The table with parameters values used in FIG. (4.8,4.9,4.10)

Parameters	S_r	μ_r	k	α	γ	μ_{rl}	k_b
Values	$2.5 * 10^{(7.2)}$	0.01	$2 * 10^{(-9.46)}$	0.2	0.008	0.008	0.4
Parameters	μ_{ra}	N	k_{11}	n^*k^*	μ_{pe}	ω	S_{pe}
Values	0.014	32	0.01	$10^{(-8)}$	0.0208	0.04	20
Parameters	k_{pi}	m	k_{tp}	r_e	n_1		
Values	0.08745	$10^{(-8)}$	0.008745	880	12		

TABLE. A.10. The table that shows the initial variables that used in FIG.(4.11,4.12, 4.13,4.14)

Variables	$R(0)$	$R_l(0)$	$R_a(0)$	$P_i(0)$	$P_e(0)$	$E(0)$
Values	$5 * 10^9$	0	0	50	0	200

TABLE. A.11. The table with parameters values used in FIG. (4.11,4.12, 4.13,4.14)

Parameters	S_r	μ_r	k	α	γ	μ_{rl}	k_b
Values	$2.5 * 10^{(7.2)}$	0.01	$2 * 10^{(-9)}$	0.2	0.0001	0.01	0.4
Parameters	μ_{ra}	N	k_{11}	n^*k^*	μ_{pe}	ω	S_{pe}
Values	0.014	32	0.01	$10^{(-8)}$	0.0208	0.04	20
Parameters	k_{pi}	m	k_{tp}	r_e	n_1		
Values	0.08745	$10^{(-8)}$	0.008745	2000	24		

TABLE. A.12. The table that shows the initial values used in FIG. (4.15,4.16)

Variables	$R(0)$	$R_l(0)$	$R_a(0)$	$P_i(0)$	$P_e(0)$	$E(0)$
Values	$5 * 10^9$	0	0	10^7	0	200

TABLE. A.13. The table with parameters and values used in FIG. (4.15,4.16)

Parameters	S_r	μ_r	k	α	γ	μ_{rl}	k_b
Values	$2.5 * 10^{(7.3)}$	0.01	$2 * 10^{(-9.25)}$	0.1	0.001	0.008	0.5
Parameters	μ_{ra}	N	k_{11}	n^*k^*	μ_{pe}	ω	S_{pe}
Values	0.014	32	0.02	$10^{(-8)}$	0.0208	0.05	20
Parameters	k_{pi}	n_1	m	k_{tp}	r_e		
Values	0.08745	12	$10^{(-8)}$	0.0009	880		

TABLE. A.14. The table that shows the initial values used in FIG. (5.2,5.3,5.4)

Variables	$S_l(0)$	$I_l(0)$	$P(0)$	$C_l(0)$	$R(0)$	$R_i(0)$	M_r
Values	10^{11}	0	0	1	$5 * 10^9$	0	1
Variables	$T(0)$	$C_r(0)$	$S_{mc}(0)$	$I_{mc}(0)$	$G(0)$	$E(0)$	
Values	1	1	10^6	0	1	200	

TABLE. A.15. The table with parameters and values used in FIG. (5.2,5.3,5.4)

Parameters	π_{il}	β_l	μ_{sl}	k_l	N	m	μ_{il}
Values	$3*10^{(7.5)}$	$4*10^{(-10)}$	0.004	0.2	32	$10^{(-8)}$	0.01
Parameters	α_p	k_{12}	n_3	μ_{imc}	μ_p	k_{cl}	k_{tp}
Values	0.2	0.2	30	0.01	0.01	0.02	0.25
Parameters	S_r	k	μ_r	k_b	μ_{ri}	μ_{il}	k_r
Values	$2.5*10^{(7.2)}$	$2*10^{(-9.25)}$	0.01	0.4	0.2	0.01	0.001
Parameters	γ	ω	μ_t	k_{11}	μ_{cr}	π_{mc}	β_{mc}
Values	0.4	$10^{(-4)}$	0.01	0.02	0.2	$2.4*10^4$	$10^{(-7)}$
Parameters	μ_g	ω_e	r_e	β_p	n_1	μ_{mr}	k_{13}
Values	0.4	0.04	$2.1*10^5$	$4*10^{(-10)}$	24	0.0208	0.6
Parameters	μ_{cl}	k_7	μ_{mc}	π_p			
Values	0.01	$10^{(-8)}$	0.025	0.08			

TABLE. A.16. The table that shows the initial values used in FIG. (5.5,5.6,5.7)

Variables	$S_l(0)$	$I_l(0)$	$P(0)$	$C_l(0)$	$R(0)$	$R_i(0)$	M_r
Values	$10^{10.5}$	0	0	1	$5*10^9$	0	1
Variables	$T(0)$	$C_r(0)$	$S_{mc}(0)$	$I_{mc}(0)$	$G(0)$	$E(0)$	
Values	1	1	10^5	0	1	200	

TABLE. A.17. The table with parameters and values used in FIG.(5.8,5.9, 5.10,5.5,5.6,5.7, 5.11,5.12, 5.13)

Parameters	π_{il}	β_l	μ_{sl}	k_l	N	m	μ_{il}
Values	$3*10^{(7.7)}$	$4*10^{(-10)}$	0.01	0.2	32	$10^{(-8)}$	0.01
Parameters	α_p	k_{12}	n_3	μ_{imc}	μ_p	k_{cl}	k_{tp}
Values	0.5	0.3	5	0.2	0.001	0.02	0.0001
Parameters	S_r	k	μ_r	k_b	μ_{ri}	μ_{il}	k_r
Values	$2.5*10^{(7.3)}$	$2*10^{(-8)}$	0.01	0.4	0.2	0.01	0.01
Parameters	γ	ω	μ_t	k_{11}	μ_{cr}	π_{mc}	β_{mc}
Values	0.4	$10^{(-4)}$	0.01	0.02	0.2	$2.4*10^4$	$10^{(-7)}$
Parameters	μ_g	ω_e	r_e	β_p	n_1	μ_{mr}	k_{13}
Values	0.4	0.04	$2.1*10^5$	$4*10^{(-9)}$	12	0.01	0.6
Parameters	μ_{cl}	k_7	μ_{mc}	π_p			
Values	0.01	$10^{(-8)}$	$10^{(-10)}$	0.08			

Bibliography

[1] R. M. Anderson, R. M. May, and S. Gupta. Non-linear phenomena in host-parasite interactions. *Parasitology*, 99:S59 – S79, 1989.

[2] R. Antia, A. Yates, and J. C. de Roode. The dynamics of acute malaria infections. I. Effect of the parasite's red blood cell preference. *Proceedings of the Royal Society B*, 275:1449 – 1458, 2008.

[3] K. Artavanis-Tsakonas and E. M. Riley. Innate immune response to malaria: Rapid induction of IFN-γ from human NK cells by live plasmodium falciparum-infected erythrocytes. *The Journal of Immunology*, 169:2956 – 2963, 2002.

[4] K. Artavanis-Tsakonas, J. E. Tongren, and E. M. Riley. The war between the malaria parasite and the immune system: immunity, immunoregulation and immunopathology. *Clinical and Experimental Immunology*, 133:145 – 152, 2003.

[5] D. J. Austin, N. J. White, and R. M. Anderson. The dynamics of drug action on the within-host population growth of infectious agents: Melding pharmacokinetics with pathogen population dynamics. *Journal of Theoretical Biology*, 194:313 – 339, 1998.

[6] P. B. Bloland. Drug resistance in malaria. *World Health Organization (WHO)*, 2001.

[7] S. M. Blower. Sensitivity and uncertainty analysis of complex models of disease transmission: An HIV model, as an example. *International Statistical Review*, 62:229 – 243, 1994.

[8] L. J. Bruce-Chwatt. Alphonse laveran's discovery 100 years ago and today's global fight against malaria. *Journal of the Royal Society of Medicine*, 74:531 – 536, 1981.

[9] L. Cao, L. Krymskaya, V. Tran, S. Mi, M. C. Jensen, S. Blanchard, and M. Kalos. Development and application of a multiplexable flow cytometry-based assay to quantify cell-mediated cytolysis. *Journal of the International Society for Advancement of Cytometry*, 77A:534 – 545, 2010.

[10] CDC. Parasite Image Library. http://dpd.cdc.gov/dpdx. Last accessed 27 September 2011.

[11] CDC. Malaria, Biology. http://www.cdc.gov/malaria/about/biology/index.html, 2010 (review). Last accessed: 1 March 2011.

[12] N. Chitnis, J. M. Hyman, and J. M. Cushing. Determining important parameters in the spread of malaria through the sensitivity analysis of a mathematical model. *Bulletin of Mathematical Biology*, 2008.

[13] C. Chiyaka, W. Garira, and S. Dube. Modelling immune response and drug therapy in human malaria infection. *Computational and Mathematical Methods in Medicine*, 9:143 – 163, 2008.

[14] K. Chotivanich, R. Udomsangpetch, J. A. Simpson, P. Newton, S. Pukrittayakamee, S. Looareesuwan, and N. J. White. Parasite multiplication potential and the severity of falciparum malaria. *Journal of Infectious Diseases*, 181:1206 – 1209, 2000.

[15] S. M. Ciupe, R. M. Ribeiro, P. W. Nelson, and A. S. Perelson. Modeling the mechanisms of acute hepatitis B virus infection. *Journal of Theoretical Biology*, 247:23 – 35, 2007.

[16] K. L. Cooke and P. van den Driessche. Analysis of an SEIRS epidemic model with two delays. *Journal of Mathematical Biology*, 35:240 – 260, 1996.

[17] A. Coppi, R. Natarajan, G. Pradel, B. L. Bennett, E. R. James, M. A. Roggero, G. Corradin, C. Persson, R. Tewari, and P. Sinnis. The malaria circumsporozoite protein has functional domains, each with distinct roles as sporozoites journey from mosquito to mammalian host. *The Journal of the Experimental Medicine*, pages 1 – 16, 2011.

[18] A. F. Cowman and B. S. Crabb. Invasion of red blood cells by malaria parasites. *Cell*, 124:755 – 766, 2006.

[19] B. C. de Sousa and C. Cunha. Development of mathematical models for the analysis of hepatitis delta virus viral dynamics. *PLoS ONE*, 5:e12512, 2010.

[20] O. Diekmann, J. A. P. Heesterbeek, and J. A. J. Metz. On the definition and the computation of the basic reproduction ratio R_0 in models for infectious diseases in heterogeneous populations. *Journal of Mathematical Biology*, 28:365 – 382, 1990.

[21] K. Dietz, G. Raddatz, and L. Molineaux. Mathematical model of the first wave of plasmodium falsiparam asexual parasitemia in non- immune and vaccinated individuals. *The American Journal of Tropical Medicine and Hygiene*, 75:46 – 55, 2006.

[22] H. Elsaesser, K. Sauer, and D. G. Brooks. IL-21 Is required to control chronic viral infection. *Science*, 324:1569 – 1572, 2009.

[23] C. R. Engwerda and M. F. Good. Interactions between malaria parasites and the host immune system. *Current Opinion in Immunology*, 17:381 – 387, 2005.

[24] L. Esteva, A. B. Gumel, and C. V. de Leon. Qualitative study of transmission dynamics of drug-resistance malaria. *Mathematical and Computer Modelling*, 50:611 – 630, 2009.

[25] A. Friedman, J. Turner, and B. Szomolay. A model on the influence of age on immunity to infection with mycobacterium tuberculosis. *Experimental Gerontology*, 43:275 – 285, 2008.

[26] H. Fujioka and M. Aikawa. Stucture and life cycle. *Chemical Immunology*, 80:1 – 26, 2002.

[27] S. Gandon, M. J. Mackinnon, S. Nee, and A. F. Read. Imperfect vaccines and the evolution of pathogen virulence. *Nature*, 414:751 – 756, 2001.

[28] M. B. Gravenor, A. R. McLean, and D. Kwiatkowski. The regulation of malaria parasitaemia: parameter estimates for a population model. *Parasitology*, 110:115 – 122, 1995.

[29] D. T. Haydon, L. Matthews, R. Timms, and N. Colegrave. Top-down or bottom-up regulation of intra-host blood-stage malaria: do malaria parasites most resemble the dynamics of prey or predator? *Proceedings of the Royal Society B*, 270:289 – 298, 2003.

[30] B. Hellriegel. Modelling the immune response to malaria with ecological concepts: short-term behaviour against long-term equilibrium. *Proceedings of the Royal Society B*, 250:249 – 256, 1992.

[31] C. Hetzel and R. M. Anderson. The within-host cellular dynamics of bloodstage malaria theoretical and experimental studies. *Parasitology*, 113:25 – 38, 1996.

[32] A. Hoare, D. G. Regan, and D. P. Wilson. Sampling and sensitivity analysis tools (SaSAT) for computational modelling. *Theoretical Biology and Medical Modelling*, 5:4, 2008.

[33] M. R. Hollingdale and U. Krzych. Immune responses to liver-stage parasites: Implications for vaccine development. *Chemical Immunology*, 80:97 – 124, 2002.

[34] M. B. Hoshen, R. Heinrich, W. D. Stein, and H. Ginsburg. Mathematical modelling of the within-host dynamics of plasmodium falciparum. *Parasitology*, 121:227 – 235, 2000.

[35] A. Iggidr, J. Kamgang, G. Sallet, and J. Tewa. Global analysis of new malaria intrahost models with a competitive exclusion principle. *SIAM Journal of Applied Mathematics*, 67:260 – 278, 2006.

[36] IUPUI. ECE680 Modern automatic control Routh's stability criterion. http://www.engr.iupui.edu/ skoskie/ECE680/Routh.pdf, 2007. Last accessed 17 September 2011.

[37] B. Jayabalasingham, N. Bano, and I. Coppens. Metamorphosis of the malaria parasite in the liver is associated with organelle clearance. *Cell Research*, 20:1043 – 1059, 2010.

[38] H. J. Kaiser. HIV/Malaria co-Infection nearly doubles HIV viral load, increases chance of transmission, study says. http://www.thebody.com/content/art9124.html, 2005. Last accessed: 1 March 2011.

[39] V. Kalia, S. Sarkar, and R. Ahmed. CD8 T-cell memory differentiation during acute and chronic viral infections. Landes Bioscience and Springer Science + Business Media, 2010.

[40] D. E. Kirschner. Dynamics of co-infection with m. tuberculosis and HIV-1. *Theoretical Population Biology*, 55:94 – 109, 1999.

[41] A. J. Knell, editor. *Malaria*. Oxford University Press, 1991.

[42] J. W. Koehler, M. Bolton, A. Rollins, K. Snook, E. de Haro, E. Henson, L. Rogers, L. N. Martin, D. J. Krogstad, M. A. James, J. Rice, B. Davison, R. S. Veazey, R. Prabhu, A. M. Amedee, R. F. Garry, and F. B. Cogswell. Altered immune responses in Rhesus macaques co-Infected with SIV and plasmodium cynomolgi: An animal model for coincident AIDS and relapsing malaria. *PLoS ONE*, 4:e7139, 2009.

[43] C. M. Kribs-Zaleta and J. X. Velasco-Hernandez. A simple vaccination model with multiple endemic states. *Mathematical Biosciences*, 164:183 – 201, 2000.

[44] G. Li and Z. Jin. Global stability of a SEIR epidemic model with infectious force in latent, infected and immune period. *Chaos, Solitons and Fractals*, 25:1177 – 1184, 2005.

[45] F. J. Lopez-Antunano and G. Schmunis, editors. *Diagnosis of Malaria*. Number 512. Scientific Publication: Pan American Health Organization, USA, 1990.

[46] MalariaSite. Control of malaria. http://www.malariasite.com/malaria /ControlOfMalaria.htm. Last accessed: 17 September 2011.

[47] MalariaSite. Life cycle. http://www.malariasite.com/malaria/LifeCycle.htm. Last accessed: 30 September 2011.

[48] G. L. Mandell, J. E. Bennett, and R. Dolin. *Principles and Practice of Infectious Diseases, 7th Edition*. Churchhill Livingstone, 2009.

[49] D. P. Mason, F. E. McKenzie, and W. H. Bossert. The blood-stage dynamics of mixed plasmodium malariae-plasmodium falciparum infections. *Journal of Theoretical Biology*, 198:549 – 566, 1999.

[50] A. Matteelli, F. Castelli, and S. Caligaris. *Life Cycle of Malaria Parasites*, chapter 2, pages 17 – 23. University of Brescia (Italy), 1997.

[51] F. E. McKenzie. Why model malaria? *Parasitology Today*, 16:511 – 516, 2000.

[52] F. E. McKenzie and W. H. Bossert. The dynamics of plasmodium falciparum blood-stage infection. *Journal of Theoretical Biology*, 188:127 – 140, 1997.

[53] F. E. McKenzie and W. H. Bossert. An integrated model of plasmodium falciparum dynamics. *Journal of Theoretical Biology*, 232:411 – 426, 2005.

[54] F. E. McKenzie, D. L. Smith, W. P. O'Meara, and E. M. Riley. Strain theory of malaria: The first 50 years. *Advances in Parasitology*, 66:1 – 46, 2008.

[55] P. G. McQueen and F. E. McKenzie. Age-structured red blood cell susceptibility and the dynamics of malaria infections. *Proceedings of the National Academy of Sciences*, 101:9161 – 9166, 2004.

[56] P. G. McQueen and F. E. McKenzie. Competition for red blood cells can enhance plasmodium vivax parasitemia in mixed-species malaria infection. *The American Journal of Tropical Medicine and Hygiene*, 75:112 – 125, 2006.

[57] P. G. McQueen and F. E. McKenzie. Host control of malaria infections: Constraints on immune and erythropoeitic response kinetics. *PLoS Computation Biology*, 4:e1000149, 2008.

[58] N. Mideo, T. Day, and A. F. Read. Modelling malaria pathogenesis. *Cellular Microbiology*, 10:1947 – 1955, 2008.

[59] S. A. Mikolajczak, V. Jacobs-Lorena, D. C. MacKellar, N. Camargo, and S. H. I. Kappe. L-FABP is a critical host factor for successful malaria liver stage development. *International Journal for Parasitology*, 37:483 – 489, 2007.

[60] L. H. Miller, D. I. Baruch, K. Marsh, and O. K. Doumbo. The pathogenic basis of malaria. *Nature*, 415:643 – 649, 2002.

[61] O. R. Millington, C. D. Lorenzo, R. S. Phillips, P. Garside, and J. M. Brewer. Suppression of adaptive immunity to heterologous antigens during plasmodium infection through hemozoin-induced failure of dendritic cell function. *Journal of Biology*, 5:5, 2006.

[62] L. A. Mohammed. Stability of linear control systems: Routh's Criterion. www.uotechnology.edu.iq/dep-production/media/pdf/FCLec8.pdf. Last accessed 21 September 2011.

[63] R. H. Morrow and W. J. Moss. *The Epidemiology and Control of Malaria*, chapter 26, pages 1087 – 1138. Jones and Bartlett Publishers, 2007.

[64] MVI. PATH malaria vaccine initiative (MVI). http://www.malariavaccine.org/. Last accessed: 17 September 2011.

[65] A. Niger and A. B. Gumel. Immune response and imperfect vaccine in malaria dynamics. *Mathematical Population Studies*, 18:54 – 86, 2011.

[66] F. Nuwaha. The challenge of chloroquine-resistant malaria in sub-Saharan Africa. *Health Policy and Planning*, 16:1 – 12, 2001.

[67] F. Nyabadza. Modelling the role of prophylaxis in malaria prevention. *International Journal of Biological and Medical Sciences*, 1:18 – 23, 2007.

[68] B. E. Petersen, W. C. Bowen, K. D. Patrene, W. M. Mars, A. K. Sullivan, N. Murase, S. S. Boggs, J. S. Greenberger, and J. P. Goff. Bone marrow as a potential source of hepatic oval cells. *Science*, 284:1168 – 1170, 1999.

[69] M. Prudencio, A. Rodriguez, and M. M. Mota. The silent path to thousands of merozoites: the plasmodium liver stage. *Nature Reviews Microbiology*, 4:849 – 856, 2006.

[70] RollBackMalaria. Key malaria facts. http://www.rollbackmalaria.org/keyfacts.html. Last accessed: 17 September 2011.

[71] P. J. Rosenthal, editor. *Anti-malarial Chemotherapy: Mechanisms of action, Resistance, and Directions in Drug Discovery*. Humana Press Inc., 2001.

[72] D. Sacks. BAC talk about cell type-specific regulation of human IL−10. *Proceedings of the National Academy of Sciences*, 106:16895 – 16896, 2009.

[73] K. J. Saliba and K. Kirk. pH Regulation in the intracellular malaria parasite plasmodium falciparum. *The Journal of Biological Chemistry*, 274:33213 – 33219, 1999.

[74] A. Saltelli, S. Tarantola, F. Campolongo, and M. Ratto. *Sensitivity Analysis in Practice: A Guide to Assessing Scientific Models*. John Wiley and Sons, Ltd, England, 2004.

[75] M. A. Sanchez and S. M. Blower. Uncertainty and sensitivity analysis of the basic reproductive rate tuberculosis as an example. *American Journal of Epidemiology*, 145:1127 – 1137, 1997.

[76] C. Shiff. Integrated approach to malaria control. *Clinical Microbiology Reviews*, 15:278 – 293, 2002.

[77] R. Shonkwiler and S. J. Aneke. Some mathematical models for malaria. *School of Mathematics*, 1999. Georgia Institute of Technology, Atlanta GA 30332.

[78] L. Simpson. Life cycle and transmission. http://dna.kdna.ucla.edu/parasitecourse−old/malariafiles /subchapters/life%20cycle.htm. Last accessed 30 September 2011.

[79] T. Smith, G. F. Killeen, N. Maire, A. Ross, L. Molineaux, F. T. G. Hutton, J. Utzinger, K. Dietz, and M. Tanner. Mathematical modelling of the impact of malaria vaccines on the clinical epidemiology and natural history of plasmodium falciparum malaria: Overview. *American Journal of Tropical Medicine and Hygiene*, 75:1 – 10, 2006.

[80] R. W. Snow, C. A. Guerra, A. M. Noor, H. Y. Myint, and S. I. Hay. The global distribution of clinical episodes of plasmodium falciparum malaria. *Nature*, 434:214 – 217, 2005.

[81] D. A. Stevens. Combination immunotherapy and antifungal chemotherapy. *Clinical Infectious Diseases*, 26:1266 – 1269, 1998.

[82] M. M. Stevenson and E. M. Riley. Innate immunity to malaria. *Nature Reviews Immunology*, 4:169 – 180, 2004.

[83] A. Sturm, R. Amino, C. van de Sand, T. Regen, S. Retzlaff, A. Rennenberg, A. Krueger, J. Pollok, R. Menard, and V. T. Heussler. Manipulation of host hepatocytes by the malaria parasites for delivery into liver sinosoids. *Science*, 313:1287 – 1290, 2006.

[84] Y. Su, S. Ruan, and J. Wei. Periodicity and synchronization in blood-stage malaria infection. *Journal of Mathematical Biology*, 63:557 – 574, 2011.

[85] A. Suhrbier, L. A. Winger, E. Castellano, and R. E. Sinden. Survival and antigenic profile of irradiated malarial sporozoites in infected liver cells. *Infection and Immunity*, 58:2834 – 2839, 1990.

[86] K. R. Tan, S. Mali, and P. M. Arguin. Malaria risk information and prophylaxis, by country. http://wwwnc.cdc.gov/travel/yellowbook/2010/chapter−2/malaria.htm. Last accessed: 29 June 2011.

[87] M. I. Teboh-Ewungkem and T. Yuster. A within-vector mathematical model of plasmodium falciparum and implication of incomplete fertilization on optimal gametocyte sex ratio. *Journal of Theoretical Biology*, 264:273 – 286, 2010.

[88] K. A. Trott, J. Y. Chau, S. Luckhart, and K. Abel. Enhanced severity of malaria infection in simian immunodeficiency virus (SIV) infected rhesus macaques. *The Journal of Immunology*, 182:129.15, 2009.

[89] J. Tumwiine, S. Luckhaus, J. Y. T. Mugisha, and L. S. Luboobi. An age-structured mathematical model for the within host dynamics of malaria and the immune system. *Journal of Mathematical Modelling and Algorithms*, 7:79 – 97, 2008.

[90] UNICEF. Promoting rational use of drugs and correct case management in basic healthy services. UNICEF programme division in cooperation with the World Healthy Organization, 2000. Last accessed: 15 August 2011.

[91] UNICEF. Malaria and children: progress in intervention coverage. UNICEF and The roll back Malaria partnership, 2007. Last accessed: 1 March 2011.

[92] USAID. Angola malaria indicator survey 2006 – 2007, 2007.

[93] P. van den Driessche and J. Watmough. Reproduction numbers and sub-threshold endemic equilibria for compartmental models of disease transmission. *Mathematical Biosciences*, 180:29 – 48, 2002.

[94] E. J. Wherry and R. Ahmed. Memory CD8 T-cell differentiation during viral infection. *Journal of Virology*, 78:5535 – 5545, 2004.

[95] WHO. Guidelines for the treatment of malaria. World Health Organization.

[96] WHO. Malaria. http://www.who.int/mediacentre/factsheets/fs094/en/, 2010. Last accessed: 1 March 2011.

[97] E. N. Wiah, I. K. Dontwi, and I. A. Adetunde. Using mathematical model to depict the immune response to hepatitis B virus infection. *Journal of Mathematics Research*, 3:157 – 167, 2011.

[98] Wikipedia. Ronald Ross. http://en.wikipedia.org/wiki/RonaldRoss. Last accessed: 17 September 2011.

[99] Wikipedia. Sensitivity analysis. http://en.wikipedia.org/wiki/Sensitivityanalysis. Last accessed 23 September 2011.

[100] Wikipedia. Adaptive immune system. http://en.wikipedia.org/wiki/Adaptive-immune-system, 2010. Last accessed: 26 January 2010.

[101] Wikipedia. Red blood cell. http://en.wikipedia.org/wiki/Red-blood-cells, 2010. Last accessed: 17 June 2010.

[102] A. Yeka, K. Banek, N. Bakyaita, S. G. Staedke, M. R. Kamya, A. Talisuna, F. Kironde, S. L. Nsobya, A. Kilian, M. Slater, A. Reingold, P. J. Rosenthal, F. Wabwire-Mangen, and G. Dorsey. Artemisinin versus nonartemisinin combination therapy for uncomplicated malaria: Randomized clinical trials from four sites in Uganda. *PLOS Medicine*, 2:0654 – 0662, 2005.

[103] S. Yeung, W. Pongtavornpinyo, I. M. Hastings, A. J. Mills, and N. J. White. Antimalarial drug resistance, artemisinin-based combination therapy, and the contribution of modelling to elucidating policy choices. *American Journal of Tropical Medicine and Hygiene*, 71:179– 186, 2004.

[104] D. Zhang, P. Shankar, Z. Xu, B. Harnisch, G. Chen, C. Lange, S. J. Lee, H. Valdez, M. M. Lederman, and J. Lieberman. Most antiviral CD8 T cells during chronic viral infection do not express high levels of perforin and are not directly cytotoxic. *Blood*, 101:226 – 235, 2003.